RECLAMATION

Managing Water in the West

Colorado River Basin Water Supply and Demand Study

Technical Report B — Water Supply Assessment

U.S. Department of the Interior
Bureau of Reclamation

December 2012

Mission Statements

The U.S. Department of the Interior protects America's natural resources and heritage, honors our cultures and tribal communities, and supplies the energy to power our future.

The mission of the Bureau of Reclamation is to manage, develop, and protect water and related resources in an environmentally and economically sound manner in the interest of the American public.

Colorado River Basin
Water Supply and Demand Study

Technical Report B — Water Supply Assessment

U.S. Department of the Interior
Bureau of Reclamation

December 2012

Contents

Tables

Figures

Appendices

Acronyms and Abbreviations

2007 Interim Guidelines Final EIS	*Colorado River Interim Guidelines for Lower Basin Shortages and Coordinated Operations for Lake Powell and Lake Mead Final Environmental Impact Statement*
°C	degrees Celsius
AMJ	April, May, and June
AMO	Atlantic Multi-decadal Oscillation
Basin	Colorado River Basin
Basin States	Colorado River Basin States
BCSD	bias correction and spatial downscaling
CDF	cumulative distribution function
CMIP3	Coupled Model Intercomparison Project Phase 3
CRSS	Colorado River Simulation System
EIS	Environmental Impact Statement
ENSO	El Nino Southern Oscillation
ET	evapotranspiration
GCM	General Circulation Model
GHG	greenhouse gas
in/d	inches per day
IPCC	Intergovernmental Panel on Climate Change
ISM	Indexed Sequential Method
JAS	July, August, and September
JFM	January, February, and March
kaf	thousand acre-feet
km	kilometer
maf	million acre-feet
Mexico	United Mexican States
mm	millimeters
mm/d	millimeters per day
netCDF	network common data format
NOAA	National Oceanic and Atmospheric Administration
NRC	National Research Council

OND	October, November, and December
PET	potential ET
PDO	Pacific Decadal Oscillation
Reclamation	Bureau of Reclamation
RMSE	root mean square error
SNOTEL	snow-telemetry
SOI	Southern Oscillation Index
SRES	Special Report on Emissions Scenarios
Study	Colorado River Basin Water Supply and Demand Study
SWE	Snow water equivalent
USGS	U.S. Geological Survey
VIC	Variable Infiltration Capacity
WCRP	World Climate Research Program
WWCRA	West-Wide Climate Risk Assessment

Technical Report B — Water Supply Assessment

1.0 Introduction

The Colorado River Basin Water Supply and Demand Study (Study), initiated in January 2010, was conducted by the Bureau of Reclamation's (Reclamation) Upper Colorado and Lower Colorado regions, and agencies representing the seven Colorado River Basin States (Basin States) in collaboration with stakeholders throughout the Colorado River Basin (Basin). The purpose of the Study is to define current and future imbalances in water supply and demand in the Basin and the adjacent areas of the Basin States that receive Colorado River water over the next 50 years (through 2060), and to develop and analyze adaptation and mitigation strategies to resolve those imbalances. The Study contains four major phases to accomplish this goal: Water Supply Assessment, Water Demand Assessment, System Reliability Analysis, and Development and Evaluation of Options and Strategies for Balancing Supply and Demand.

Spanning parts of the seven states of Arizona, California, Colorado, New Mexico, Nevada, Utah, and Wyoming, the Colorado River is one of the most critical sources of water in the western United States. The Colorado River is also a vital resource to the United Mexican States (Mexico). It is widely known that the Colorado River, based on the inflows observed over the last century, is over-allocated and supply and demand imbalances are likely to occur in the future. Up to this point, this imbalance has been managed, and demands have largely been met as a result of the considerable amount of reservoir storage capacity in the system, the fact that the Upper Basin States are still developing into their apportionments, and efforts the Basin States have made to reduce their demand for Colorado River water.

Concerns regarding the reliability of the Colorado River system to meet future needs are even more apparent today. The Basin States include some of the fastest growing urban and industrial areas in the United States. At the same time, the effects of climate change and variability on the Basin water supply has been the focus of many scientific studies which project a decline in the future yield of the Colorado River. Increasing demand, coupled with decreasing supplies, will certainly exacerbate imbalances throughout the Basin.

It is against this backdrop that the Study was conducted to establish a common technical foundation from which important discussions can begin regarding possible strategies to reduce future supply and demand imbalances. The content of this report is a key component of that technical foundation and describes the Study's assessment of water supply. The purpose of the Water Supply Assessment is to determine the probable magnitude and variability of historical and future natural flows in the Basin. Natural flow represents the flow that would have occurred at a location, had depletions and reservoir regulation not been present upstream of that location.

Because the magnitude and variability of future water supply is uncertain, a set of future water supply scenarios were developed to explore that uncertainty, including the potential effects of future climate variability and climate change. The water supply projections were used to analyze future reliability of the river system to meet water demands, with and without future options and strategies. The Water Supply Assessment drew on the expertise of researchers and analysts worldwide who have been investigating the hydrology of the Basin and the dynamics of global climate change.

Initially published in June 2011 under Interim Report No. 1 with updates published in February 2012, this report replaces these earlier publications.

2.0 Approach to Water Supply Scenario Development

A scenario planning process was implemented to examine the uncertainty in future water supply and demand and is detailed in *Technical Report A – Scenario Development*. As noted in that report, a collaborative process that engages stakeholders was essential to the successful development of future scenarios. Numerous organizations participated in the Water Supply Assessment, including representatives of the Reclamation, Reclamation's Technical Service Center, the Basin States, U.S. Fish and Wildlife Service, National Oceanic and Atmospheric Administration (NOAA), federally recognized tribes, conservation organizations, and others interested in the Basin. This collaboration was accomplished through a variety of means, including participation in a Water Supply Sub-Team and direct contact with the organizations listed above. The Water Supply Sub-Team members and the points of contact are identified in appendix B1 of this report.

A scenario is an alternative view of how the future might unfold. Scenarios are not predictions or forecasts of the future. The scenario planning process involved identifying the key driving forces (i.e., the factors that will likely have the greatest influence on the future state of the system and thereby the performance of the system over time), ranking the driving forces as to their relative importance and relative uncertainty, and associating the highly uncertain and highly important driving forces, identified as critical uncertainties, with either water supply or water demand. The process is shown in figure B-1, which is also presented in *Technical Report A – Scenario Development*. The critical uncertainties that were identified and associated with water supply (the step, "Associate Critical Uncertainties with Water Supply and Demand," shown in figure B-1) are:

- Changes in Streamflow Variability and Trends
- Changes in Climate Variability and Trends

See *Technical Report C – Water Demand Assessment* for a discussion of the critical uncertainties associated with water demand.

The subsequent process (shown on the left-hand side of figure B-1 and labeled "Supply") was used by the Water Supply Sub-Team to move from the critical uncertainties to supply scenarios. Each step of this process is described in the following sub-sections.

FIGURE B-1
Scenario Development Process

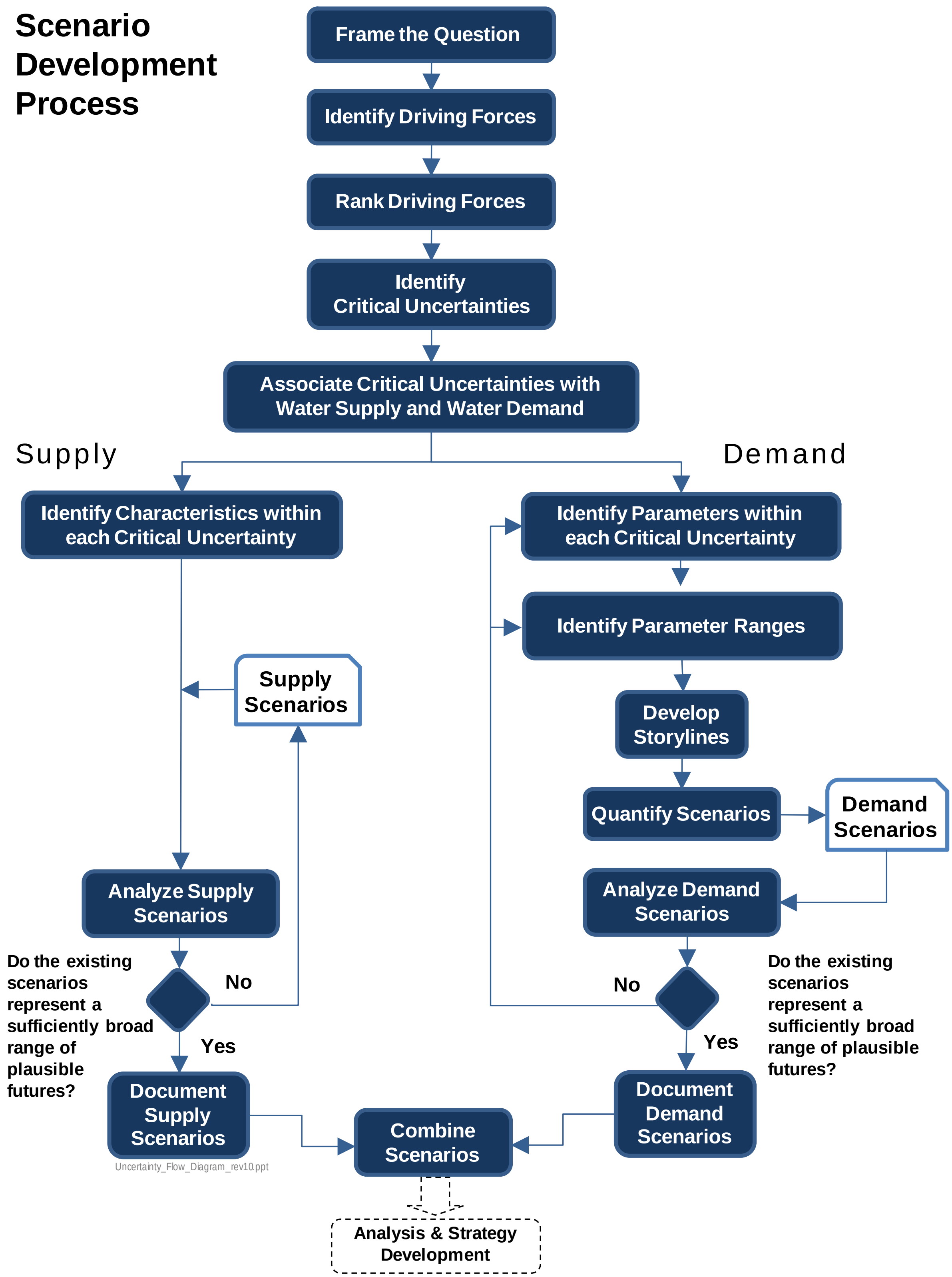

2.1 Identify Characteristics within each Critical Uncertainty

Characteristics can be either qualitative or quantitative descriptions of the trend or values over time that describe the trajectory of the critical uncertainty. In 2004, Reclamation initiated a multi-faceted research and development program to enable the use of methods beyond those that use the observed record for projecting possible future inflow sequences for Basin planning studies. Through this effort, two additional water supply scenarios were developed and have been used in previous Basin planning studies; these scenarios assume that characteristics of the water supply critical uncertainties are represented by the observed and paleo-reconstructed streamflow records. These scenarios, Paleo Resampled and Paleo Conditioned, have most recently been published in appendix N of the *Colorado River Interim Guidelines for Lower Basin Shortages and Coordinated Operations for Lake Powell and Lake Mead Final Environmental Impact Statement* (2007 Interim Guidelines Final Environmental Impact Statement [EIS]) (Reclamation, 2007).

For purposes of the Study, it was determined that these previously used scenarios did not represent a sufficiently broad range of plausible futures because they did not include the consideration of changing climate beyond what has occurred in history. For this reason, a fourth scenario was developed that assumes the characteristics of the critical uncertainties Changes in Streamflow Variability and Trends, and Changes in Climate Variability and Trends are indicated by Downscaled General Circulation Model (GCM) projections and simulated hydrology.

2.2 Water Supply Scenarios

The following scenarios and associated themes were considered in the Study:

- **Observed Record Trends and Variability (Observed Resampled):** Future hydrologic trends and variability are similar to the past approximately100 years.
- **Paleo Record Trends and Variability (Paleo Resampled):** Future hydrologic trends and variability are represented by reconstructions of streamflow for a much longer period in the past (nearly 1,250 years) that show expanded variability.
- **Observed Record Trends and Increased Variability (Paleo Conditioned):** Future hydrologic trends and variability are represented by a blend of the wet-dry states of the longer paleo reconstructed period (nearly 1,250 years), but magnitudes are more similar to the observed period (about 100 years).
- **Downscaled GCM Projected Trends and Variability (Downscaled GCM Projected):** Future climate will continue to warm with regional precipitation and temperature trends represented through an ensemble of future Downscaled GCM Projections and simulated hydrology.

The scenarios each use well-established techniques to represent plausible future water supply conditions. The Observed Resampled, Paleo Resampled, and Paleo Conditioned scenarios use approaches previously developed to represent a range of hydroclimatic variability (annual to decadal scales) under a broad retrospective view. These scenarios are considered plausible in that they represent the range of hydroclimatic conditions experienced in the past. Future changes in climate variability and trends, and their influence on streamflow and Basin water supply, have been studied by several researchers in recent years. The Study represents the first time future climate scenarios have been included in Reclamation's Basin planning studies. For these reasons, greater detail is provided for the Downscaled GCM Projected scenario in this report. This scenario is considered plausible in that it reflects a growing body of scientific research suggesting future changes in hydroclimatic conditions globally and in the Basin. Each of the scenarios in the Study is considered a plausible future condition and is informative for future Basin planning.

3.0 Summary of the Water Supply Assessment Approach

A plausible range of future water supply scenarios was considered to analyze the future reliability of the system. An assessment of historical supply conditions was performed to facilitate an understanding of how the projected future supply conditions under each scenario differ from historical supply conditions. This section describes the water supply indicator groups analyzed for historical and future conditions and includes a summary of published research related to Basin supply.

3.1 Tools and Methods

The assessment of historical and future supply conditions focused on four main groups of water supply indicators, presented in figure B-2. The water supply indicator groups are interrelated: climate influences hydrologic processes; hydrologic processes generate streamflow; and teleconnections (defined below) influence the oscillation of climate patterns.

FIGURE B-2
Water Supply Indicator Groups Used in the Study

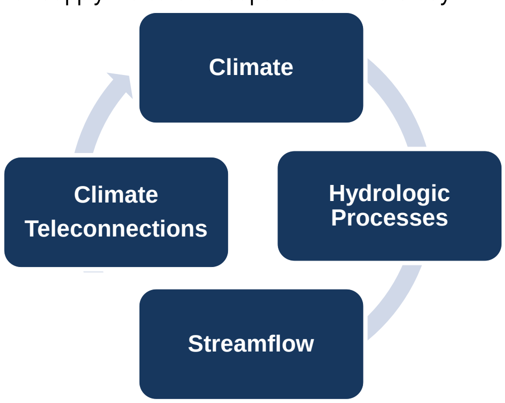

Although the primary indicator of water supply in the Basin is streamflow, a fundamental understanding of the processes that influence the quantity, location, and timing of streamflow is beneficial. Comparisons for each indicator group were made between historical supply and future supply under the Downscaled GCM Projected scenario because this scenario assumes a changing climate. For the Observed Resampled, Paleo Resampled, and Paleo Conditioned scenarios, which assume a climate similar to the past, streamflow is the primary indicator. Methods applied to project streamflow under the future supply scenarios are described in their respective sections.

Climate indicators considered in this assessment were temperature and precipitation. Hydrologic process indicators were runoff, evapotranspiration (ET), snowpack accumulation (snow water equivalent [SWE]), and soil moisture. Climate and hydrologic process indicators were primarily derived from gridded data sets (Maurer et al., 2002; Maurer et al., 2007; Reclamation, 2011a), and spatial averaging was performed for selected sub-basins associated with Reclamation's natural flow computation points. The sub-basin averaging of climate and hydrologic process information allowed assessment of broader regions of the Basin than the detailed grid cell calculations.

Climate teleconnection indicators considered were the El Nino Southern Oscillation (ENSO), Pacific Decadal Oscillation (PDO), and Atlantic Multi-decadal Oscillation (AMO) indices. Teleconnections refer to the linkage between large-scale, ocean-atmosphere patterns (such as ENSO, PDO, and AMO) and weather or climate changes within a separate region of the globe (e.g., precipitation patterns in the Basin). Finally, streamflow indicators considered were natural flows at select locations in the Basin.

Natural flow represents the flow that would have occurred at the location had depletions and reservoir regulation not been present upstream of that location. Natural flow has been computed historically by Reclamation[1] and is currently available for 29 locations throughout the Basin: 20 locations in the Upper Basin upstream of and including the Lees Ferry gaging station in Arizona; and nine additional locations below Lees Ferry, including the Paria River and other inflow points in the Lower Basin. These locations are shown in figure B-3. At this time, Basin-wide, natural flow estimates extend from 1906 through 2008[2]. Although all gages were not in place back to 1906, the existing records were extended back to 1906 using methods described in Lee et al. (2006).

For some tributaries in the Lower Basin (specifically the Little Colorado River, Virgin River, and Bill Williams River), U.S. Geological Survey (USGS)-gaged flows at specific locations near the confluence of the tributary and the Colorado River mainstream were used in place of natural flows. This approach was also taken for the Paria River, which joins the Colorado River just downstream of Lees Ferry, Arizona. In addition, the Gila River is not included in the Colorado River Simulation System (CRSS) and is therefore not included as one of the 29 locations where natural flow is estimated throughout the Basin. See *Technical Report C – Water Demand Assessment, Appendix C11 – Modeling of Lower Basin Tributaries in the Colorado River Simulation System,* for further discussion.

CRSS is Reclamation's primary Basin-wide simulation model used for long-term planning studies and, in its current configuration, requires natural flow inputs at these 29 locations on a monthly time step over the Study's planning horizon. This report describes the specific methods used to quantify, and results of, the water supply scenarios considered in the Study.

Additional information related to water supply data and methods is provided in appendix B2.

---

1 Additional information, documentation, and the natural flow data are available at http://www.usbr.gov/lc/region/g4000/NaturalFlow/index.html.

2 At the time the analysis for this report was performed, natural flow data were available only through 2008.

FIGURE B-3
Colorado River Basin and 29 Natural Flow Locations (Reclamation, 2011a)

Of the 29 streamflow locations, a subset was used for analysis in this report. Circled stations are used for describing climate and streamflow in this report; red dashed circled stations are used to describe climate, orange dashed circled stations are used to describe both climate and streamflow, and solid orange circled stations are used to describe only streamflows.

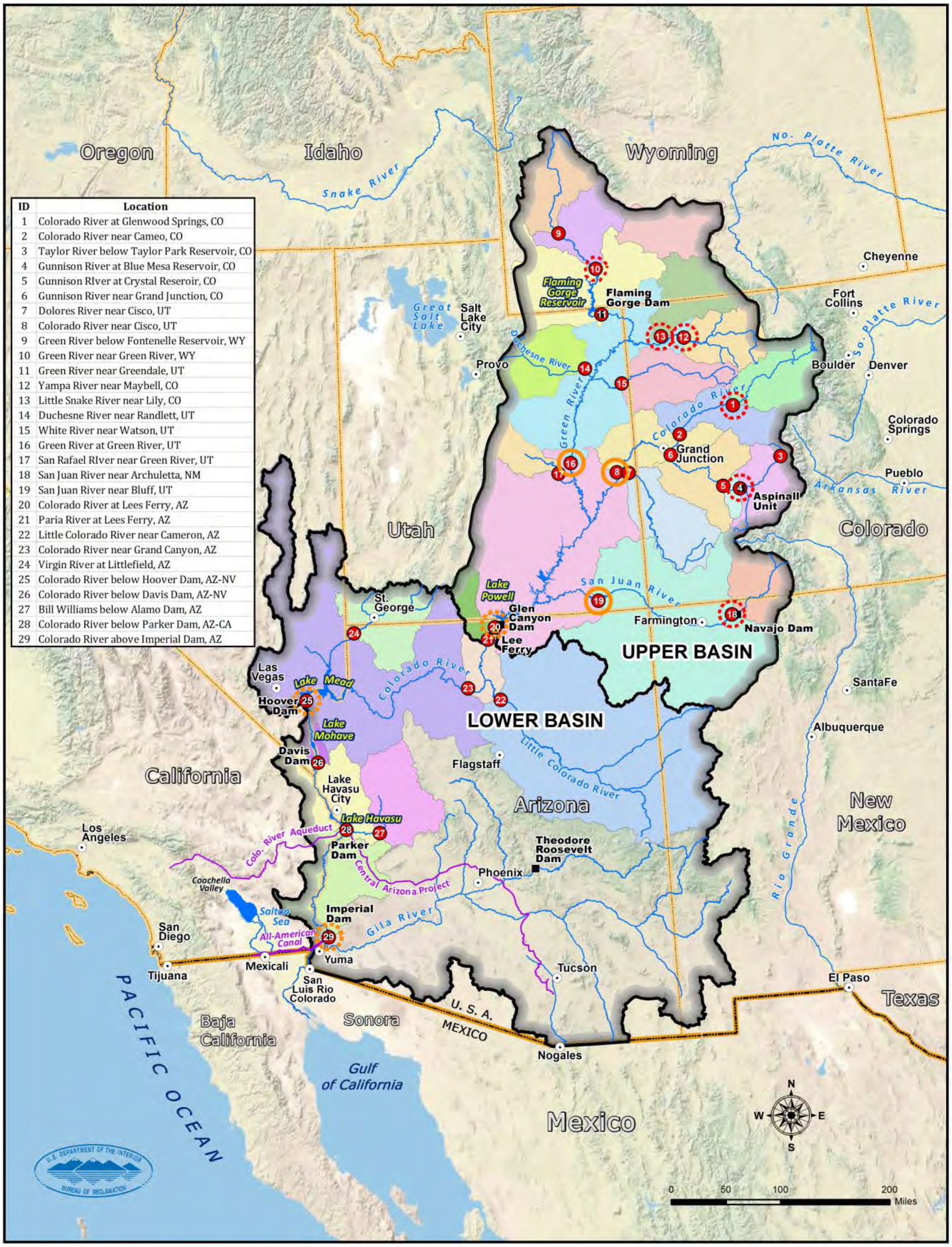

3.2 Sources of Data and Information

An extensive review of relevant literature, water supply studies, and hydroclimatic data was performed as part of the Water Supply Assessment. The Basin supply has been studied by numerous researchers, and a wealth of information is available, including several recent studies directly relevant to the Study. Relevant hydroclimate data were collected throughout the Water Supply Assessment, with particular emphasis on gridded climate data sets and natural flows for the 29 natural flow locations in the Basin.

3.2.1 Literature Review

Due to its strategic importance as a source of water for the western United States, the Colorado River is one of the most studied river systems in the world. The Basin water supply has been assessed using a variety of hydrologic analyses for many decades, but efforts accelerated in the 1990s with the availability of GCMs and observed increased streamflow variability (Pagano and Garen, 2005). Reclamation published an extensive literature review of Colorado River climate and hydrology studies in appendix U of the 2007 Interim Guidelines Final EIS (Reclamation, 2007). This appendix summarizes the state of the science in 2007. In 2011, Reclamation's Technical Service Center published a second edition of the *Literature Synthesis on Climate Change Implications for Water and Environmental Resources* (Reclamation, 2011b) that summarizes relevant research through the summer of 2010. Provided below is a brief summary of past efforts and research that were used to assess Basin supply.

- The following studies: Gleick (1987); Nash and Gleick (1991, 1993); Hamlet and Lettenmaier (1999); McCabe and Wolock (1999a, 1999b); and Wilby et al. (1999) discuss climate change impacts on the hydrology and water resources of western U.S. river basins. All these studies assume or predict increasing temperatures, but disagree about both the magnitude and direction of precipitation changes.

- Nash and Gleick (1991) evaluate prescribed changes of +2 degrees Celsius (°C) and +4 °C, coupled with precipitation reductions of 10 and 20 percent. The 2 °C increase per 10 percent precipitation decrease resulted in a 20 percent streamflow reduction, while the 4 °C increase per 20 percent precipitation decrease resulted in a 30 percent runoff decrease.

- Christensen et al. (2004) project average temperature increases of 1.0 °C, 1.7 °C, and 2.4 °C, and precipitation decreases of 3, 6, and 3 percent for the Basin for the periods 2010 to 2039, 2040 to 2069, and 2070 to 2099, respectively, relative to the period 1950 to 1999 means. The temperature and precipitation changes lead to reductions of April 1 SWE of 24, 29, and 30 percent, and runoff reductions of 14, 18, and 17 percent for the three periods.

- Updated analyses by Christensen and Lettenmaier (2007) using a larger ensemble of climate projections, result in smaller mean projected reductions in Lees Ferry flows (less than 11 percent).

- Hoerling et al. (2009), in an attempt to reconcile streamflow estimates by several researchers, summarize the recent hydroclimatic analyses of the Basin and find that the projections range from a 5 to 20 percent reduction in streamflow by 2050.

- A recently released *Colorado River Water Availability Study* (Colorado Water Conservation Board, 2010) focuses on the State of Colorado's hydrometeorological contribution to the

Colorado River system. The study describes the tools available to simulate river hydrology, agricultural demands, water allocation, and decision support.

- Several papers in a special issue of the *Proceedings of the National Academy of Sciences* on climate change and water in southwestern North America (Sabo et al., 2010) focus on the climate and water supply in the Basin. Cayan et al. (2010) provide an analysis of the current Colorado River drought and suggest that, although the current drought is exceptional in the observed record, future droughts in the Basin may be more severe and longer in duration. Woodhouse et al. (2010) provide the 1,200-year perspective on Southwestern drought, draw linkages of warming to paleo drought severity, and place the drought in context with the medieval period worst-case drought. Seager and Vecchi (2010) attribute the current and future Southwest drying to a broader expansion of the Hadley cell that causes storms to track farther north. It is important to note that the latter study (Seager and Vecchi, 2010) suggests decreases in winter (October through March) precipitation, although many other studies (including Cayan et al., 2010) suggest increases during this same period for much of the Basin. It is not clear whether this discrepancy is due to the large domain (southwest North America, from southern Mexico to the Oregon-California border and from the Pacific Ocean to the High Plains) that is being averaged, or due to the lack of regional/local spatial resolution of the GCM-based information.
- Das et al. (2011) further evaluate the effect of seasonal differences in warming on Colorado River streamflow changes. The Intergovernmental Panel on Climate Change (IPCC) Fourth Assessment Report group of climate models indicates that climate warming over the Basin may be greater in summer than in winter. Das et al. (2011) find that annual Colorado River streamflow is more sensitive to warm season (April through September) warming than cold season warming (October through March), and is the most sensitive of the four western river basins evaluated. A 3 °C warming in the warm season results in a 13.3 percent reduction in annual flow, while the same warming applied during the cool season results in an annual flow reduction of only 3.5 percent. Climate warming, especially if amplified in summer as projected, may drive significant reductions in available supply, even if there is no reduction in precipitation.

Common to nearly all this research is the projection of continued and accelerated warming in the Basin and very likely increases in the severity of future droughts. However, the research suggests continued uncertainty in projections of the magnitude and direction of potential future changes in annual precipitation. Effective treatment of this uncertainty is important in making credible estimates of future water supply.

3.2.2 Data Sources

The Water Supply Assessment relied on a variety of peer-reviewed datasets collected by Reclamation, other recognized federal sources, and hydrologic modeling results obtained from Reclamation’s West-Wide Climate Risk Assessment study (Reclamation, 2011c). The data sources and methods are described further in subsequent sections of this report and a complete listing is collectively included in appendices B2, B3, and B4.

4.0 Historical Supply

An assessment of the Basin's historical climate and hydrology is critical for a robust understanding of the projected changes associated with each of the four future water supply scenarios. For this reason, an assessment of the historical supply of the Basin is first presented. This presentation begins with a discussion of the methods used to perform the assessment, followed by the results for the four groups of water supply indicators: climate, hydrologic processes, climate teleconnections, and streamflow.

4.1 Methods

Historical daily temperature and precipitation data for 1950 to 2005 (Maurer et al., 2002[3]) were processed into average temperature and total precipitation for each month and year of the period. Monthly, seasonal, and annual statistics were computed for each grid cell (1/8th-degree resolution, or about 12 kilometers [km]) of the gridded meteorological dataset for the 1971 to 2000 historical period to represent the historical climatology and compare to future projected climates. The historical dataset was derived from individual NOAA Cooperative Observer station observations and gridded to the 1/8th-degree using mapping algorithms that account for station elevation, orographic effects, and other characteristics (Maurer et al., 2002).

Climate is defined by the World Meteorological Organization (2011) as the "average weather," or a statistical description in terms of the mean and variability of variables such as temperature, precipitation, and wind. Climate change is the shift in the long-term weather statistics, or trend, that a region experiences. Thus, climate change cannot be represented by single annual events or individual anomalies. That is, a single large flood event or particularly hot summer is not an indication of climate change, although a series of floods or warm years that statistically change the average precipitation or temperature over time may indicate climate change. The World Meteorological Organization recommends the use of a 30-year period for evaluating climate. At the time the Study was initiated, the established 30-year climatological period as described by NOAA (2011) was the 1971 to 2000 historical period. This period was used in the study to define the historical base climate. While NOAA has recently updated its climatological period to 1981 to 2010, climate and hydrologic information from various sources were not available at the time required to support this assessment for the Basin.

The historical climatological period allows for the averaging of individual year and multi-year variability over a longer period to capture the average conditions. A longer period could have been selected as the historical base period, but ensuring consistency with NOAA's period definition, and establishing a period consistent with tracking future changes (desire to estimate future changes for similar 30-year time slices), were considered important to define time-varying changes in this analysis. The seasons are defined as follows: Fall (October, November, and December); Winter (January, February, and March); Spring (April, May, and June); and Summer (July, August, and September).

Historical hydrologic parameter data were generated by the Variable Infiltration Capacity (VIC) model for the period 1950 to 2005. The VIC model (Liang et al., 1994; Liang et al., 1996; Nijssen et al., 1997) is a spatially distributed macro-scale hydrologic model that solves the water balance at each model grid cell. The VIC model is populated with the historical temperature and

[3] Subsequent to Maurer et al. (2002), the climate dataset was extended to 2005 using identical methods.

precipitation data to simulate historical hydrologic parameters (Maurer et al., 2002). Appendix B4 provides details on the VIC model and its application in the Study. The simulated hydrologic parameters include ET, runoff (surface runoff), baseflow (subsurface runoff), soil moisture (in each of three soil layers), and SWE. Representative statistics describing these parameters were generated on monthly, seasonal, and annual bases. The statistical analysis was conducted on both grid cell and watershed bases. The results of the grid cell analysis produce the most informative map graphics and clearly show spatial variation at the greatest resolution possible, while the watershed basis provides an aggregate graphic of the variation across a natural flow station's watersheds.

Climate teleconnections were analyzed first by selecting indices that could have potential influence in streamflow changes for the Basin. Published research (such as Redmond and Koch, 1991; Diaz and Kiladis, 1992; and McCabe et al., 2004) indicates that the strongest correlations with Basin flows were observed with the ENSO and PDO indices. For ENSO, data were collected for both the ocean component (sea surface temperature anomalies) and the atmospheric component (sea level pressure anomalies). The sea surface temperature anomalies indicate the relative temperature state of the tropical Pacific Ocean as compared to normal (warm phase indicating El Nino conditions), while the sea level pressure anomalies are one measure of large-scale fluctuations in air pressure occurring between the western and eastern tropical Pacific. The two components are highly correlated and, combined, describe ENSO. The Southern Oscillation Index (SOI) was the primary dataset used in the Study to describe ENSO due to the longer period of data availability. The PDO indicates the longer-term (about 15 to 25 years) oscillation of the north Pacific Ocean sea surface temperatures. The PDO index, which indicates the warm or cool phase of the sea surface temperatures, has been linked to decadal-length period of above average or below average precipitation and was used directly in this assessment. The quantitative teleconnections analysis was based on the SOI and the PDO indices.

Only a qualitative discussion of the AMO is included in this report. For additional information pertaining to indices' choice, refer to appendix B2.

Annual average values for the SOI were computed using different annual windows. The average SOI presented in the Study refers to the June through November period, which was identified as a strong indicator of ENSO events (Redmond and Koch, 1991). Once the SOI averages were computed, ENSO events were determined by years where the averaged SOI was below -1 (classified as an El Niño year) or above 1 (classified as a La Niña year). Annual averages of the PDO on a water year basis were calculated and compared with the same water year annual flows. A warm PDO was defined as a value greater than or equal to 0.0 and a cold PDO was a PDO value less than 0.0.

Two historical streamflow data sets, the observed record spanning the period 1906 to 2007, and the paleo reconstructed record spanning the period 762 to 2005 (Meko et al., 2007), were used in the Study to characterize historical streamflow patterns and variability. Period comparisons were made between the full extent of the data and a more recent period. For the observed dataset spanning 1906 to 2007, the second comparison period (1978 to 2007) was selected as the most recent 30-year period. For the paleo dataset spanning 762 to 2005, the second comparison period was selected as 1906 to 2005 so that direct comparisons could be made of the observed and paleo timeframes.

4.2 Results

4.2.1 Climate

The Basin contains climate zones ranging from alpine to desert and is fundamentally influenced by climate variability from seasonal to millennial scales (National Research Council [NRC], 2007). The Basin water supply, as is typical in many western river systems, strongly depends on snowmelt from high elevation portions (figure B-4) of the Upper Basin, with about 15 percent of the watershed area producing about 85 percent of the entire Basin's average annual runoff. Annual precipitation ranges from 84 millimeters (mm) (less than 4 inches) in southwestern Arizona to nearly 1,600 mm (63 inches) in the headwaters of Colorado, Utah, and Wyoming, as shown in figure B-5. Average temperatures vary considerably by season, Basin location, and elevation, as also shown in figure B-5. Warmest temperatures are seen in the southwestern Arizona summer and coolest in the headwaters during the winter.

The climate of the Basin exhibits important spatial and seasonal variability. To illustrate this variability, figure B-6 shows monthly average temperature and precipitation as watershed averages for the areas immediately upstream of the Colorado River near Glenwood Springs (Colorado), Colorado River at Lees Ferry (Arizona), and Colorado River above Imperial Dam (Arizona/California). These three locations reflect a coarse transect of the Basin from the headwaters to Imperial Dam.

As illustrated in figure B-6, the average temperature varies by more than 20 °C seasonally at each of the three locations and similarly across the Basin within seasons. Cool winter temperatures at the higher elevation portions of the Upper Basin cause much of the precipitation to fall in the form of snow. At lower elevations, warmer conditions exist and liquid precipitation is the dominant form. For most regions, the majority of the precipitation occurs in the cool season (fall and winter). Warmer temperatures in the spring and summer induce snowmelt at the higher elevations, and storms tend to be shorter and more intense. The summer precipitation does not contribute a significant portion of the Basin annual total. In the southwest portions of the Basin (Arizona, California, and Nevada), summer precipitation is locally important. The North American monsoon season plays a significant role in bringing moisture from the sub-tropical Pacific and Gulf of California and causes intense summer storms in the southwestern desert. The monsoon influence extends into Upper Basin states as well and can contribute to significant summer precipitation in New Mexico, Utah, and Colorado.

FIGURE B-4
Colorado River Basin Elevation (feet above mean sea level)
Derived from National Elevation Dataset, USGS, (HTTP://NED.USGS.GOV).

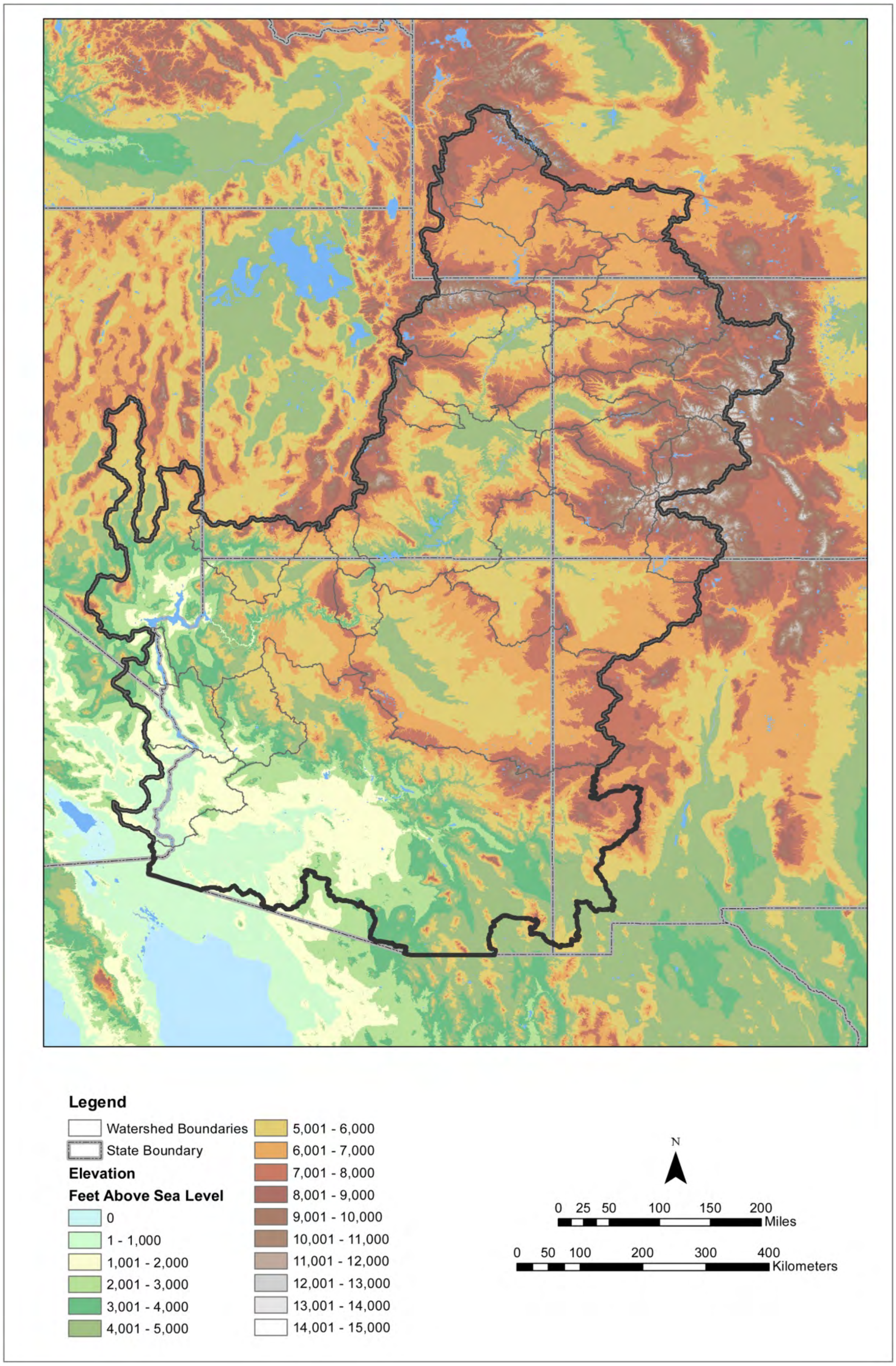

FIGURE B-5
Average Annual Temperature (°C) and Average Annual Precipitation (mm) for the Period 1971–2000
Derived from Maurer et al., 2002.

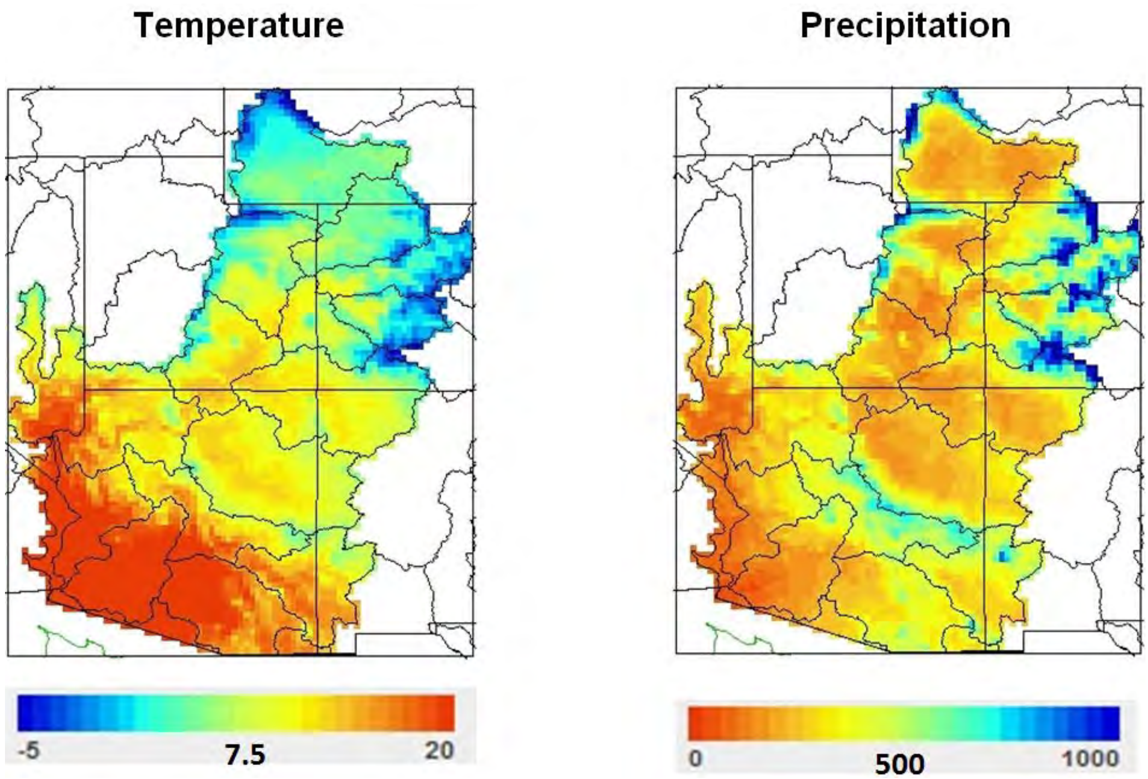

FIGURE B-6
Monthly Average Temperature and Precipitation for Three Representative Locations in the Colorado River Basin
Derived from daily gridded observed meteorology (Maurer et al., 2002) and averaged for the local watershed immediately upstream of the indicated point.

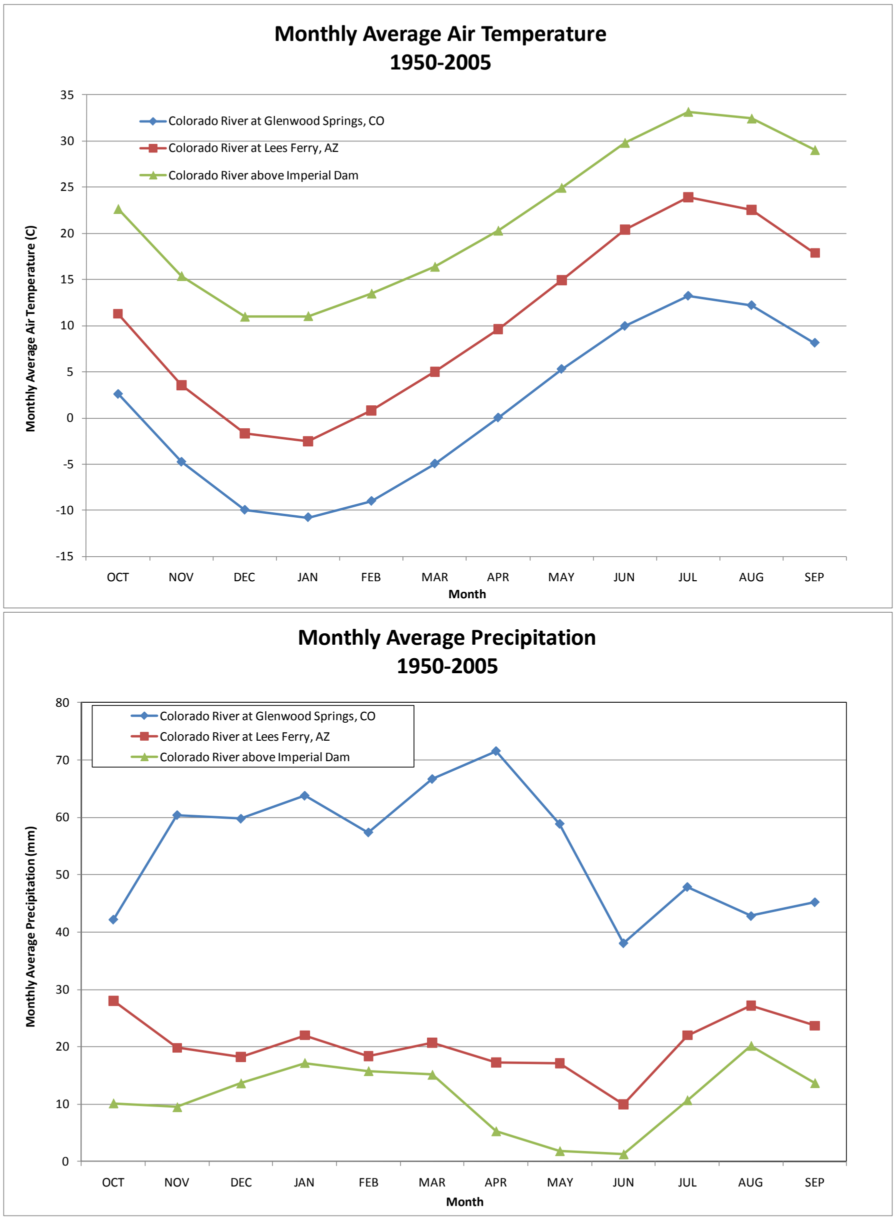

Trends in temperature and precipitation for the Basin have been studied by Groisman et al. (2001), McCabe et al. (2002), Piechota et al. (2004), Hamlet et al. (2005), Pagano and Garen (2005), Regonda et al. (2005), Andreasdis et al. (2006), Fassnacht (2006), Mote (2006), Christensen and Lettenmaier (2007), and several others. Long-term trends are summarized in the 2007 NRC summary report on hydroclimatic variability in the Basin (NRC, 2007). The long-term annual temperatures and precipitation amounts from the period 1895 to 2005 are shown in figure B-7. A significant increase in temperature is apparent in this figure, although periods of cooling have occurred historically. Most important is the warming trend that has occurred since the 1970s. This warming trend is also seen in the Upper and Lower Basins and with observed North American and global trends.

Annual precipitation shows substantial variability and periods of dry and wet spells. Most notable in the precipitation record is the lack of a significant long-term annual trend, yet the annual variability appears to be increasing. Both the highest and lowest annual precipitation years appear in the most recent 30-year record.

FIGURE B-7
Annual Average Surface Air Temperature for the Colorado River Basin, 1895–2005 (top); and Annual Water Year Average Precipitation for the Colorado River Basin above Lees Ferry, Arizona (bottom)
Red lines show annual values; blue lines show the 11-year running mean. Source: NRC (2007) and Western Regional Climate Center.

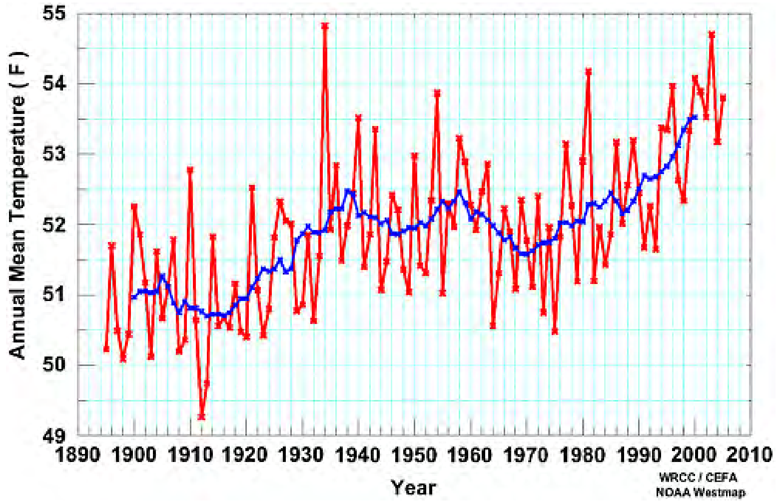

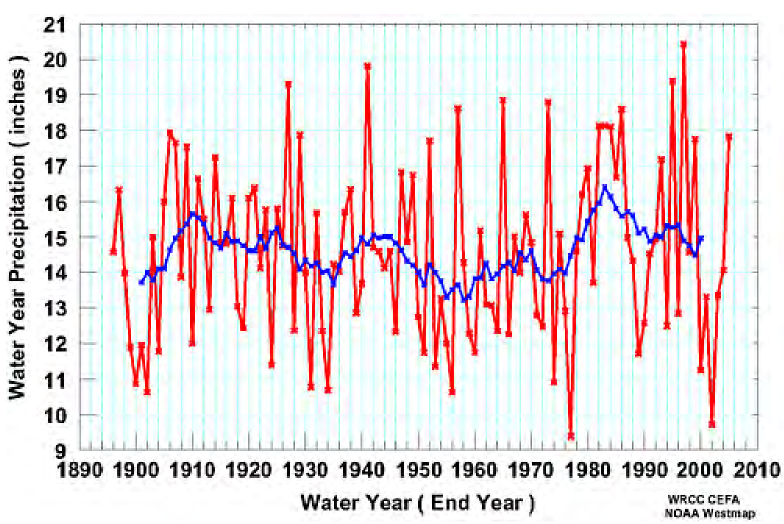

A 2008 publication by Miller and Piechota summarizes Basin temperature, precipitation, and streamflow trends and also examines the possibility that a “step change” in these parameters occurred during the mid 1970s. The step-change time series data were divided into the first 24 years of data (1951 to 1974) and the later 31 years of data (1975 to 2005) for temperature and precipitation datasets. Miller and Piechota (2008) find that increasing temperature trends and step changes were observed consistently throughout the year, often times at greater than a 95 percent confidence level. Temperature trends were most significant in the first quarter of the year, January through March. Precipitation trends and step changes were not as evident as those for temperature. An increasing precipitation trend was observed January through March, but not at all stations and not significant for other months.

4.2.2 Hydrologic Processes

The hydrologic processes that describe the interaction between climate and the watershed landscape are critically important in determining water availability and the manner in which the Basin response may change under future climate. The regions of greatest precipitation in the Basin are those at high elevation in the headwaters of the Green, Colorado, and San Juan Rivers. Due to cold temperatures, these areas accumulate substantial snowpack that is critical to the Basin supply. Figure B-8 provides an estimate of the average spatially distributed April 1 SWE for the period 1971 to 2000 derived from a historical simulation of the VIC hydrology model. Important in this figure is the relatively small portion of the watershed that offers significant seasonal water storage in the form of snowpack. Although snow falls in other portions of the Basin, temperatures are generally not sufficiently cold to retain the snowpack for any great length of time. The remainder of this lower elevation portion of the watershed is primarily dominated by rainfall.

One way to synthesize many complex hydrologic processes at the watershed scale is to introduce the concept of runoff efficiency. Runoff efficiency is a measure of the effectiveness of a particular watershed in converting precipitation into runoff. Watersheds with very high runoff efficiencies dominate the overall contribution toward streamflow and have relatively lower losses. Watersheds with low runoff efficiencies have high losses and tend to be dominated by infiltration to soil moisture and consumptive use through ET. ET is the sum of evaporation from the land surface and plant transpiration. As can be seen in figure B-8, the watersheds with the highest efficiencies are the headwaters of the Colorado, Green, and San Juan Rivers. These watersheds are able to convert about 20 to 30 percent of the precipitation into runoff and baseflow; however, even in the headwater regions there is considerable variability in runoff efficiencies, with some values less than 10 percent. In the Lower Basin, average runoff efficiencies are all less than 10 percent and many watersheds have runoff efficiencies less than 5 percent. The runoff efficiency Basin-wide is about 12 percent.

ET is the dominant hydrologic flux on the annual scale, consuming more than 70 percent of the precipitation supply. As can be seen in figure B-8, ET is highest in regions with greatest precipitation. This is not to say that the ET demand is highest in these regions, but rather that ET tends to be supply-limited in the Basin. The ET demand (potential ET [PET]) is actually higher in the warmer climate of the Lower Basin, but water supply in the form of soil moisture is less and what is available is depleted earlier than in the Upper Basin watersheds.

FIGURE B-8
Estimated Average Annual ET and Runoff (mm), April 1 SWE (mm), and Annual Average Runoff Efficiency (fraction of precipitation converted into runoff) for 1971–2000
Derived from historical VIC simulations.

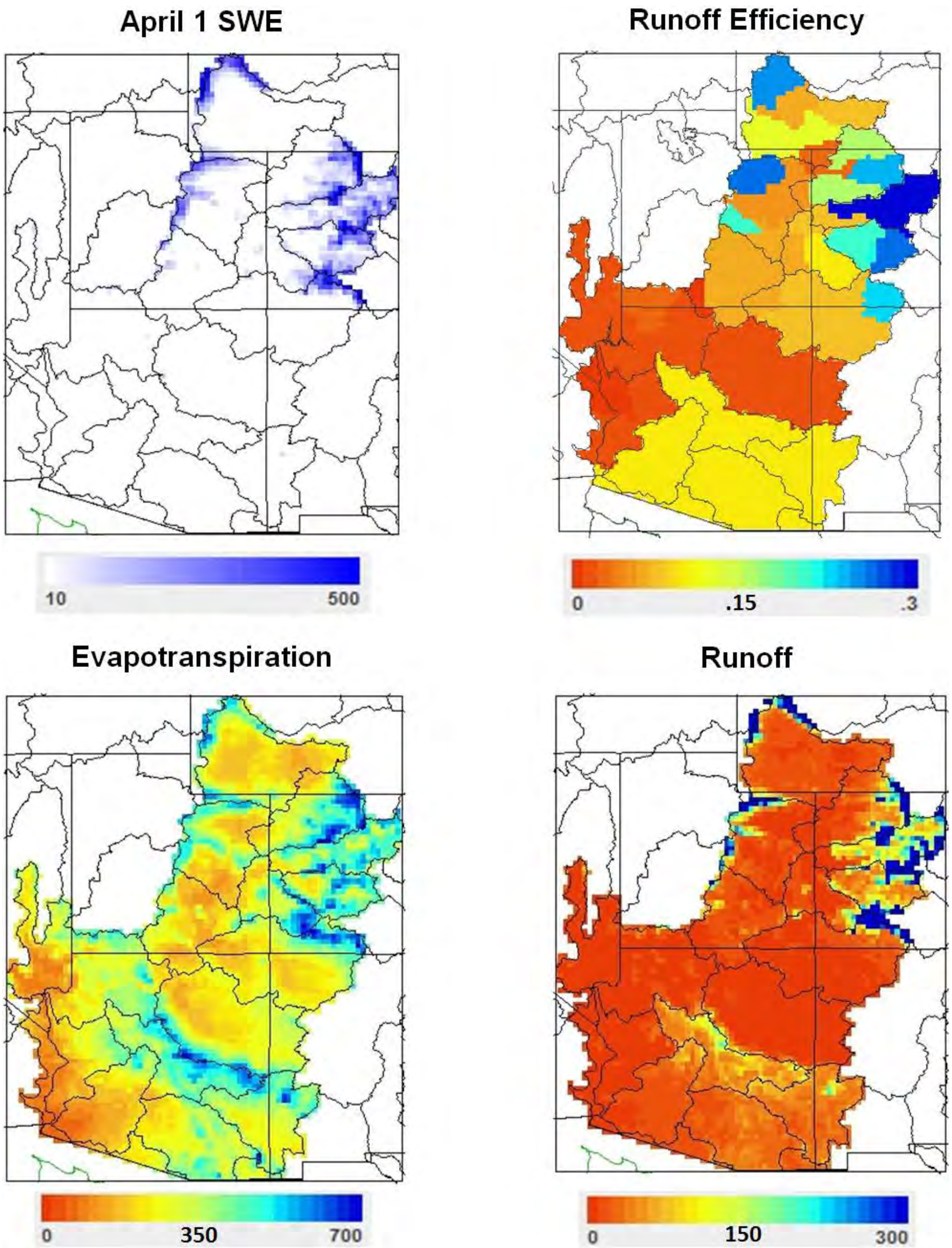

Previously published research was relied on to assess observed snowpack trends in the Basin. Research by Mote (2003), Mote et al. (2008), Clark et al. (2001), Cayan et al. (2001), and Pederson et al. (2011) indicate a general decline in April 1 SWE for Pacific Northwest and northern Rocky Mountain locations, and increases in parts of the Great Basin and southern Rockies, as shown in figure B-9.

FIGURE B-9
Left panel: Linear Trends in April 1 SWE at 594 Locations in the Western United States and Canada, 1950–2000 (Mote et al., 2008) (Negative trends are shown by open circles, positive by solid circles.)
Right panel: April 1 SWE Trends (1950–2000) Plotted against Elevation of Snow Course (Mote et al., 2008) (Units on y-axis are incorrectly labeled by author as mm and should be meters.)

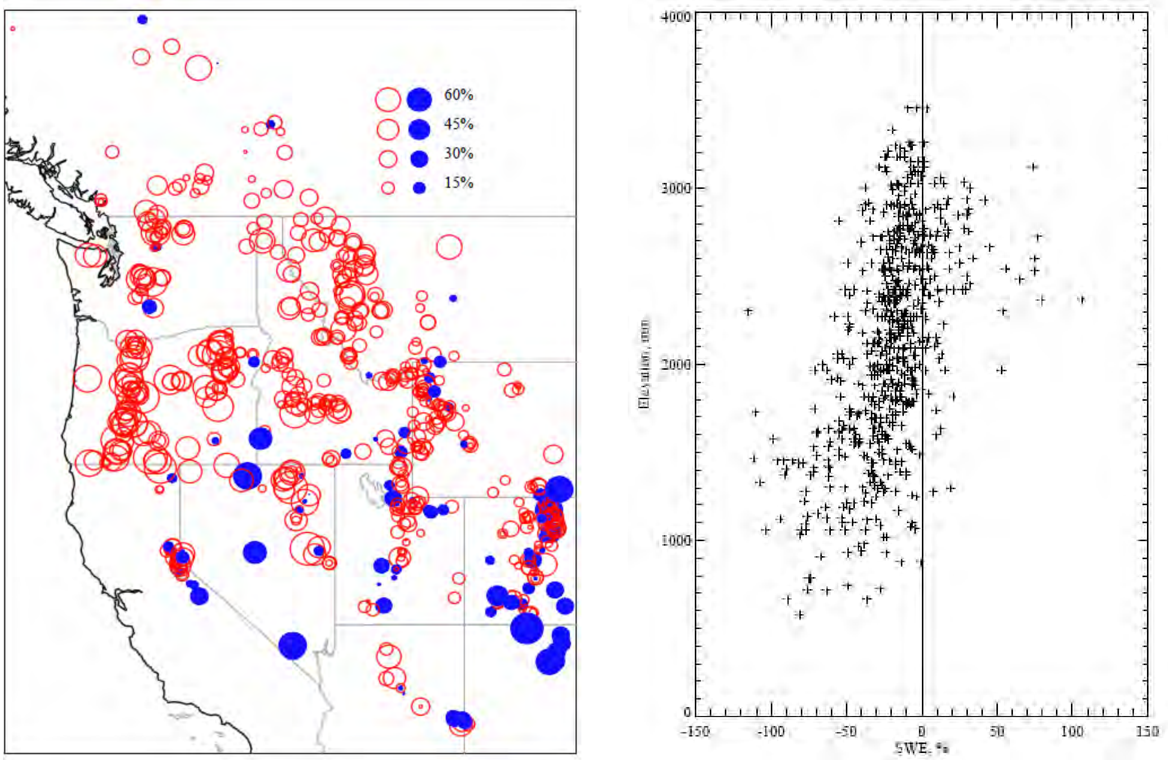

Widespread decreases in springtime snowpack are observed with consistent results across the lower elevation northern latitudes of the western United States. The high-elevation and thus cooler Rockies do not consistently produce decreasing trends for SWE. To assess the vertical characteristics of SWE, Mote plotted April 1 SWE trends (1950 to 2000) against elevation of snow course (figure B-9). Losses of SWE tend to be largest at low elevations and strongly suggest a temperature-related effect.

Finally, Mote et al. (2008) used the VIC model to simulate SWE accumulation and depletion for western U.S. basins. From this analysis, it was clear that changes in SWE are not simply linear, but fluctuate on decadal time scales. SWE was estimated to have declined from 1915 to the 1930s, rebounded in the 1940s and 1950s, and despite a peak in the 1970s, declined since mid-century.

Additionally, recent research demonstrates dust-on-snow events have the ability to alter the timing and magnitude of runoff (Painter et al., 2010). Dust-on-snow events reduce snow albedo, or reflectivity, thereby increasing the solar radiation that reaches and warms the snow, potentially contributing to changes in timing of snowmelt and seasonal streamflows.

4.2.3 Climate Teleconnections

Research indicates a relationship between Pacific Ocean climate indices and Basin streamflow (Redmond and Koch, 1991; Webb and Betancourt, 1992; Cayan et al., 1999; Mo et al., 2009; and others). The June through November SOI is identified by Redmond and Koch (1991) as a strong indicator of ENSO events. For the Study, relationships between the PDO and ENSO and natural flows in the Upper Basin were examined. Figure B-10 presents the annual PDO index and indicates when June through1 November SOI average values are below -1.0 or above 1.0. The solid red bars indicate a positive PDO index, or warm PDO phase, while the solid blue bars indicate the cold PDO phase. The light red and blue shading indicate the SOI condition. Evident in this figure is the low frequency phasing of the PDO (multi-decadal scales) and the significant year-to-year variability in the ENSO events. Indicated by the line on this figure is the 11-year, center-weighted annual flow departure from long-term mean for the Colorado River at Lees Ferry, Arizona. Correlation between the low frequency PDO and decadal scale Colorado River flows appears prominent since the mid-1940s with lower decadal-scale flows during cool PDO phases and higher flows during warm PDO phases. However, significant variability exists even at these scales and prior to the mid-1940s, the correlation is poor.

There are other climate teleconnections that appear to influence multi-decadal variations in precipitation patterns (e.g., AMO) and others that can modify the characteristics of seasonal precipitation (e.g., Madden-Julian Oscillation and Arctic Oscillation) (Becker et al., 2011; Bond and Vecchi, 2003; Hu and Feng, 2010). The understanding of the influence of these teleconnections on the Colorado River precipitation, and their usefulness as an indicator, is still evolving.

FIGURE B-10
Plot of Water-Year Average PDO Values and ENSO Events Defined by SOI Averages for the Period June–November

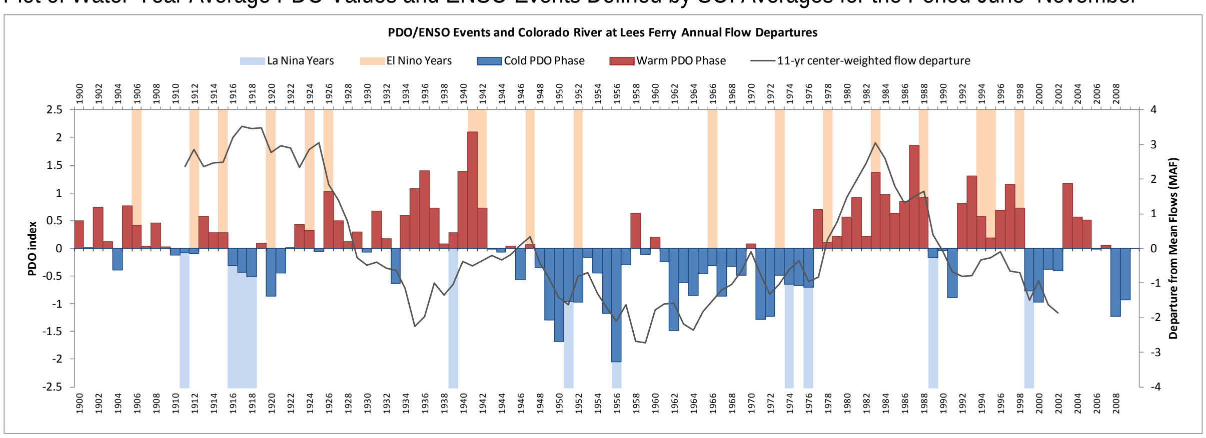

Figure B-11 illustrates water year departure from median streamflows in percent during warm and cold PDO and ENSO periods sampled from the period 1906 to 2007 for Upper Basin natural flow locations. The red bars indicate the streamflow departures for the warm phase of PDO (top) and ENSO (bottom), while the blue bars reflect the departures during the cool phases. Although significant streamflow variability exists from year to year, the majority of the flows are higher than normal during the warm PDO and ENSO (El Niño) phases. Conversely, the majority of the flows are lower than normal during the cool PDO and ENSO (La Niña) phases. It should be noted that the PDO and ENSO relationship is essentially inverted for the northern Basin in Wyoming (Green River Basin) where flows tend to be higher during the cool PDO and ENSO (La Niña) phase. The dividing line separating typical ENSO influence varies considerably from year to year, but is often referred to as a line from San Francisco to Cheyenne (Edwards and Redmond, 2005).

Overall, the natural inter-annual variability in streamflow tends to be more dominant than the relationships to either ENSO or PDO. ENSO has considerably more skill (strength as a predictor of seasonal precipitation or streamflow) in the coastal watersheds of the Pacific, than over the Basin. PDO, on the other hand, is a low-frequency signal (multi-decadal scale) that limits the number of events that could be correlated. However, it is important to note that in 2011 to 2012 the climate was entering a strong combined cool phase of both ENSO and PDO. The alignment of both signals in the cool phase suggests a propensity for continued drying trends in the coming years. The ability to predict the future state of PDO, however, is limited at this time.

FIGURE B-11
Median Change in Flows from Long-term Average for Warm and Cold PDO (top) and ENSO (bottom) Years

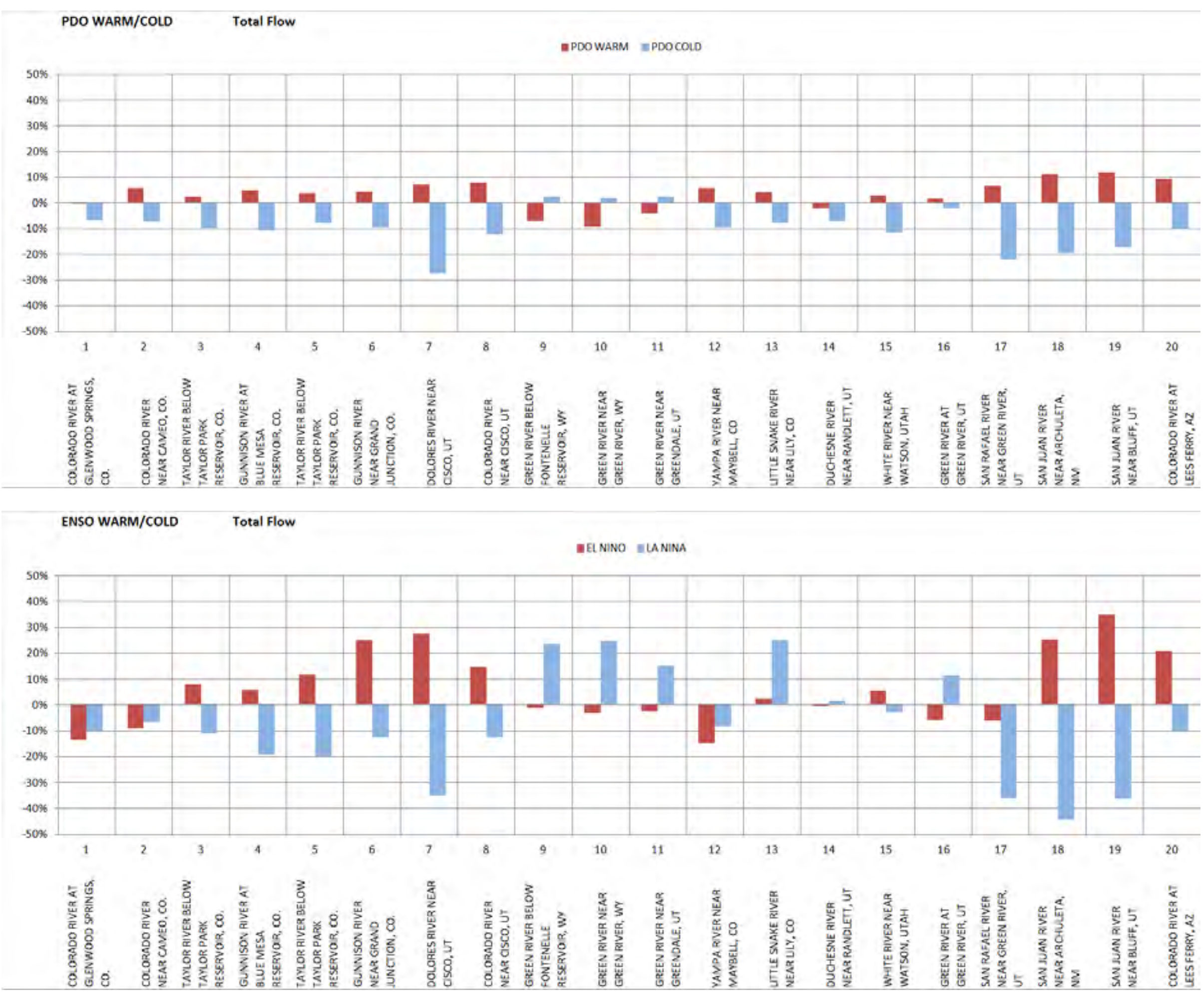

4.2.4 Streamflow

Analysis of streamflow records for the 29 natural flow locations indicated that about 92 percent of the total Colorado River at Imperial Dam, Arizona natural flow is contributed by runoff upstream of Lees Ferry, Arizona (figure B-12). As shown graphically in figure B-12, the Green River contributes about 33 percent of the total natural flow, the Colorado River at Cisco, Utah about 42 percent, and the San Juan River about 13 percent based on long-term annual natural flows from 1906 to 2007. Due to the importance of these rivers to the overall supply, they were selected as key locations for historical assessment. In addition, the Colorado River at Lees Ferry, Arizona is used because approximately 92 percent of the Basin natural flow (measured at Imperial Dam, Arizona) has accumulated there.

FIGURE B-12
Colorado River Basin Average Annual Natural Flow Contribution (% of total) for each of the 29 Natural Flow Locations
Streamflow derived from the observed period (1906–2007). See figure B-2 for names of locations.

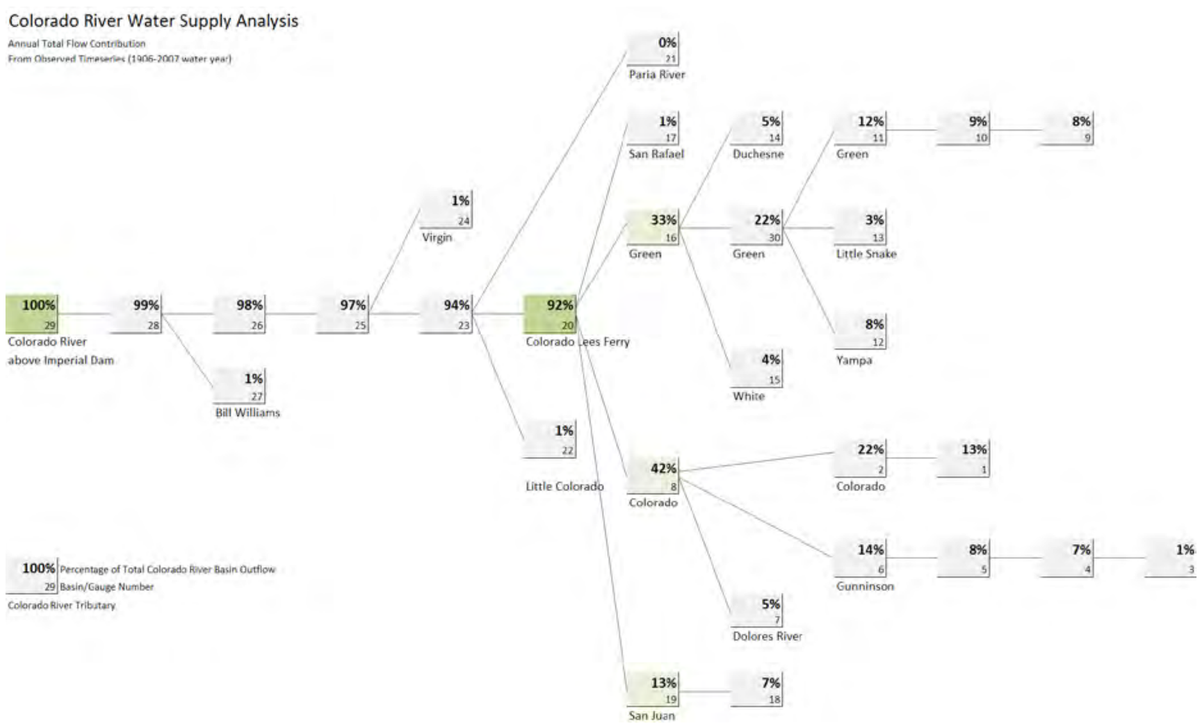

The mean annual flows for 1906 to 2007 at each of the 20 Upper Basin natural flow locations are shown in figure B-13. Also shown is the variability of annual flows as “box-whisker” ranges. The mean annual flow of the Colorado River at Lees Ferry, Arizona (location 20) is approximately 15.0 million acre-feet (maf), but ranged from 5.6 maf (1977) to 25.2 maf (1984) over this period. The upper Colorado River at Cisco, Utah (location 8), Green River at Green River, Utah (location 16), and San Juan River at Bluff, Utah (location 19) have mean annual flows of 6.8 maf (ranging from 2.6 to 12.6 maf), 5.4 maf (ranging from 1.9 to 5.3 maf), and 2.1 maf (ranging from 0.5 to 4.5 maf), respectively.

FIGURE B-13
Upper Basin Average Annual Total Natural Flows
kaf/yr = thousand acre-feet per year
Box represents the 25th, 50th, and 75th percentiles; whiskers represent the maximum (max) and minimum (min), and triangle represents the mean flow. Streamflow derived from the observed period (1906–2007).

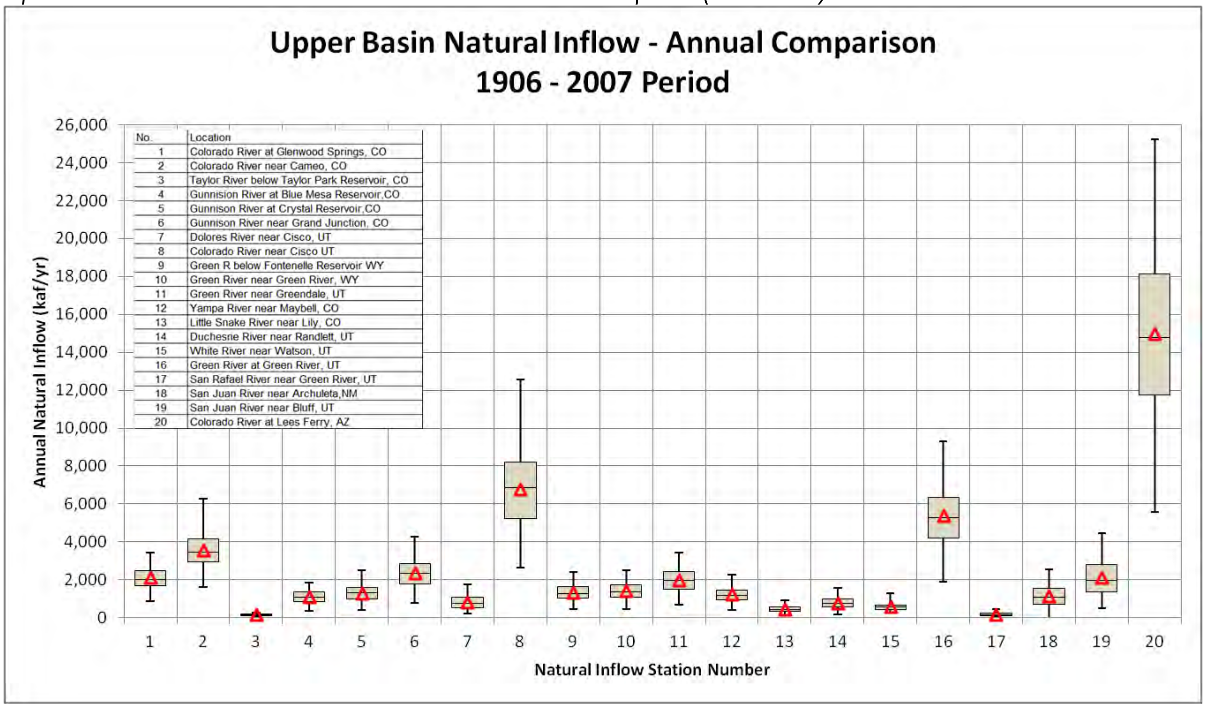

Streamflow analysis summaries (snapshots) were prepared for all 29 natural flow locations to evaluate the trends and variability of flows. Four snapshot summaries are presented in this report for the following key locations: Colorado River near Cisco, Utah (location 8); Green River at Green River, Utah (location 16); San Juan River near Bluff, Utah (location 19); and Colorado River at Lees Ferry, Arizona (location 20). Additional streamflow analysis figures for each of the major contributing flow locations are included in appendix B5. This supplemental material includes a table reporting specific monthly streamflow averages, annual averages including minimum and maximum values with the years they occurred, and a more-detailed analysis of deficit/surplus periods.

The snapshot results were developed from the natural flows dataset using data for water years 1906 to 2007 (figures B-14 to B-17). The top plot in each figure shows the annual flow volumes and the moving averages for 3, 5, and 10 years. This plot provides a visual assessment of streamflow variability, minimum and maximum flows, and long-term trends. For most selected locations, greater variability and more frequent events of greater magnitude are observed after 1976. Generally lower flows are observed from the mid 1930s to mid 1960s and a slightly downward trend in flows is observed in all locations for this time period. As an example, the Colorado River at Lees Ferry, Arizona plot (figure B-14) shows a period of generally below average streamflow and a period of moderate variability for the period 1930 to 1976. Beginning in 1977, streamflow amplitude and variability increased, with a decrease in streamflows in the most recent two decades. These recent changes in streamflow are attributed, in part, to shifts in the atmospheric-oceanic conditions as represented by PDO and ENSO and hydrologic response to recent warming.

FIGURE B-14
Colorado River at Lees Ferry, Arizona Natural Streamflow Snapshot Analysis

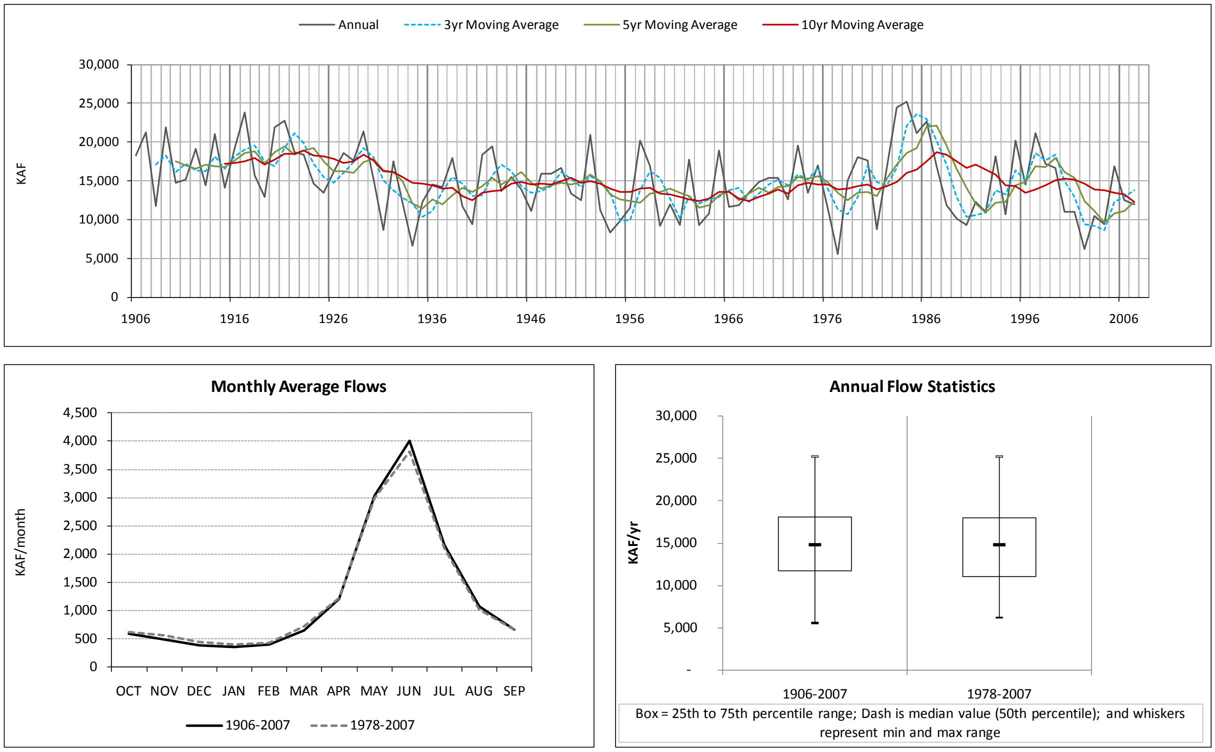

The bottom left plot shows a two-period comparison of monthly average streamflow. The first period spans 1906 to 2007, while the second period captures the more recent 30-year period, 1978 to 2007. For the period 1978 to 2007, all selected locations exhibit a reduction in late spring streamflows and a slight increase in winter streamflows when compared to the long-term (1906 to 2007) averages. The annual mean flow was slightly lower at most of the Upper Basin locations during the 1978 to 2007 period, while annual variability, based on the inter-quartile (25th to 75th percentile) range of flows, was higher during this period. The mean annual flow for the 1978 to 2007 period is 14.6 maf—about 3 percent lower than the 1906 to 2007 period mean annual flow of 15.0 maf. The increase in variability can be explained largely by the two significant high-flow periods (the early-mid 1980s and the late 1990s) and the recent extended drought conditions during this period. The two periods show similar maximums and minimums for the 1-, 3-, and 5-year averages because the annual flow extremes (both high and low) have mostly occurred in the most recent 30-year period and are thus represented in both periods (the most recent period is also included in the long-term period).This finding is consistent with precipitation trends that show increased variability in the recent period. However, these changes are not universal. For example, the Colorado River at Cisco, Utah station shows an increase in variability in the more recent period, and also a slight increase in annual mean flow. Conversely, the San Juan River near Bluff, Utah station shows a lower mean flow, but a slightly lower variability in the recent period as compared to the longer 1906 to 2007 period. The two highest flows at this location occurred in 1941 and 1973.

FIGURE B-15
Green River at Green River, Utah Natural Streamflow Snapshot Analysis

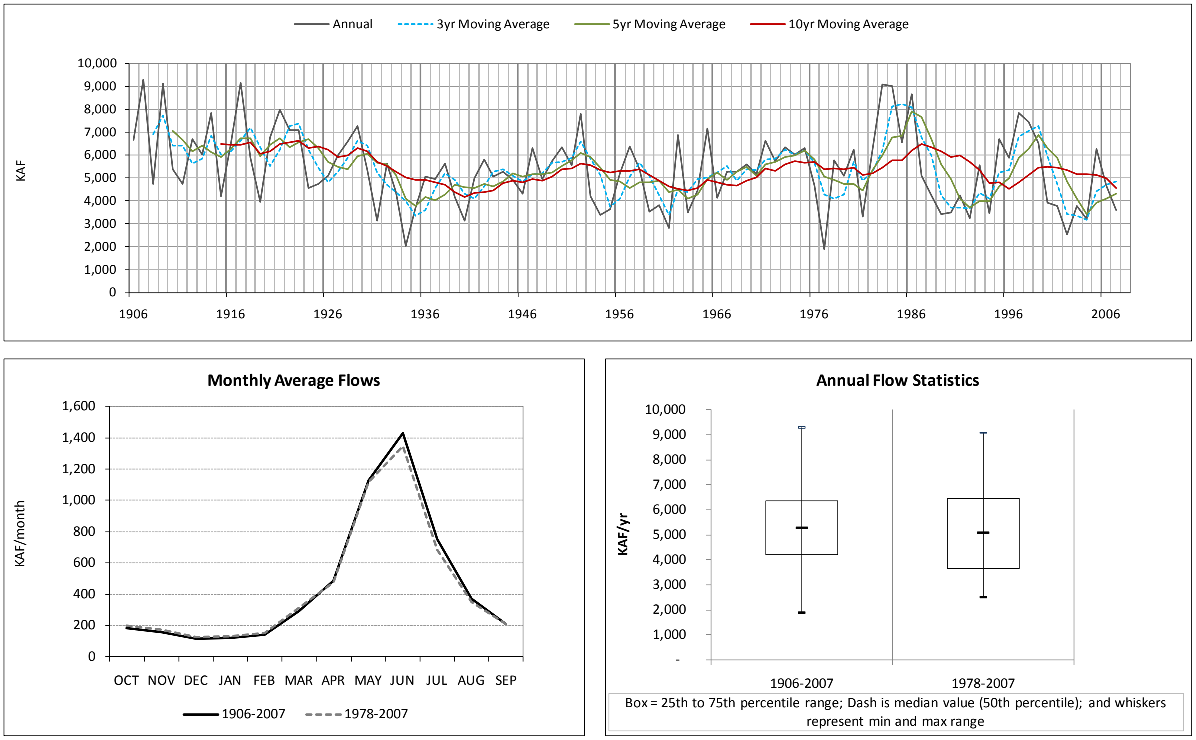

FIGURE B-16
Colorado River near Cisco, Utah Natural Streamflow Snapshot Analysis

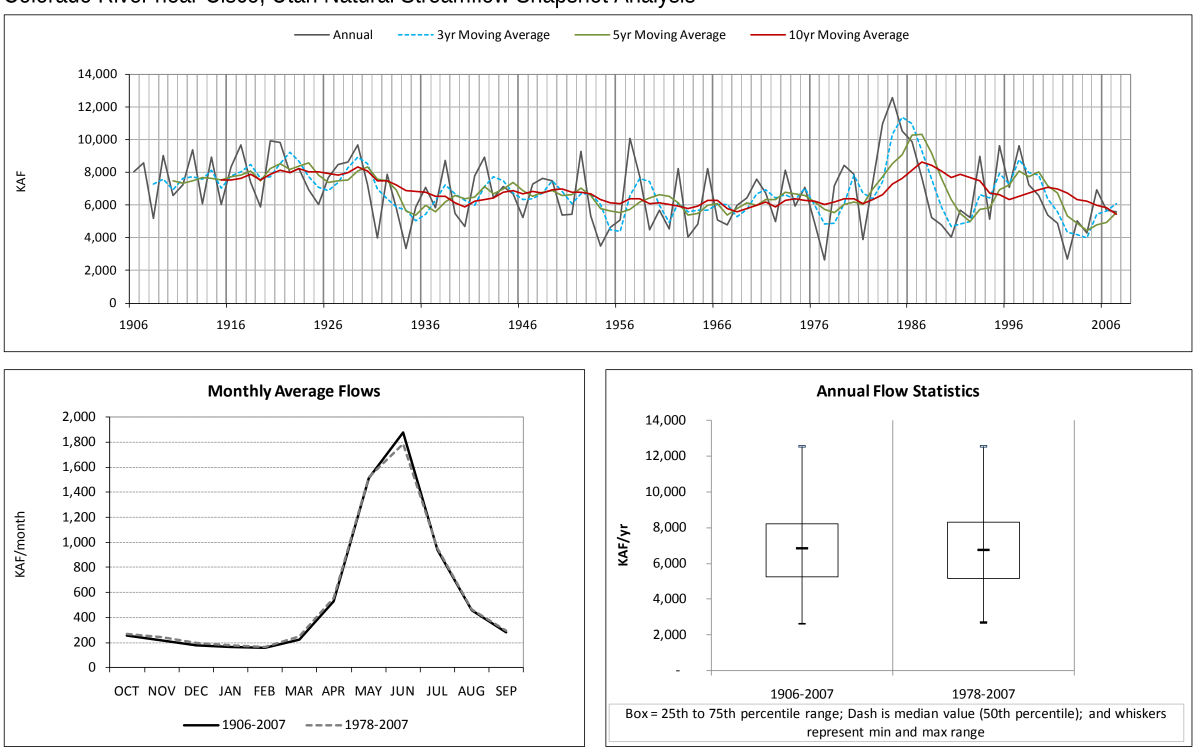

FIGURE B-17
San Juan River near Bluff, Utah Natural Streamflow Snapshot Analysis

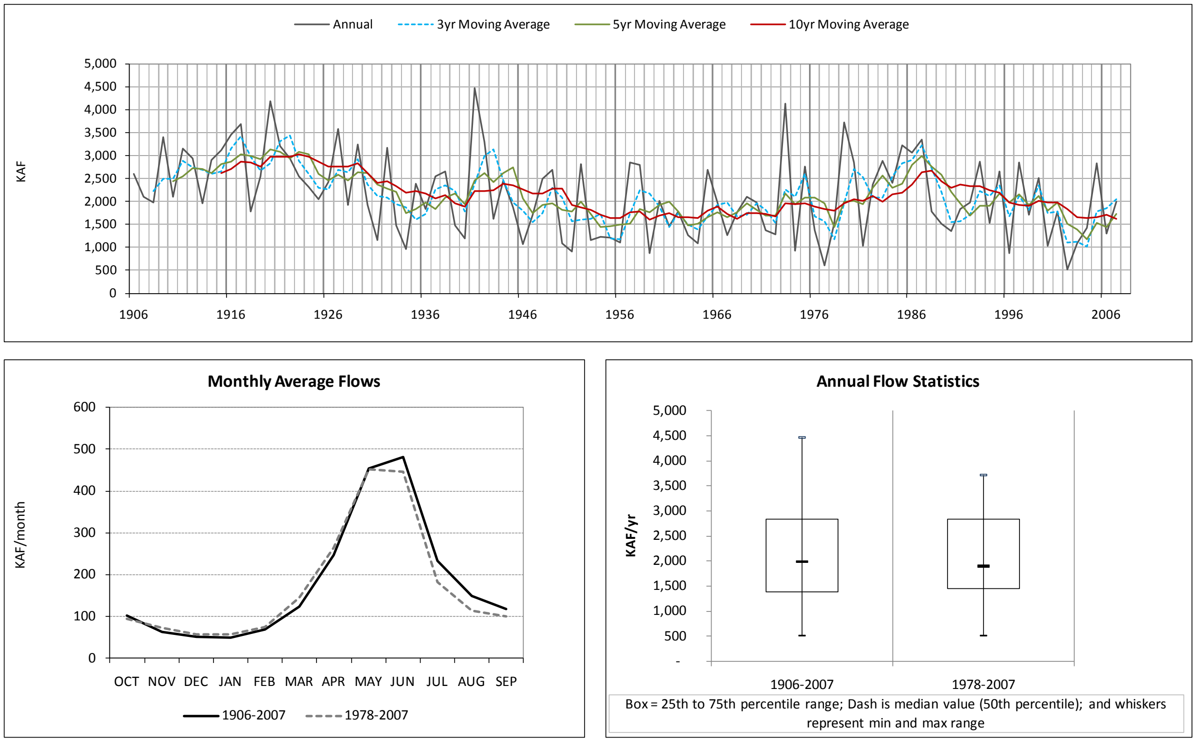

As with temperature and precipitation, Miller and Piechota (2008) also evaluated streamflow trends and explored the significance of a step change in streamflow, which occurred during the mid 1970s. The step change time series data were divided into the first 69 years of data (1906 to 1974) and the latter 31 years of data (1975 to 2005). Increasing streamflow trends in January through March and decreasing streamflow trends during peak runoff months (April through July) were reported in the authors' study. The authors also note that decreasing streamflow trends were apparent at the 99 percent confidence level throughout the Basin during the traditional peak flow months, despite the high variability of streamflow rates that historically occurred in the Basin (e.g., Pagano and Garen, 2005; Woodhouse and Lukas, 2006). Because streamflow trends are more apparent than precipitation trends, the authors speculate that it is possible that the form of precipitation (rain or snow) and other components of the water budget (e.g., evaporation and seepage losses) are changing. Based on these studies, a general warming in the Basin is shifting winter precipitation to a higher rain-snow ratio when compared to historical data. These changes are consistent with earlier peak streamflows in the spring.

The inter-annual variability of climate and hydrology within the Basin produces frequent periods when the mean flow during that period is below the long-term mean. These occurrences are referred to as periods of streamflow deficit or deficits for the purpose of this report. As part of the analysis conducted for this report, different averaging periods for determining and measuring deficits were considered. The use of a 1-year averaging period was discarded because it implied that any 1 year above 15 maf of natural flow at Lees Ferry, Arizona, would break a multi-year deficit. The use of a 2-year averaging period implies that it may take 2 consecutive, above-normal years (or 1 extremely wet year) to end a deficit. The definition used in the remainder of this report is the following: a deficit occurs whenever the 2-year average flow falls below 15 maf, the long-term mean annual flow of the 1906 to 2007 period.

Applying this definition, figure B-18 presents the severity of 2-year deficits in the observed record. For each year of the 1906 to 2010 period[4,] the 2-year running average annual flow was calculated. The difference between the 2-year running average flow and the long-term mean annual flow was computed. If the difference was negative, it was labeled "deficit" and the volumes were accumulated until the difference was once again positive. The deficit length and cumulative amount were recorded for each year. Three significant deficit spells that occurred in the observed period beginning in 1931 (7-year deficit), 1959 (7-year deficit), and 2000 (9-year deficit) are shown on the figure in green, orange, and red, respectively. As can be seen from the figure, the deficit that began in 2000 accumulated a 9-year deficit of more than 28 maf. This recent deficit is more severe than any other deficit in the observed period.

FIGURE B-18
Cumulative Streamflow Deficits (defined as 2-year running mean below 15 maf) for the Colorado River at Lees Ferry, Arizona
2008–2010 natural flows are provisional.

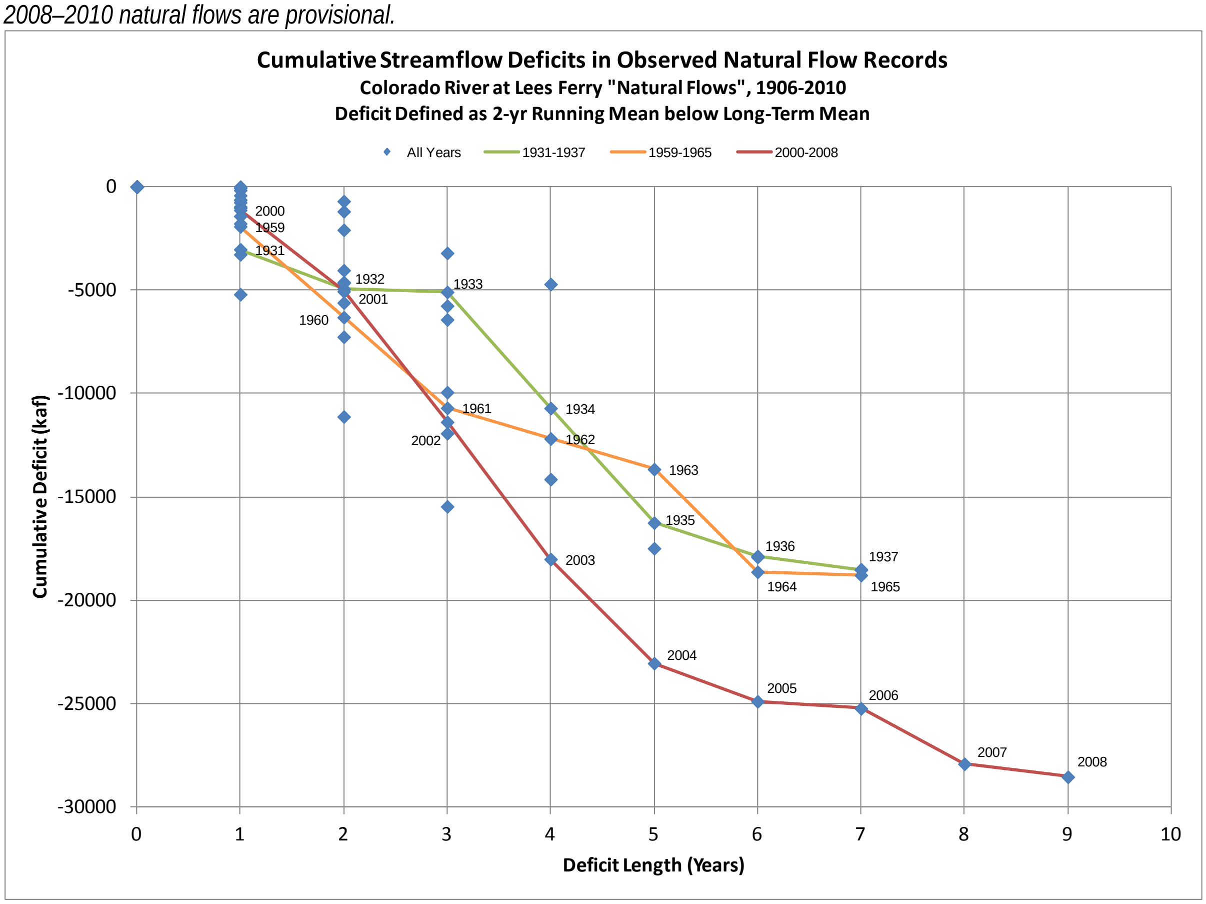

4 The natural flow at Lees Ferry, Arizona extended to 2010, based on provisional natural flow estimates is used here to better reflect the current state of streamflow deficit.

4.3 Paleo Reconstruction of Streamflow

A summary of the snapshot results for Colorado River at Lees Ferry, Arizona from the paleo-reconstructed 762 to 2005 period is shown in figure B-19. The top plot shows the annual flow volumes and the moving averages for 3, 5, 10, 20, and 30 years for the period of record. This plot provides a visual assessment of streamflow variability, minimum and maximum flows, and long-term trends. Period comparisons between long-term paleo reconstruction (762 to 2005) and a segment of the observed record (1906 to 2005) are shown. The annual flow box plot shows the minimum, 75th, 50th, and 25th percentiles, and maximum annual streamflows for the two analysis periods. The minimum, 25th percentile, median, and 75th percentile are all slightly less in the paleo reconstructed record, indicating that the paleo reconstructed streamflows are lower than the observed record. Variability is increased in the paleo reconstructed record, as illustrated by the broader inter-quartile range and minimum/ maximum values. Finally, the bottom panel shows the annual (left axis) and cumulative (right axis) deviations from the mean annual flow to illustrate the wet and dry periods in this long-term record.

Streamflow deficits using the same methods as described in the previous section were similarly computed for the 762 to 2005 period and the 1906 to 2005 period, and statistics are presented in three exceedance plots (duration, magnitude, and intensity) in figure B-20. The 762 to 2005 period contains deficits that are longer in duration (16 years) and larger (as much as 35 maf) than those in the 1906 to 2005 period. Thus, the sequences of wet-dry from the much longer paleo record suggest that deficits of greater severity than the recent deficit are possible. Interestingly, the deficit intensity (defined as the cumulative deficit divided by the duration of the deficit, which can give an indication of the annual severity of deficits) is similar between the two periods, suggesting that the paleo record produces longer deficits, but that they may not be any more intense on an annual basis than the observed record.

In summary, the trends over the observed period and over the recent climatological regime suggest declining streamflows, increases in variability, and seasonal shifts in streamflow that are likely linked to warming. The paleo reconstruction indicates a slightly lower mean than the observed record. The paleo reconstruction suggests the annual and inter-annual flows have been more variable in terms of both wet and dry sequences, as compared with the observed record period. Deficits of longer duration and greater magnitude can be expected based on the paleo record, although the paleo record shows that past deficits were not significantly more intense than the observed record.

FIGURE B-19
Colorado River at Lees Ferry, Arizona Paleo Streamflow Snapshot Analysis
cum=cumulative

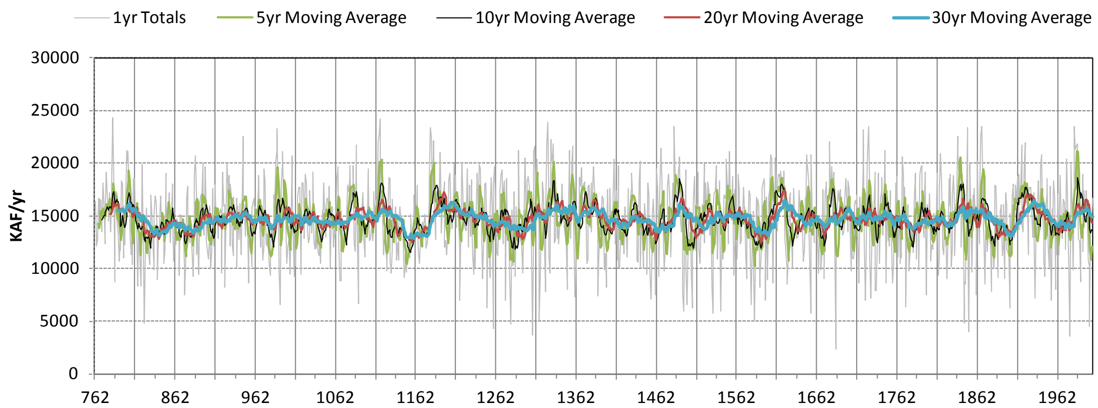

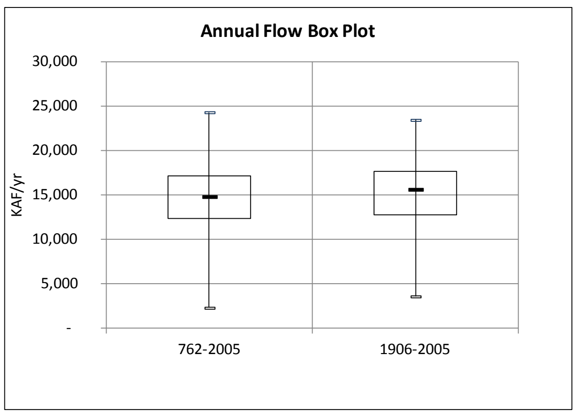

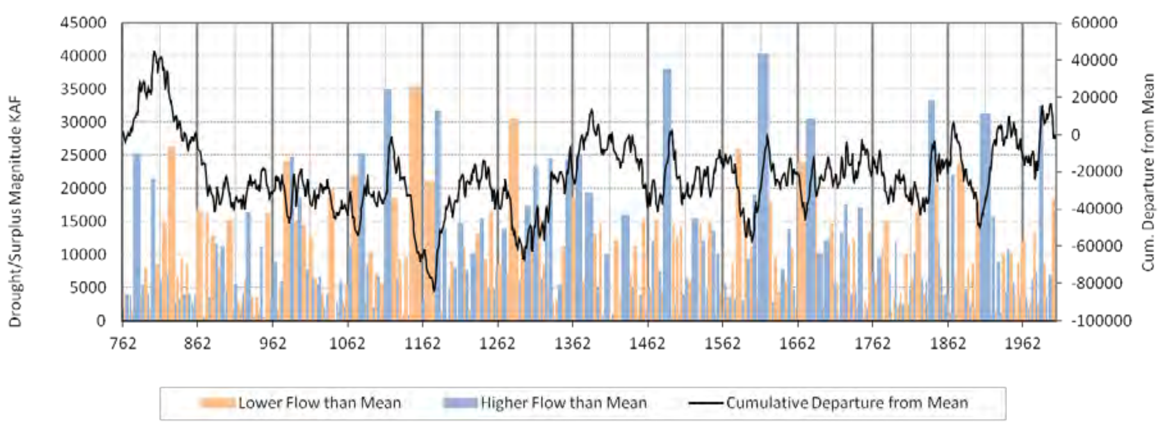

FIGURE B-20
Comparison of Drought Characteristics between a Segment of the Observed Period (1906–2005) and the Paleo Period (762–2005)

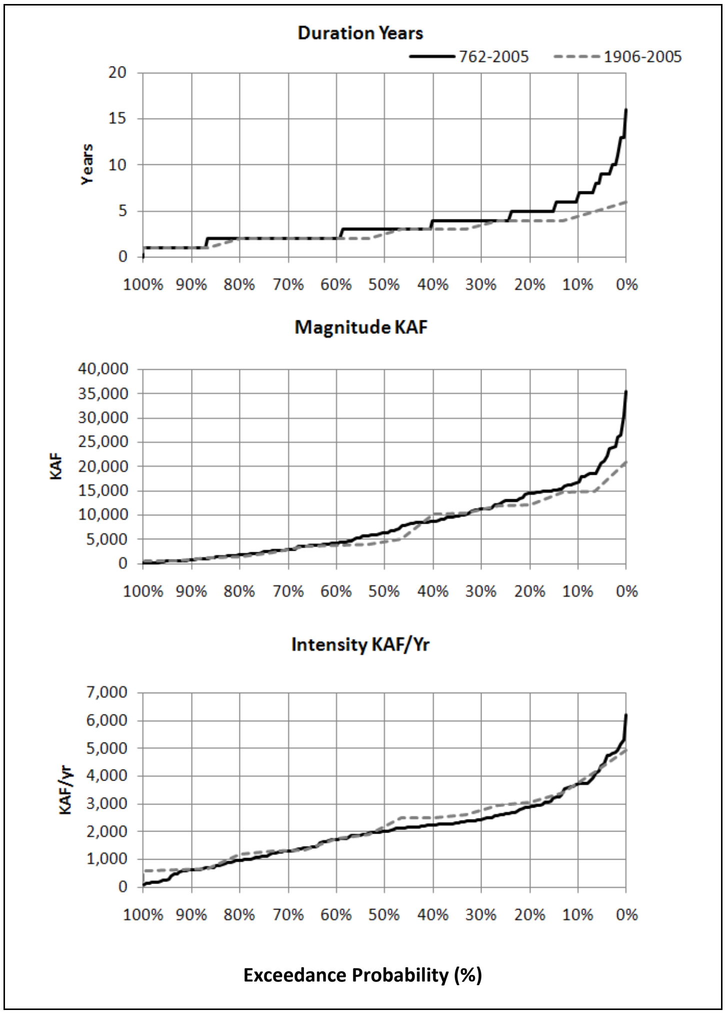

5.0 Future Supply under the Observed Resampled Scenario

5.1 Methods

Used by Reclamation in several past planning studies (such as Reclamation, 2007), the Observed Resampled[5] scenario is quantified by applying the Indexed Sequential Method (ISM) (Ouarda et al., 1997) to the 1906 to 2007 observed natural flow record to generate 102 sequences, each 50 years in length. ISM is a stochastic resampling method that creates a number of different future hydrologic sequences (or realizations). The length of the hydrologic sequence is determined by the simulation horizon (2011 to 2060, or 50 years in the Study) and the number

[5] The analysis of the Direct Natural Flow, Direct Paleo, and Nonparametric Paleo Conditioning scenarios discussed in appendix N of the 2007 Interim Guidelines Final EIS (Reclamation, 2007) are synonymous with the analysis of the Observed Resampled, Paleo Resampled, and Paleo Conditioned scenarios discussed in this report, respectively.

of sequences is determined by the length of the record that is being resampled (1906 to 2007, or 102 years in this scenario). The ISM cycles through the observed record generating 102 hydrologic sequences, based on the assumption that the record "wraps around" at the end (i.e., 1960 to 2007, followed by 1906, 1907, and 1908).

Strengths of this method are that it is based on the best available measured data, provides the basis for a quantification of the uncertainty and an assessment of risk with respect to future inflows, and is widely accepted by Basin stakeholders. The major drawback of this approach is that future scenarios are limited to the magnitudes and sequencing that occurred in the observed record, with the exception of new sequences generated as a result of the wrap. Therefore, a wider range of plausible future streamflows (including flow magnitudes and wet and dry sequences not seen in the observed record) are not possible in the Observed Resampled scenario.

5.2 Results

The results for the Observed Resampled scenario are presented as summary figures for annual and monthly flows at Colorado River at Lees Ferry, Arizona in figures B-21 through B-24. Because each supply scenario included multiple hydrologic sequences, there is a range associated with the flow statistics. Figure B-21 displays all of the individual 102 sequences in the Observed Resampled scenario. The sequence bolded in figure B-21 also appears in figure B-22, which is a representative trace of the 102 sequences for illustration purposes. Figure B-22 also depicts the annual range of natural flows when applying the ISM technique, and figure B-23 provides the annual statistics.

Annual natural flows are generally in the range of 5 to 25 maf, with a mean of approximately 15 maf. The standard deviation is almost one-third of the mean annual flow, providing a representation of the inter-annual variability of this flow record. Skew is a measure of the shape of the annual flow distribution. A skew of zero implies a normal distribution in which wetter years and magnitudes are evenly balanced with drier years. The skew and backward lag correlation indicate that the flows are slightly biased to the lower side of the distribution (more dry years than wet years) and that year-to-year correlation of flows (indicated by the backward lag correlation) is relatively high.

FIGURE B-21
Colorado River at Lees Ferry, Arizona Natural Flow for 102 Sequences for the Observed Resampled Scenario
The bolded line indicates a representative trace.

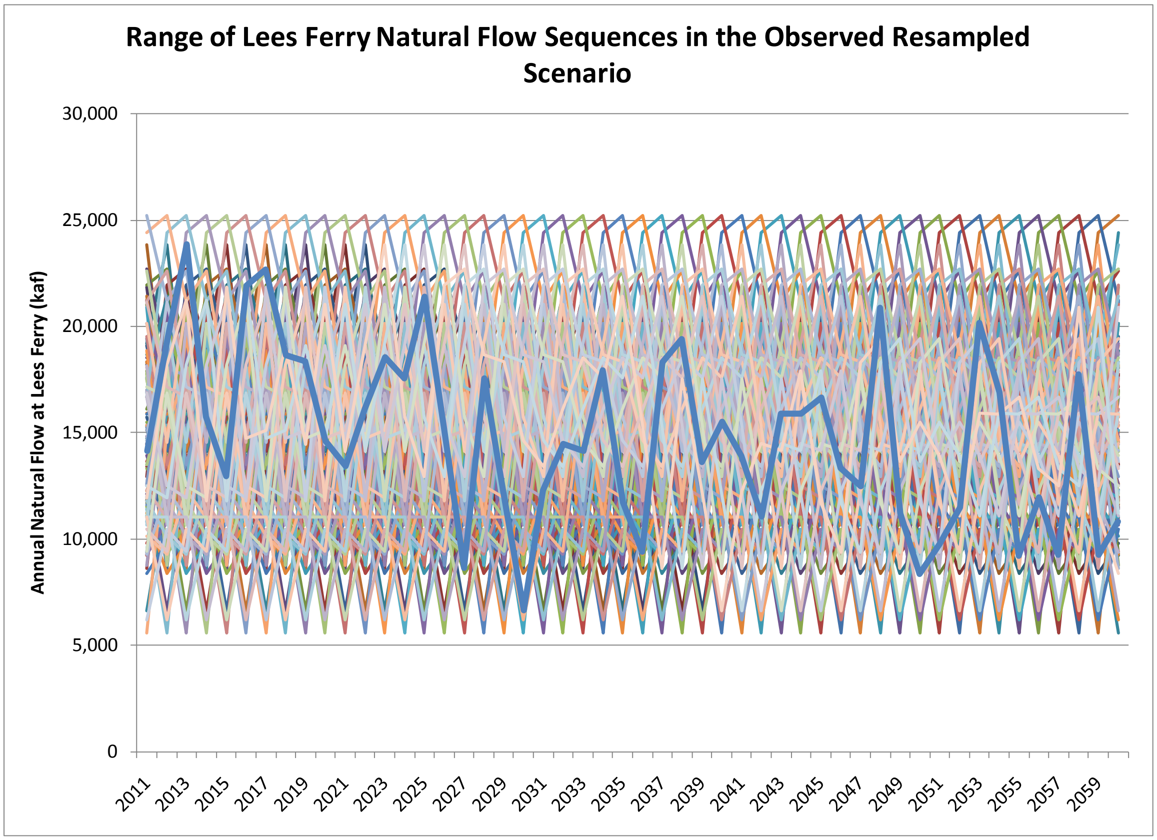

FIGURE B-22
Simulated Annual Colorado River at Lees Ferry, Arizona Natural Flow Statistics for 102 Realizations, 2011–2060
Figure shows the median (line), 25th–75th percentile band (dark shading), 10th–90th percentile band (light shading), max/min (whiskers), and 1906–2007 observed min and max (dashed lines). The blue line indicates a representative trace.

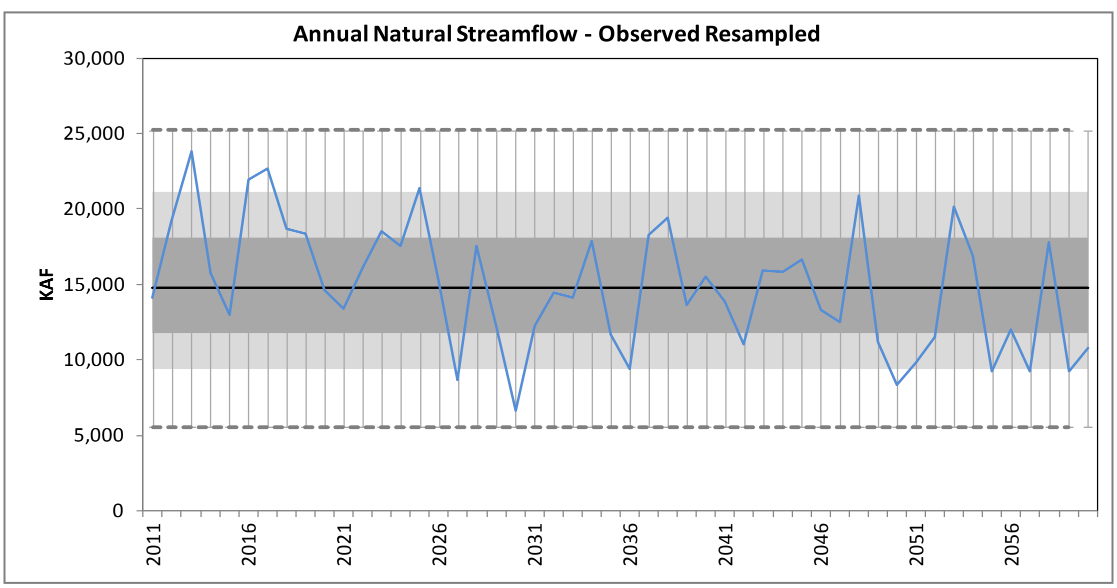

FIGURE B-23
Summary Statistics for Annual Colorado River at Lees Ferry, Arizona Natural Flows for the Observed Resampled Scenario
Figure shows the median (dash), 25th–75th percentile band (box), and max/min (whiskers).

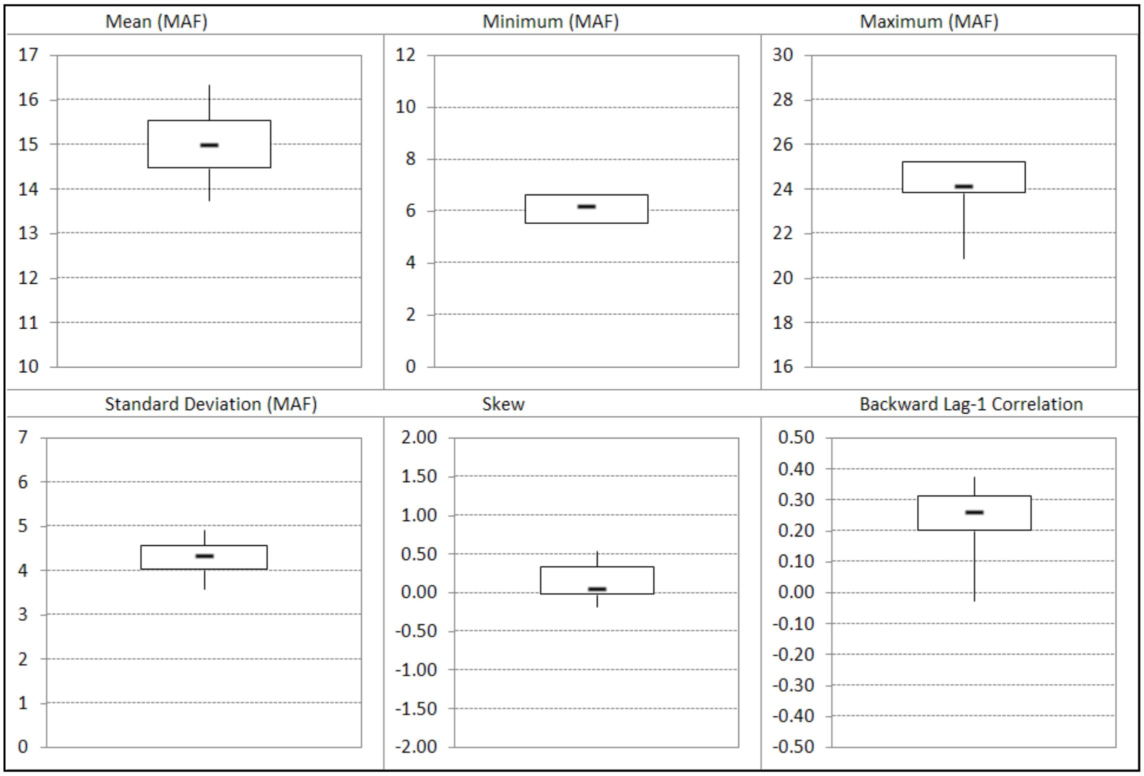

River flow peaks in late spring due to delayed snowmelt from the higher elevation upstream watersheds, with May, June, and July exhibiting the highest flows (figure B-24). June flows are both the highest and most variable with mean monthly flows averaging about 4 maf per month and ranging from about 1 to 9 maf per month. Late summer and fall flows are considerably lower and exhibit significantly less variability.

FIGURE B-24
Simulated Monthly Colorado River at Lees Ferry, Arizona Natural Flow Statistics for 102 Realizations, 2011–2060
Figure shows the median (dash), 25th–75th percentile band (shading), and max/min (whiskers).

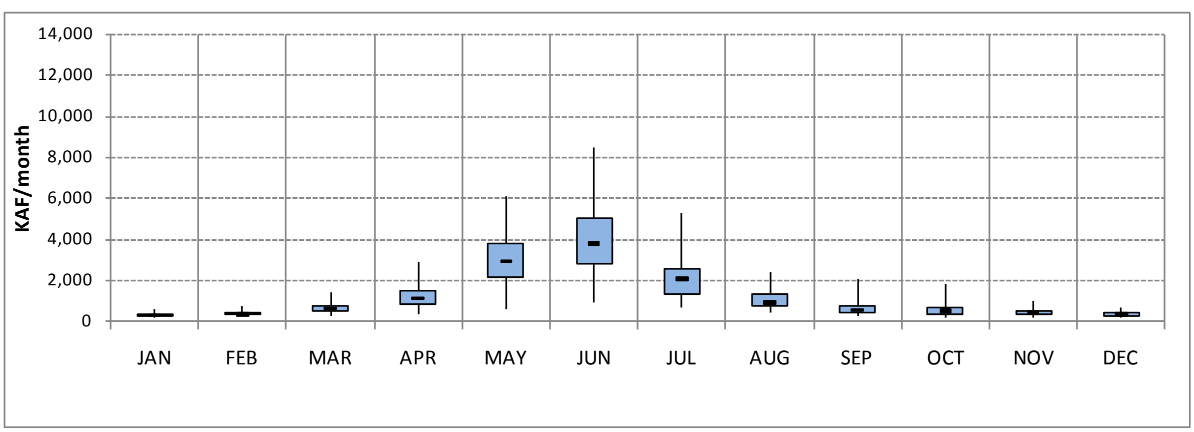

Another measure of the inter-annual variability and persistence of streamflow states (wet and dry) is characterized by determining the frequency, duration, and magnitude of deficit and surplus periods. Recall that for the purpose of this report, “deficit” is defined as a consecutive 2-year period when the mean is less than the observed long-term mean of 15.0 maf. Similarly, “surplus” is defined as a consecutive 2-year period when the mean is above 15.0 maf.

Figure B-25 illustrates four characteristics of deficit and surplus spells throughout the Study period (2011 to 2060): spell length, spell magnitude, the frequency of specific spell lengths occurring, and the relationship between deficits and surpluses in the scenario. Box plots displaying spell length are shown in the left figure (deficit, below the x-axis, and surplus, above the x-axis). The exceedance plot shown in the right figure displays the exceedance probabilities for spell lengths. Probabilities for deficit spells are shown in the bottom half of the plot. Probabilities for surplus spells are shown in the top half of the plot.

FIGURE B-25
Simulated Deficit and Surplus Spell Length and Magnitude for all 102 Realizations in the Observed Resampled Scenario
Box plots show the median (dash), 25th–75th percentile band (shading), and max/min (whiskers).

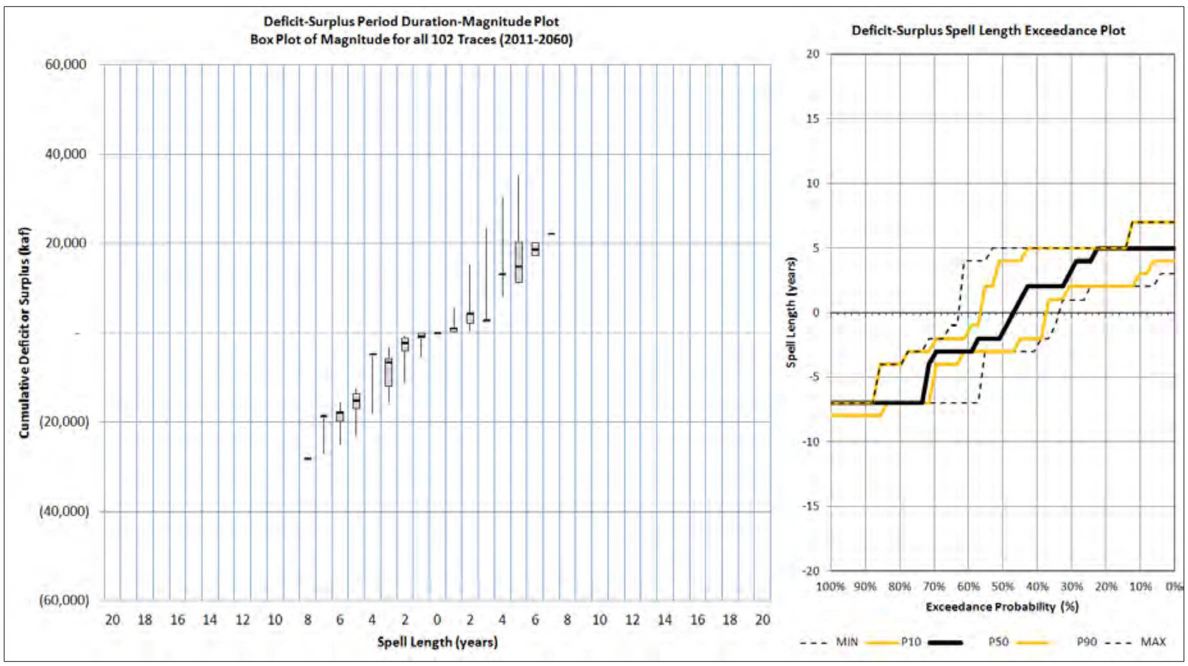

Spell length: the maximum deficit is 8 years (note that this length would be 9 years if the observed record extended through 2010), and the maximum surplus is 7 years. This information is provided in both the box plots and the exceedance plot.

Spell magnitude: referring to the box plots, the magnitude of the maximum deficit and surplus is about 27 maf and 22 maf, respectively. Deficit or surplus intensity can be computed by dividing the spell magnitude by the spell length.

Frequency of specific spell lengths occurring: the exceedance plot inset provides information regarding the frequency of the length of deficit and surplus spells. As such, the median exceedance probability of a deficit spell of 5 years is about 70 percent, meaning there is about a

30 percent chance of a deficit longer than 5 years. Similarly, at the 30 percent median exceedance probability is a surplus spell of 3 years, meaning there is about a 30 percent chance of a surplus period lasting more than 3 years.

Relationship between deficits and surpluses in the scenario: the median (50 percent exceedance probability) corresponds to a deficit of 3 years. This result indicates that under the Observed Resampled scenario, there is a greater probability of being in a deficit (lasting at least 3 years) than in a surplus period.

6.0 Future Supply under the Paleo Resampled Scenario

6.1 Methods

The Paleo Resampled scenario is generated by applying the ISM to paleo reconstructed streamflow data (762 to 2005) to develop 1,244 traces, each 50 years in length. The major strength of this method is the ability to produce sequences with magnitudes and deficit/surplus spells not found in the Observed Resampled scenario. In addition, as is true for the Observed Resampled scenario, this method is based on relationships to measured data. Although there is a wealth of literature documenting the strong link between streamflow and tree-ring growth in moisture limited regions, the exact magnitudes of a paleo reconstruction are not as reliable as historical flow data, particularly at the extremes (Woodhouse and Brown, 2001). This is attributed to a variety of factors in the reconstruction process, such as model selection to relate tree-ring width to streamflow. Furthermore, because ISM sequentially resamples the paleo record to generate hydrologic sequences, the sequences will only consist of flow magnitudes and sequences that are present in the paleo record, with the exception of the sequences created as a result of the wrap. The inclusion of the Paleo Conditioned scenario addresses this issue and the weakness of the paleo record in capturing magnitudes at the extremes.

Because the paleo flow data are only available at the annual time step for a single location (Colorado River at Lees Ferry, Arizona), annual flows at this location were disaggregated, spatially and temporally, throughout the Upper Basin natural flow locations using a non-parametric disaggregation method (Nowak et al., 2010). The disaggregation method relies on the observed record to model the spatial and temporal distribution properties of the monthly and annual flow. Disaggregated flows at the Lower Basin natural flow locations are generated by selecting an “analog” year from the observed record. These methods have been demonstrated to be appropriate and effective for the Basin and time step. For a more detailed explanation of these methods, please see Nowak et al., 2010, and appendix N of the 2007 Interim Guidelines Final EIS (Reclamation, 2007).

6.2 Results

The results for the Paleo Resampled scenario are presented as summary figures for annual and monthly flows for the Colorado River at Lees Ferry, Arizona in figures B-26 through B-29. As with the Observed Resampled scenario, multiple realizations are simulated, producing a range associated with the flow statistics. Figure B-26 displays all of the individual 1,244 sequences in the Paleo Resampled scenario. The sequence bolded in figure B-26 also appears in figure B-27, which is a representative trace of the 1,244 sequences for illustration purposes. Figure B-27 also depicts the annual range of natural flows, while figure B-28 provides the annual statistics.

Annual natural flows are generally in the range of 3 to 25 maf, with a mean of approximately 14.7 maf. The minimum annual flow is much lower than the Observed Resampled scenario, while the maximum annual flow is similar. Conversely, the standard deviation is smaller than the Observed Resampled scenario, suggesting that a greater number of traces are closer to the mean value. In the Paleo Resampled scenario, the skew is slightly negative (compared to slightly positive in the Observed Resampled scenario), suggesting a greater frequency of wet years than dry years (compared to the Observed Resampled scenario). Finally, the backward lag correlation is slightly higher than the Observed Resampled scenario, suggesting a greater year-to-year correlation than in the observed record. The latter likely results from the reconstruction techniques and relatively few chronologies in the distant past.

FIGURE B-26
Colorado River at Lees Ferry, Arizona Natural Flow for 1,244 Sequences for the Paleo Resampled Scenario
The bolded line indicates a representative trace.

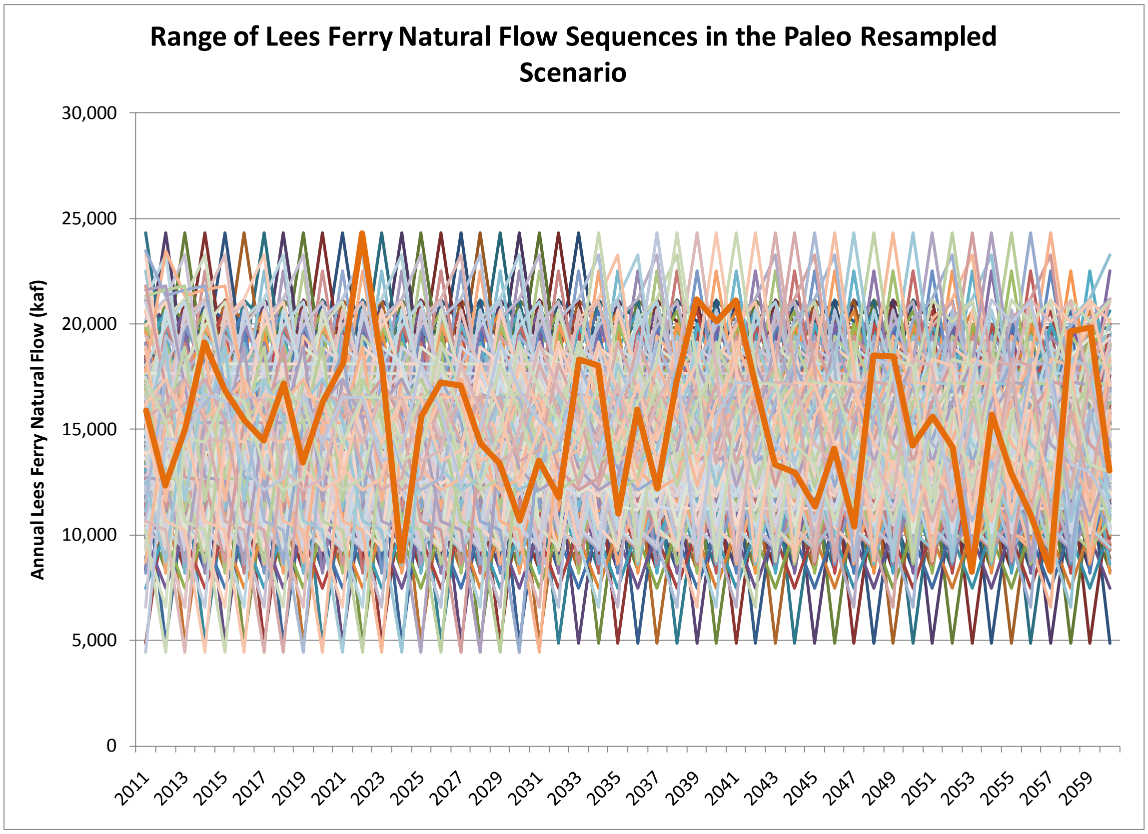

FIGURE B-27
Simulated Annual Colorado River at Lees Ferry, Arizona Natural Flow Statistics for 1,244 Traces, 2011–2060
Figure shows the median (line), 25th–75th percentile band (dark shading), 10th–90th percentile band (light shading), max/min (whiskers), and 1906–2007 observed min and max (dashed lines). The orange line indicates a representative trace.

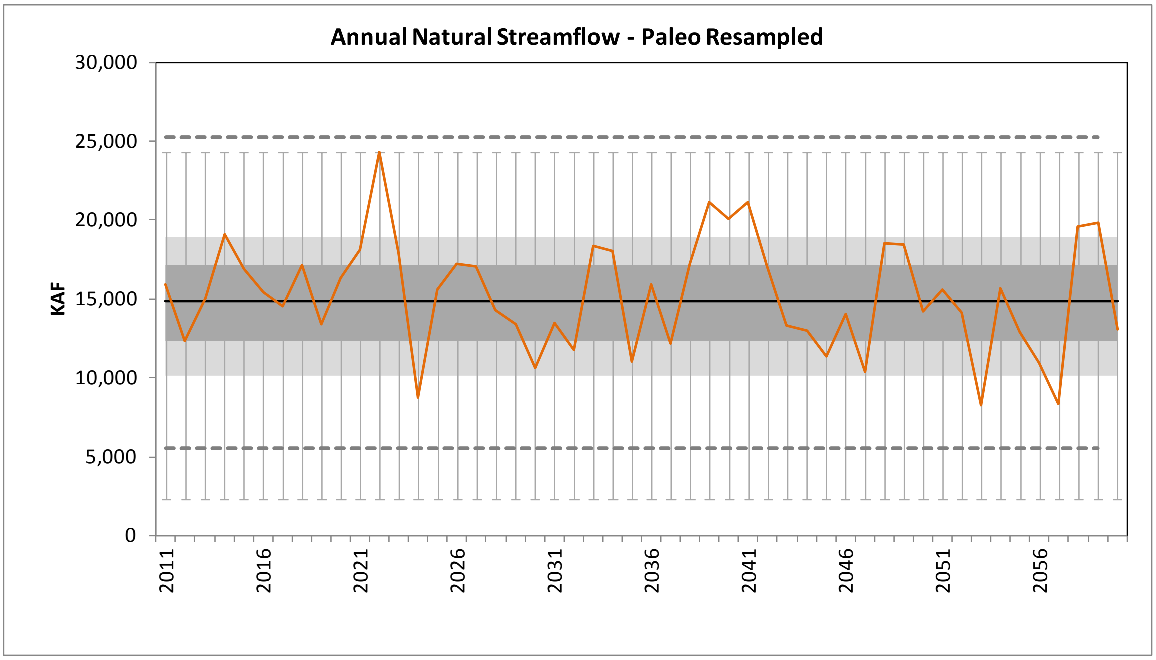

FIGURE B-28
Summary Statistics for Annual Colorado River at Lees Ferry, Arizona Natural Flows for the Paleo Resampled Scenario
Figure shows the median (dash), 25th–75th percentile band (box), and max/min (whiskers).

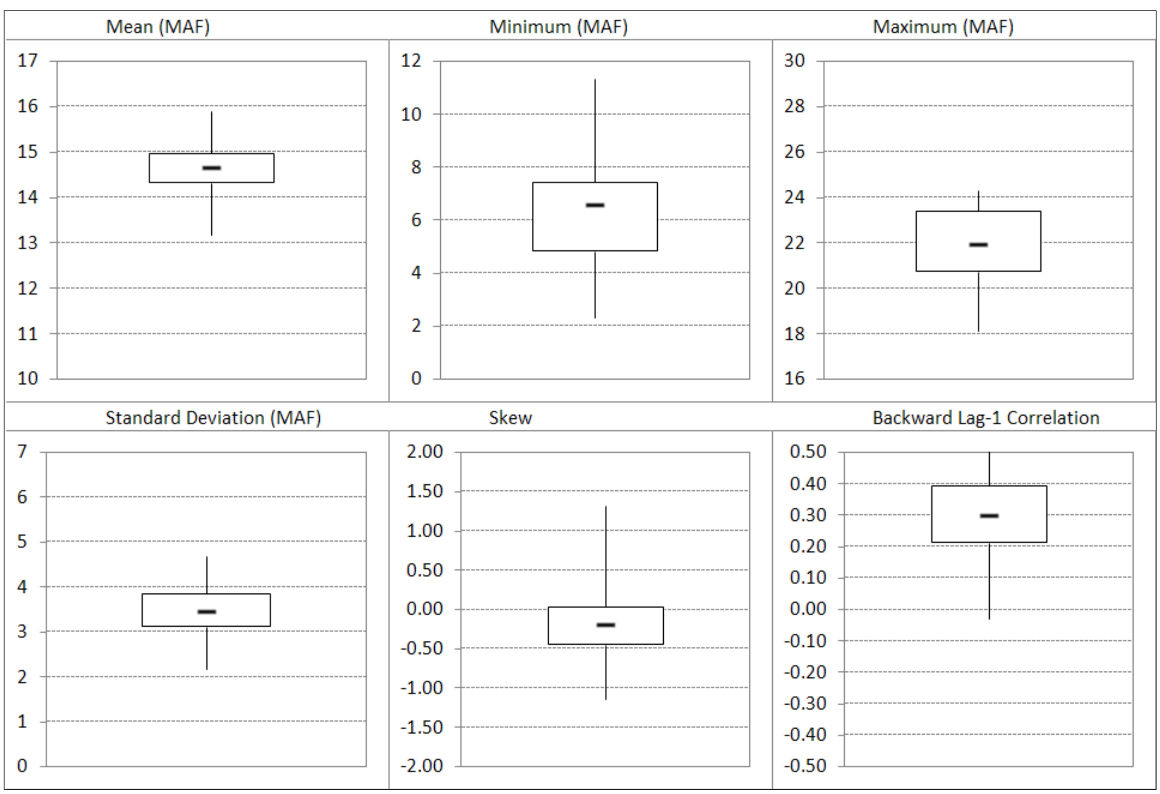

Monthly river flows suggest no significant change from the Observed Resampled scenario. Peak flows occur in late spring, with May, June, and July exhibiting the highest flows (figure B-29). As in the Observed Resampled scenario, June flows are both the highest and most extreme, with mean monthly flows averaging about 4 maf per month and ranging from about 1 to 9 maf per month. This was expected because the disaggregation applied to the annual paleo reconstruction was trained on the observed natural flow data. Also similar to the Observed Resampled scenario, late summer and fall flows are considerably lower and exhibit significantly less variability.

FIGURE B-29
Simulated Annual Colorado River at Lees Ferry, Arizona Natural Flow Statistics for 1,244 Realizations, 2011–2060
Figure shows the median (dash), 25th–75th percentile band (shading), and max/min (whiskers).

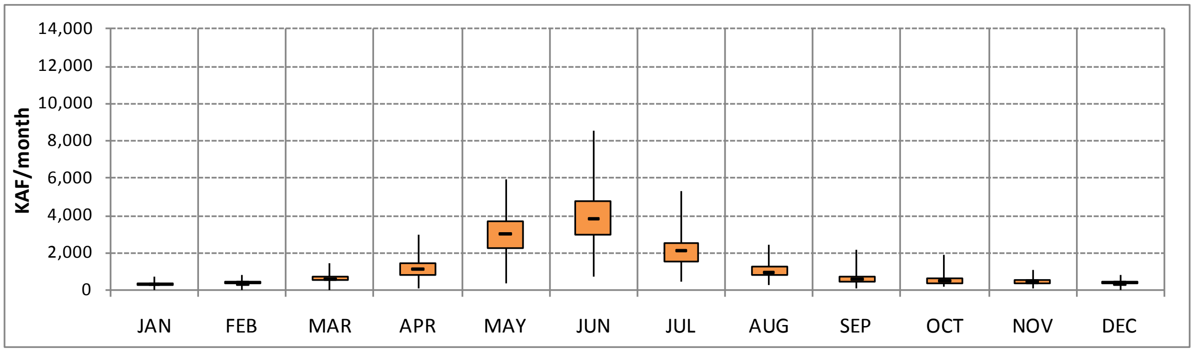

Figure B-30 illustrates the length, magnitude, and frequency of deficit and surplus spells. Under the Paleo Resampled scenario, maximum deficit and surplus periods are significantly longer in duration than those in the Observed Resampled scenario. Maximum deficit spell length under the Paleo Resampled scenario is about 17 years, and the maximum surplus spell length is about 15 years. The 17-year deficit period contains approximately 35 maf of total deficit. For comparison, the recent deficit persisted for 9 years (through 2008) with an accumulated deficit of about 29 maf. Thus, from a measure of deficit intensity, although the deficit is sustained longer in the Paleo Resampled scenario, the annual deficits are not dissimilar from the Observed Resampled scenario.

FIGURE B-30
Simulated Deficit and Surplus Spell Length and Magnitude for all 1,244 Realizations in the Paleo Resampled Scenario
Box plots show the median (dash), 25th–75th percentile band (shading), and max/min (whiskers).

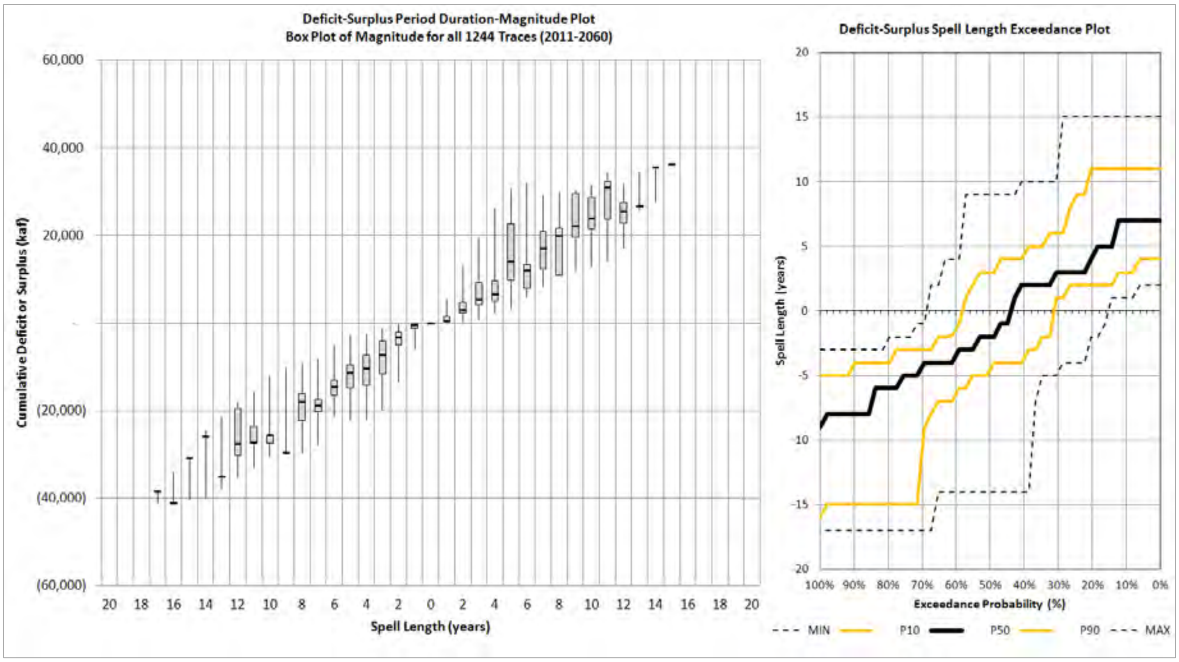

7.0 Future Supply under Paleo Conditioned Scenario

7.1 Methods

The Paleo Conditioned scenario is generated by applying a non-parametric technique to "blend" the observed historical and paleo reconstructed records to generate 1,000 traces, each 50 years in length. Flow magnitudes vary significantly across multiple reconstructions for a particular site (Stockton and Jacoby, 1976; Hildalgo et al., 2009; Hirschboeck and Meko, 2005; Woodhouse et al., 2006). However, the paleo hydrologic state agreement (i.e., wet or dry) is quite reliable across different reconstructions (Woodhouse et al., 2006).

The paleo conditioned technique blends the rich variety of drought/surplus found in the paleo reconstruction with reliable magnitudes from the observed natural flow data by first extracting a sequence of years represented simply as wet or dry from the streamflow reconstruction. Flow magnitudes are then conditionally resampled from the observed record for each year in the sequence, based on the current and previous hydrologic state. Thus, any underlying relationship between magnitude and sequencing is preserved while circumventing issues associated with magnitude reliability. For example, if an observed flow value occurred as the first year of a drought, it can only be assigned to a "dry state year" that was preceded by a "wet state year" as part of a paleo conditioned trace. Similarly, if an observed flow magnitude was the second year of a multi-year surplus period, that value can only be assigned to a "wet state year" that was preceded by another "wet state year." This logic holds true for all wet/dry sequencing combinations. Following this method, a wealth of traces can be generated (at least 1,000 are recommended to limit sample variability) by simply changing the initial wet/dry sequence information extracted from the paleo data. Different from the ISM technique, the number of sequences is not limited to the length of the streamflow record being resampled. For a more detailed explanation of the method, see appendix N of the 2007 Interim Guidelines Final EIS (Reclamation, 2007) and Prairie et al., 2008. As was the case with the Paleo Resampled scenario, the Paleo Conditioned scenario introduces considerable variability when compared with the observed data, yet maintains the reliability of the observed magnitudes. Paleo conditioned traces were also generated at the annual time scale for Colorado River at Lees Ferry, Arizona and required the same disaggregation process employed for the Paleo Resampled scenario in order to produce monthly data at multiple locations.

7.2 Results

The results for the Paleo Conditioned scenario are presented as summary figures for annual and monthly flows at Colorado River at Lees Ferry, Arizona in figures B-31 through B-34. Figure B-31 displays all of the individual 1,000 sequences in the Paleo Conditioned scenario. The sequence bolded in figure B-31 also appears in figure B-32, which is a representative trace from the 1,000 sequences. Figure B-32 depicts the annual range of natural flows, and figure B-33 provides the annual flow statistics.

Annual natural flows are generally in the range of 5 to 25 maf, with a mean of approximately 14.9 maf. The annual statistics are similar to the Observed Resampled scenario, largely due to the paleo conditioned technique that borrows the magnitudes from the observed record when combining with state information from the paleo reconstructions. Similarly, the standard deviation, skew, and backward lag correlation indicate that the annual flow statistics are similar to the Observed Resampled scenario. Monthly flows are also similar in pattern and magnitude to the Observed Resampled and Paleo Resampled scenarios, as shown in figure B-34.

The most significant difference between the Paleo Conditioned scenario and the Observed Resampled and Paleo Resampled scenarios is in the inter-annual variability and persistence of streamflow states (wet and dry). Figure B-35 illustrates the frequency, length, and magnitude of deficit and surplus spells. Deficit periods of 15 years or longer are observed in this scenario and produce accumulated deficits greater than 60 maf. Similarly, extended surplus periods of similar length produce surpluses greater than 60 maf. Under this scenario, deficit periods could persist considerably longer than the Observed Resampled and produce deficits almost twice as large. However, interestingly, the median probability of exceeding a deficit spell of greater than 7 years is only 20 percent, and there is only a 10 percent likelihood of exceeding a 5-year surplus period.

FIGURE B-31
Colorado River at Lees Ferry, Arizona Natural Flow for 1,000 Sequences for the Paleo Conditioned Scenario
The bolded line indicates a representative trace.

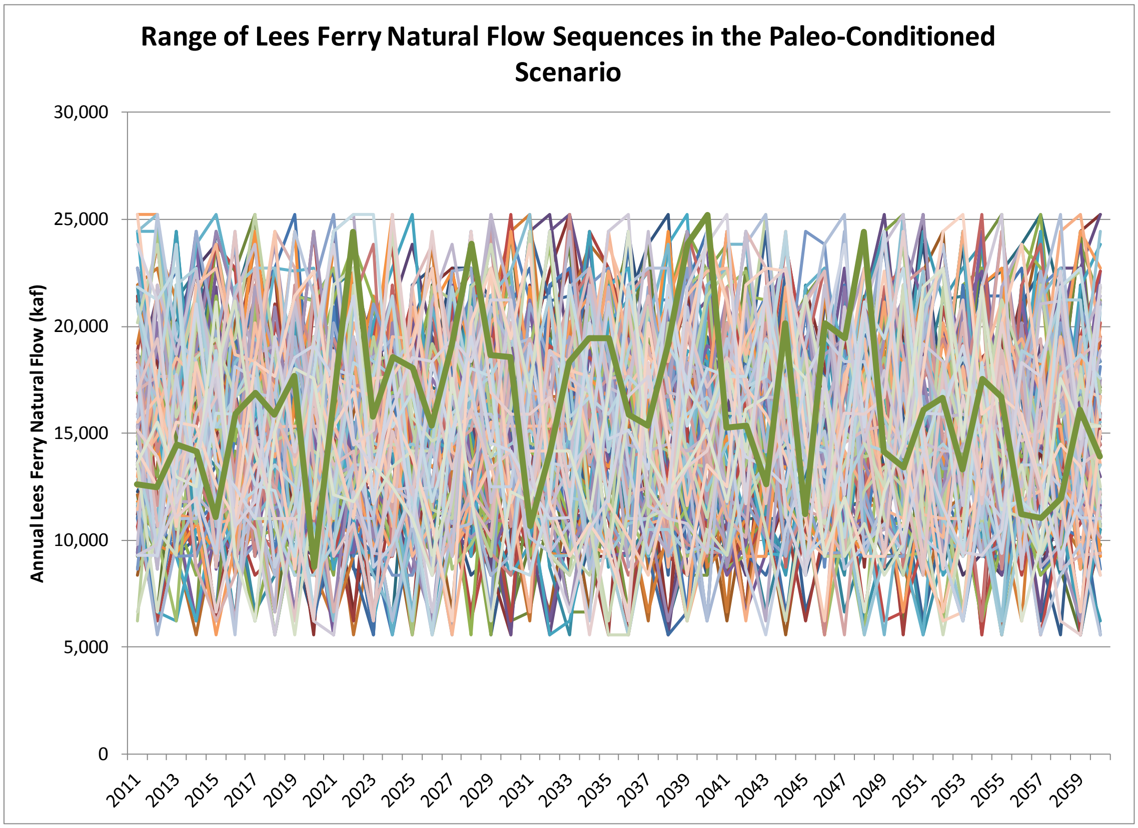

FIGURE B-32
Simulated Annual Colorado River at Lees Ferry, Arizona Natural Flow Statistics for 1,000 Realizations, 2011–2060
Figure shows the median (line), 25th–75th percentile band (dark shading), 10th–90th percentile band (light shading), max/min (whiskers), and 1906–2007 observed min and max (dashed lines). The bolded line indicates a representative trace.

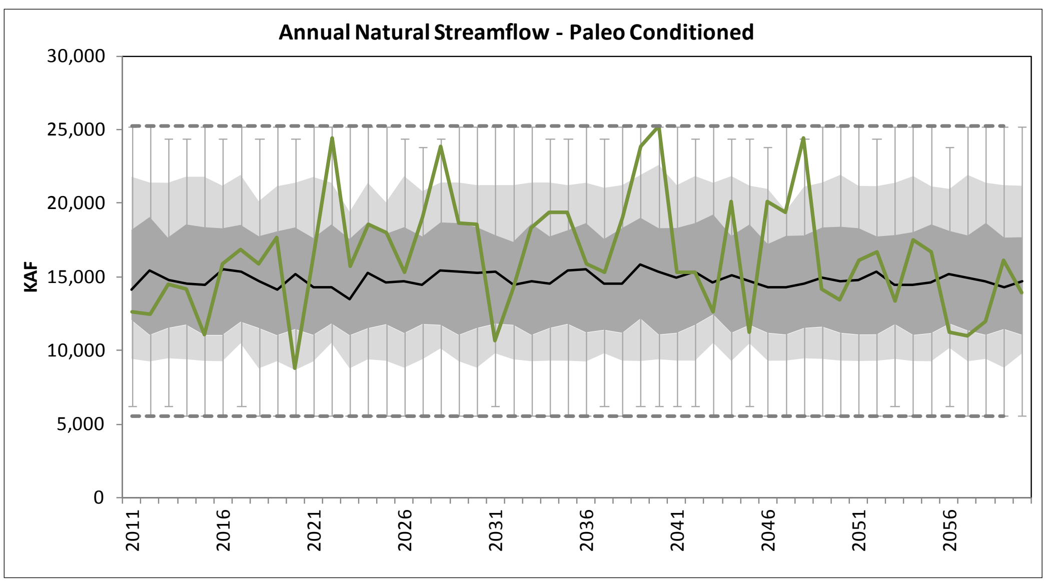

FIGURE B-33
Summary Statistics for Annual Colorado River at Lees Ferry, Arizona Natural Flows for the Paleo Conditioned Scenario
Figure shows the median (dash), 25th–75th percentile band (box), and max/min (whiskers).

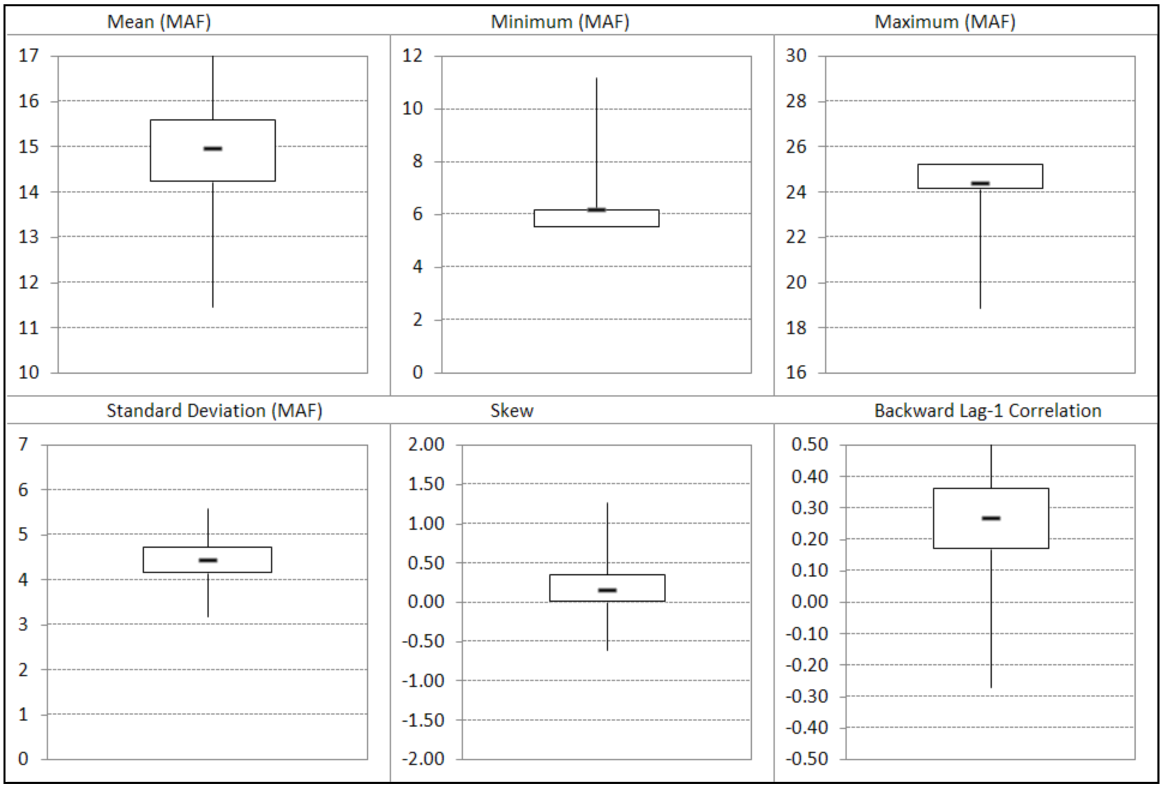

FIGURE B-34
Simulated Annual Colorado River at Lees Ferry, Arizona Natural Flow Statistics for 1,000 Realizations, 2011–2060
Figure shows the median (dash), 25th–75th percentile band (shading), and max/min (whiskers).

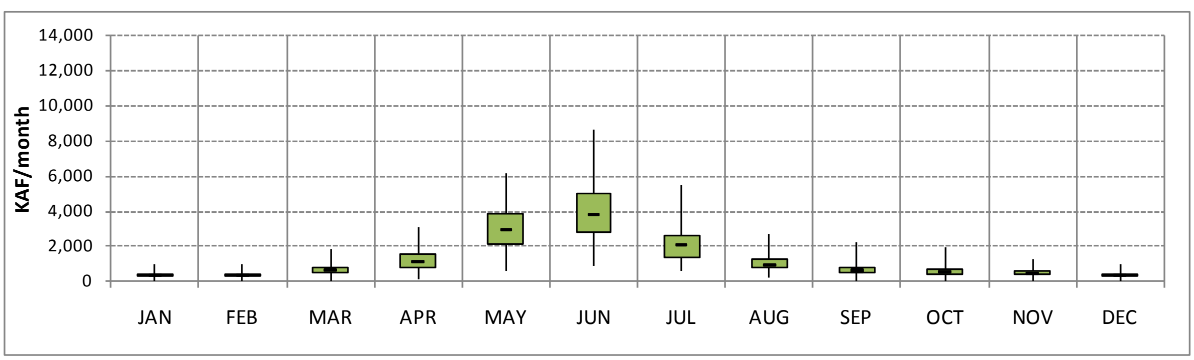

FIGURE B-35
Simulated Deficit and Surplus Spell Length and Magnitude for all 1,000 Realizations in the Paleo Conditioned Scenario
Box plots show the median (dash), 25th–75th percentile band (shading), and max/min (whiskers).

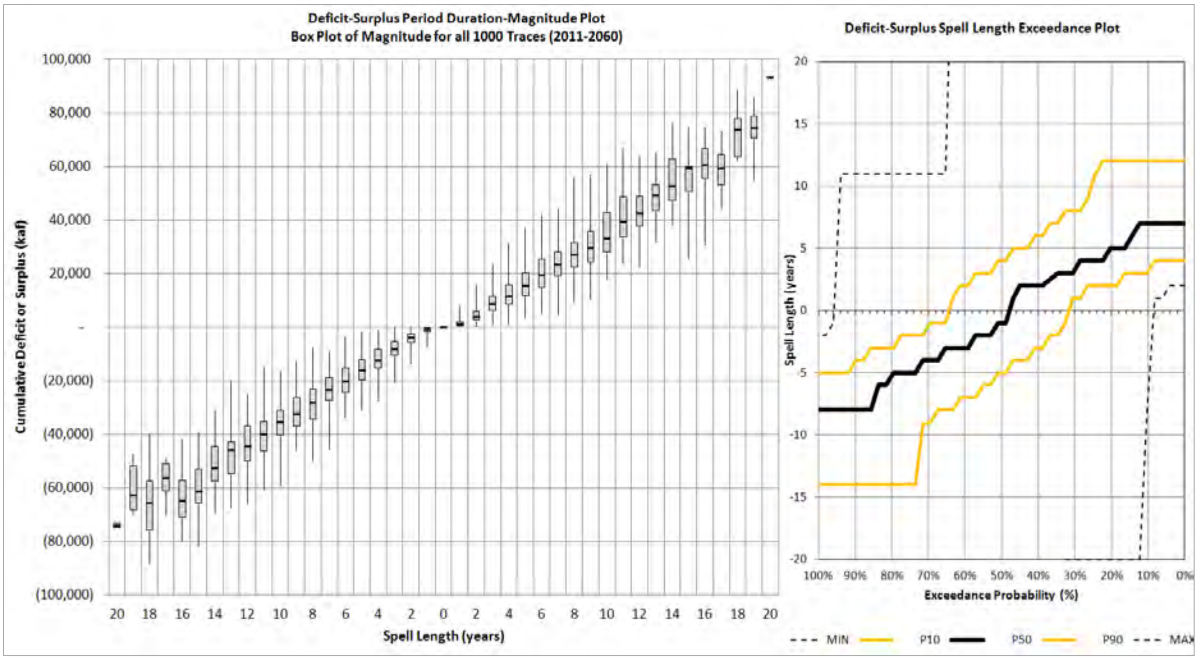

8.0 Future Supply under the Downscaled GCM Projected Scenario

8.1 Methods

Future changes in climate variability and trends, and their influence on streamflow and Basin water supply, have been studied by several researchers in recent years, and GCM future projections indicate that the climate may exhibit trends and variability over the next 50 years beyond what has occurred historically. The Downscaled GCM Projected scenario is one representation of this plausible future condition.

A number of methods for incorporating climate information in planning studies are available and have been summarized by Reclamation (2007) and others (Hamlet et al., 2010). Methods range from simple adjustments to the temperature and precipitation inputs (Delta method), to application of regional climate models for weather generation, to bottom-up risk-based approaches targeting system vulnerabilities. No one approach is better than the other; rather, each serves a specific planning purpose and consists of a set of analysis tools. The approach taken in the Study incorporates future climate information from GCMs, subsequently bias corrected and statistically downscaled, to drive a hydrologic model of the Basin. The hydrologic model simulates the effects of future climate on hydrologic processes in the Basin and provides information relating to streamflow at all major inflow points to the Colorado River and tributaries. The streamflow and ET information is then used as input into CRSS, Reclamation's primary Basin-wide simulation model used for long-term planning studies. This approach is shown graphically in figure B-36. Using this approach of linking global and regional climate information, physically based hydrologic processes, streamflow routing, and systems modeling allows for a consistent linkage between climate and system responses that are desired as part of this scenario and the overall study of future Basin reliability. The methodological approach to develop the Downscaled GCM Projected scenario consists of five major elements depicted graphically in figure B-36. A total of 112 future climate projections used in the IPCC Fourth Assessment Report (2007), subsequently bias corrected and statistically downscaled, were obtained from the Lawrence Livermore National Laboratory under the World Climate Research Program's (WCRP) Coupled Model Intercomparison Project Phase 3 (CMIP3) (Maurer et al., 2007)[6]. These data were incorporated in the first three elements of the approach in figure B-36.

Each of the 112 downscaled climate projections was then used as input into the VIC hydrology model. The VIC hydrology model used the climate projections along with land cover, soils, elevation, and other watershed information to simulate hydrologic fluxes. The hydrologic fluxes were then routed to each of the 29 natural flow locations using a routing network derived from the topography (Lohmann et al., 1996; Lohmann et al., 1998). The result of this approach was 112 unique sequences of natural flow under future climate projections. Notably, the simulated natural flows can contain significant monthly and annual biases when compared to the natural flows of the historical period. These biases are generally small for mainstem Colorado River locations, but can be large for smaller watersheds and in areas where the VIC model was not specifically calibrated. To account and compensate for these biases, the VIC-simulated streamflows for both the historical and future periods were first adjusted for biases before incorporating into systems modeling. Details on the methods used to correct for biases are included in appendix B4.

The same Downscaled GCM Projected scenario was also employed to develop the results described in the *SECURE Water Act Section 9503(c) – Reclamation Climate Change and Water 2011* (Reclamation, 2011c) Report. The SECURE Report was prepared by Reclamation's Office of Policy and Administration and includes projections of how climate change may impact the water supply on the Basin. The SECURE Report was prepared by Reclamation to provide consistent, reconnaissance-level information focused on the future risks to water supply throughout the eight Reclamation basins.

While the results are consistent between this report and the SECURE Report, the SECURE Report was limited to the evaluation of the meteorological and hydrologic changes under projected climate change. The Study also considered how hydrological changes may impact the performance of the Colorado River system through CRSS modeling. The differences in study objectives led to some differences in approach. The methodological differences consist primarily of the application of a streamflow bias correction method before using the simulated natural flows in the CRSS model. Reporting differences between this report and the SECURE Report consist of the selection of baseline climate conditions and the future analysis periods. Specifically, the SECURE Report computed future decadal changes from a 1991 to 2000 baseline condition, whereas the streamflow change statistics reported here were computed between the long-term historical record (1906 to 2007) and the Study period of 2011 to 2060. This period provides a long-term record consistent with that used in the Observed Resampled

---

[6] These data are available via the website, Bias Corrected and Downscaled World Climate Research Program Coupled Model Intercomparison Project Phase 3 Climate Projections (http://gdo-dcp.ucllnl.org/downscaled_cmip3_projections/), which is jointly hosted by the Green Data Oasis, Santa Clara University, Reclamation, and Lawrence Livermore National Laboratory.

scenario, captures a sufficiently long period necessary to describe drought and surplus statistics, and represents a mean annual flow of importance to Colorado River management. The 1906 to 2007 mean annual flow for the Colorado River at Lees Ferry, Arizona is 15.0 maf; the mean annual flow is 15.5 maf for the 1971 to 2000 period, 15.0 maf for the 1978 to 2007 period, 15.3 maf for the 1991 to 2000 period, and 14.6 maf for the 1950 to 1999 period. The 1950 to 1975 period contained lower annual flows and lower interannual variability than many of the other periods, likely influenced by conditions associated with the cold phase of PDO. To capture the projected future trends in streamflow changes associated with the Downscaled GCM Projected scenario, additional information has been provided in this report for three future 30-year time periods (2011 to 2040, 2041 to 2070, and 2066 to 2095). While the last of these periods extends beyond the Study period, it provides an important reference for understanding the potential direction of the future Basin hydrology. Therefore, results between the Study and the SECURE Report are not identical; however, work from the Study will be used to inform future reports under the SECURE Water Act.

FIGURE B-36
Methodological Approach for the Development of the Downscaled GCM Projected Scenario

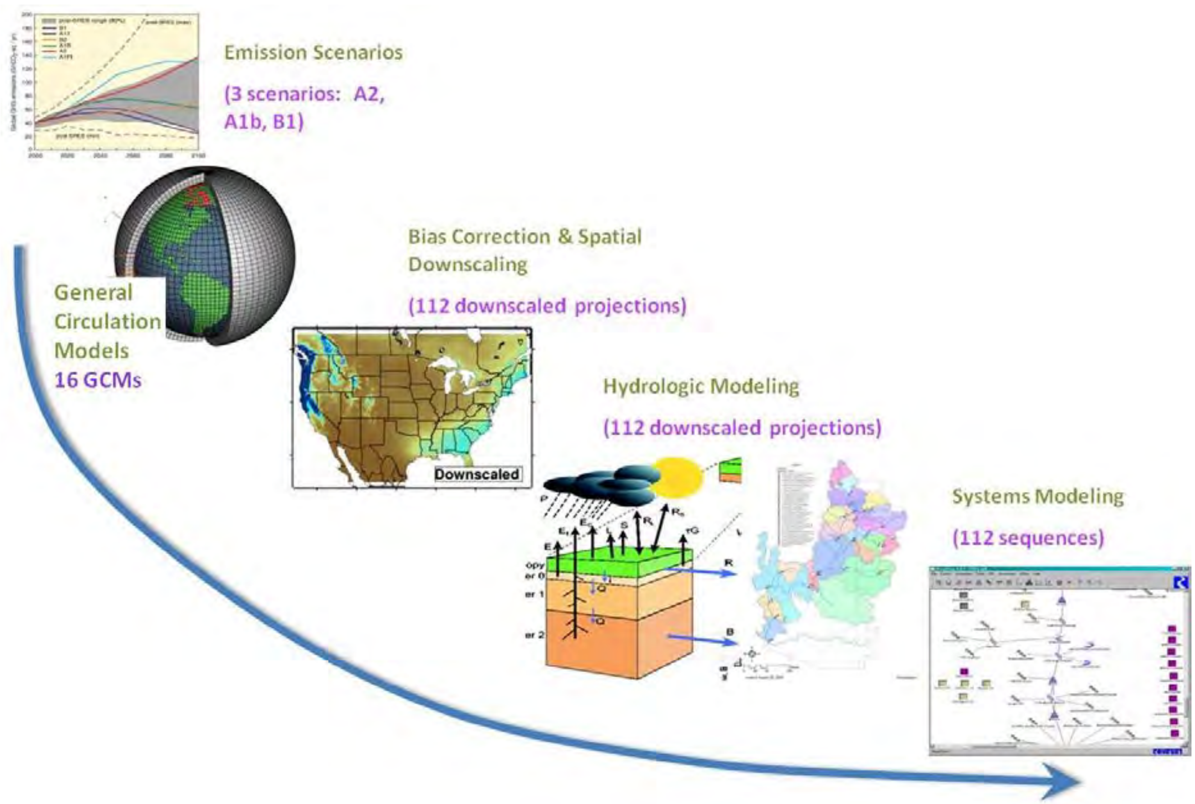

8.1.1 *Emission Scenarios*

As discussed previously, the downscaled climate projections were obtained from the World Climate Research Program's CMIP3 database. This database includes downscaled climate projections from 16 different GCMs simulated with three different IPCC emission scenarios (IPCC, 2000). The emission scenarios are those from the *Special Report on Emissions Scenarios* (SRES) (IPCC, 2000), emission scenarios A2 (high), A1B (medium), and B1 (low), and reflect a range of future greenhouse gas (GHG) emissions. The A2 scenario is representative of high population growth, slow economic development, and slow technological change. It is characterized by a continuously increasing rate of GHG emissions, and features the highest annual emissions rates of any scenario by the end of the 21st Century. The A1B scenario features a global population that peaks mid-century and rapid introduction of new and more efficient technologies balanced across both fossil- and non-fossil intensive energy sources. As a result, GHG emissions in the A1B scenario peak around mid-century. Last, the B1 scenario describes a world with rapid changes in economic structures toward a service and information economy, with reductions in material intensity, and the introduction of clean and resource-efficient technologies. GHG emission rates in this scenario peak prior to mid-century and are generally the lowest of the scenarios.

SRES emission scenarios exist that have both higher (A1FI) and lower (A1T) GHG emissions than those considered in the Study (see appendix B2). However, the three scenarios included in the analysis span the widest range available for which consistent, comprehensive GCM modeling has been performed and for which downscaled climate information is available. Furthermore, while it is possible that higher rates of warming and resulting effects on streamflows are possible, it should be noted that the atmospheric response to emission increases is not immediate. Climate response to increases in GHG emissions is on the decadal scale. Uncertainty in the projected climate system response due to increased emissions (GCM uncertainty) tends to be a greater determinant of the range of climate conditions through mid-century than the uncertainty associated with future emission scenarios themselves.

Assumptions related to parameter characteristics included in the SRES emission scenarios (such as high population growth and slow economic development) are not related to parameter characteristics of the Water Demand scenarios (see *Technical Report C – Water Demand Assessment*) because they describe a global set of drivers rather than those directly associated with the Colorado River. When considering water demand scenarios combined with water supply scenarios that incorporate climate change, outdoor water demands and reservoir evaporation rates were modified to reflect estimates of changes in ET and open water surface evaporation rates consistent with the assumptions for water supply.

8.1.2 GCMs

Sixteen GCMs were coupled with the three emissions scenarios to simulate the global atmosphere and oceans and provide projections of specific climatological forcings (principally temperature and precipitation) during the period 1950 to 2099. Many of the GCMs were simulated multiple times for the same emission scenario due to differences in starting climate system state (initial oceanic and atmospheric conditions); thus, the number of available projections (112) is greater than simply the product of the number of GCMs and emission scenarios. Appendix B2 provides a summary of the GCMs, initial conditions, and emissions scenario combinations featured in the Study. Recent research (Pierce et al., 2009; Gleckler et al., 2008) has shown the importance of incorporating multiple climate projections (even when derived from the same GCM) and the superiority of the multi-model ensemble for a wide array of climate metrics. The subsequent results presented on future climate (primarily temperature and precipitation) and, indirectly, streamflow rely on the data generated by these GCMs.

8.1.3 Bias Correction and Spatial Downscaling

Due to the coarseness of the GCM grids and inherent biases in their results, the GCM results were transformed to a local scale (~12 km) through a process called bias correction and spatial downscaling (BCSD). The methods of this process are described in detail in Wood et al., 2002; Wood et al., 2004; and Maurer, 2007.

The purpose of bias correction was to adjust a given climate projection for inconsistencies between the simulated historical climate data and observed historical climate data. In the BCSD approach, GCM projections were bias corrected at a 2-degree resolution using a quantile mapping technique which corrects the simulated historical monthly temperature and precipitation projections to be consistent with the observed distributions at the same resolution. Following bias correction, the adjusted climate projection data were statistically consistent (monthly cumulative distribution functions were identical) with the observed climate data for the historical overlap period of 1950 to 1999. The bias correction quantile maps derived from the historical overlap period were then used to adjust the GCM projections for the future period. Note that this method assumes that the GCM biases have the same structure during the 20th and 21st Centuries' simulations.

Downscaling spatially translated bias corrected climate data from the coarse, 2-degree (~200 km), spatial resolution typical of climate models to a Basin-relevant resolution of 1/8th-degree (~12 km), which is more useful for hydrology and other applications. The spatial downscaling process generally preserves observed spatial relationships between large- and fine-scale climates. This approach assumes that the topographic and climatic features that determine the fine-scale distribution of large-scale climate will be the same in the future as in the historical period.

8.1.4 Daily Weather Generation (Temporal Dissaggregation)

The resulting BCSD climate projections provided a representation of future monthly temperature and precipitation through 2099. However, to be useful for hydrologic modeling, this information was required on a daily temporal scale. The monthly downscaled data was temporally disaggregated to a daily temporal scale to create realistic weather patterns using the sampling methods described in Wood et al. (2002). To generate daily values, for each month in the simulation a month was randomly selected from the historic record for the same month (e.g., for the month of January, a January is selected from the 1950 to 1999 period). The daily precipitation and temperature data from the historic record were then adjusted (rescaled precipitation and shifted temperature) such that the monthly average matches the simulated monthly value. The same historic month was used throughout the domain to preserve plausible spatial structure to daily storms. The results of the temporal disaggregation were daily weather sequences that preserve the monthly values from the downscaled climate projections. Some uncertainties were introduced depending on the method employed to produce the daily data from the monthly climate values. A comparison of two available methods (Wood et al., 2002, and extension of Wood et al., 2002, described in Salathé, 2005) to generate daily weather patterns for the Study favored the use of the Salathé, 2005, method employed in the SECURE Report to produce the daily downscaled data. An additional description of the comparative analysis is presented in appendix B3.

8.1.5 Hydrologic Modeling

The daily weather sequences were used as input to the VIC hydrologic model to generate estimates of hydrologic fluxes and streamflow under various climate futures. For each of the 112 climate projections, the VIC hydrologic model produced a distinct trace of natural flows at each of the 29 natural flow locations.

Developed at the University of Washington, the VIC model is a semi-distributed, macro-scale hydrologic model that solves the water balance at each model grid cell. A VIC model of the Basin was previously developed by the University of Washington (Christensen and Lettenmaier, 2007), and was provided to Reclamation for the Study. The model has not been further calibrated or refined as part of the Study, but the model performance and bias correction has been evaluated and is discussed in the next section. A thorough description of the VIC model is provided in appendix B4.

Analysis shows (presented in appendix B4) that there are some biases in the VIC streamflows as driven by historical observed and downscaled climate model simulated historical meteorological forcings in comparison with the natural flows for the Basin for the overlapping period of 1950 to 1999. These biases are generally small for mainstem Colorado River locations, but can be large for smaller watersheds and in areas where the VIC model was not specifically calibrated. The mean annual flow bias for the Colorado River at Lees Ferry, Arizona, is positive 1.1 percent. Moving upstream to the three largest contributors to flow at Lees Ferry, the bias is negative 3 percent for the Green River near Green River, Utah, less than 1 percent for the Colorado River near Cisco, Utah, and negative 6 percent for the San Juan River near Bluff, Utah. The VIC model appears to have higher biases in the upper watersheds and lower biases farther downstream as more of the watershed contributes to the flow. In general, the upper Colorado River locations exhibited a positive bias, while the Green River and San Juan River locations exhibited a negative bias.

These biases are due to differences between the GCM-simulated historical climate and observed climate data, differences in hydrology model inputs and parameterization, and differences between the VIC-simulated hydrologic responses and observed watershed responses implied in the natural flows. The lack of calibration of the VIC model for lower order streams within the Basin is believed to be a significant source of the bias at these scales.

A streamflow bias correction method was developed and applied to the “raw” VIC-simulated flows to account for any systematic bias in the hydrology model and/or climate data sets. The method corrected for monthly and annual biases, while ensuring that the corrected flows maintained the system and local mass balance. The raw VIC-simulated streamflows for both the historical and future periods were first adjusted for biases before incorporating into the CRSS modeling. The streamflow bias correction step was an important component for the use of climate-driven hydrologic modeling and results in subsequent systems modeling. Without this step, the VIC-simulated historical flow biases would be carried forward into future assessments and the potential existed for misattribution of some streamflow changes to changes in climate, while these may be partially associated with model/data bias. Details on the methods used to correct for biases are included in appendix B4.

In addition to producing routed natural flows, the VIC model also provided output for other water supply indicators, including precipitation, runoff, baseflow, ET, soil moisture, and SWE. The subsequent results presented on hydrologic processes relied on these parameters generated by the VIC model.

Additional detail on VIC and its application for the Study can be found in appendix B4.

8.1.6 Systems Modeling

A total of 112 realizations at the 29 natural flow locations were taken from the VIC model simulations and subsequently corrected for streamflow biases. Differing from the three other future water supply scenarios, which do not address changes in climate, each Downscaled GCM Projection hydrologic sequence of streamflow exhibits a long-term future trend and increased variability beyond what occurred historically. For the Study, no differentiation was applied for each of the sequences, based on emission scenario or historical GCM skill. In essence, each of the 112 sequences was treated as equally likely when applied in CRSS in later phases of the Study. Included in this report is an evaluation of the relative sensitivity of streamflows to emission scenarios. From a mechanical standpoint, the Downscaled GCM Projected scenario was implemented as 112 distinct projections of the future, each starting in the year aligned with the Study period start year of 2011.

8.2 Uncertainty

The process outlined above and shown graphically in figure B-36, in which climate projections are used to generate projections of future streamflow, contains a number of areas of uncertainty. Each step in the process contains uncertainty, and it is important to recognize these in the interpretation of results. First, emission scenarios describing the global emissions of GHGs over the century were used as the primary input to GCMs. The SRES emission scenarios were used to project a range of future global development pathways. Each emission scenario was considered plausible, but the fact that the range may not be sufficiently broad cannot be ruled out. In addition, the climate system responds to a number of factors that contribute to radiative forcings affecting the warming of the earth’s surface. Factors such as aerosols, solar activity, surface albedo, and variations in the earth’s orbit, all influence the earth’s energy balance. These mechanisms are included in the climate models to the degree they are understood and can be projected into the future, but represent an inherent uncertainty in attempting to simulate the global climate system on decadal and century scales. Anthropogenic carbon dioxide emissions, which are directly represented in the emission scenarios, are believed to represent the largest component of the estimated radiative forcing (IPCC, 2007).

Second, GCMs are used to simulate global climate patterns resulting from atmospheric forcings and feedbacks throughout the land, ocean, and atmosphere interactions. The GCMs were applied at relatively coarse scales (~150- to 200-km resolution) in relation to what is required for watershed assessments, and therefore are not likely to capture important regional phenomena. Because of the atmospheric lag from GHG emissions, much of the uncertainty in climate projections through mid-century is associated with the structure and application of the many different GCMs themselves, rather than the emission scenarios driving them. The GCM results were necessarily bias corrected and spatially downscaled to be useful at the watershed scale. These bias correction and downscaling processes, while necessary, removed some of the physical linkages from the climate projections and introduced an aspect of further uncertainty. High-resolution regional climate modeling may help resolve some of the scale mismatch (both spatially and temporally) in the future, but the availability of these simulations over a broad ensemble of models and emission scenarios is limited. The statistical downscaling method employed in the Study preserves monthly observed precipitation and temperature statistics for the overlapping period at the 2-degree spatial scale. However, the statistics at finer spatial scales (i.e., 1/8th-degree scale) or longer temporal scales (seasonal, annual, and longer scales) are not necessarily preserved. Analysis included in appendix B3 provides further information on this topic.

Finally, hydrologic models are approximations of the complex physical processes that occur on the watershed scale. The VIC model is considered a strong, physically based hydrology model, but simulates hydrologic processes at the macro scale. The model necessarily needs to parameterize certain aspects of the hydrologic cycle to capture the effects at smaller scales. Several assumptions in the VIC modeling approach carry considerable uncertainty. First, the VIC modeling assumes that land use and vegetative cover are fixed throughout the simulation period. Future assumptions of land use that are consistent with the socioeconomic assumptions in the water demand scenarios were not integrated into the water supply scenarios. Changes in climate are likely to drive changes in native and invasive species (vegetative, terrestrial, avian, and aquatic) distribution and these will influence the physical watershed and future hydrologic processes and streamflow. The magnitude of these impacts is believed to be relatively small compared to the effects of changes in direct temperature and precipitation; however, the magnitude has not yet been quantified.

In addition, the VIC model, as described in this report, has been adopted without re-calibration. Results appear reasonable at the larger watershed scale, but there is observed bias in particular watersheds and at the sub-watershed scale. A bias correction method has been applied to compensate for some of the biases, but in doing so it necessarily introduces assumptions on the linkages between past and future climates that are not yet known.

8.3 Results

The results of the 112 future climate projections are presented in this section for climate, hydrologic processes, and streamflow. Climate teleconnections are discussed primarily in a qualitative manner due to the broad uncertainty in projecting future states of coupled ocean-atmosphere conditions. For climate, results are presented in terms of annual precipitation and temperature trends, followed by an analysis of seasonal trends. For hydrologic processes, results are presented for ET, snowpack, soil moisture, and runoff. Both annual and seasonal analyses are presented. The last section of the results focuses on projected changes in streamflow, both annual and seasonal, and predominately at the Colorado River at Lees Ferry, Arizona location.

Climate and hydrologic process results are presented as changes from the 30-year historical climatological period (1971 to 2000) to three future 30-year periods (2011 to 2040, 2041 to 2070, and 2066 to 2095). Thirty-year periods were chosen to span the almost 90-year future projection period (2011 to 2099). In addition, due to the difference in initial atmospheric-ocean conditions between the GCMs, a 30-year period is sufficient to separate projected average conditions from individual and multi-year variability. For simplicity, these periods are referred to as the year in which they are centered: i.e., 1985, 2025, 2055, and 2080.

Although the Study period is through 2060, the 112 future climate projections extend through 2099. The additional approximate 40 years of projections have been included in the analyses for the climate and hydrologic processes results because they offer additional insight into the projected changes of these parameters. To facilitate a more direct comparison with the projected streamflow from the other three scenarios (Observed Resampled, Paleo Resampled, and Paleo Conditioned), streamflow results are presented through 2060.

Under the scenario planning approach employed in the Study, each future climate projection was viewed as a plausible future. The probability or likelihood of each future projection is unknown, hence summary statistics of the resulting projections such as mean or median of the ensemble projection is not the most likely future, but simply the central tendency of the ensemble. For the Observed Resampled, Paleo Resampled, and Paleo Conditioned scenarios summary statistics are grounded by a stationary hydroclimate assumption. Given the increasing debate concerning the validity of a stationary hydroclimate assumption, it is tenuous to assert that the past record is predictive of future conditions. Thus, while summary statistics such as mean and median are used in part to present these data, it is important to consider the full range of outcomes, which are also provided throughout these results.

In the case of the Downscaled GCM Projected scenario, this consideration is further complicated by the ensemble of results. Each of these traces is a unique combination of initial conditions, GCM choice, and future emission scenario. The resulting streamflows are all considered plausible futures. However, summary statistics can be computed by various approaches, which influence the outcome of these values. Thus, understanding the full range of results is even more paramount in this supply scenario. Recent literature on the topic has found that an ensemble of results with multiple realizations from a single GCM can inadvertently bias the ensemble statistics favoring the GCM with multiple realizations. Hence, in some cases it may be prudent to combine realizations from each GCM such that each contributes equally to the ensemble and associated statistics. The alternate perspective suggests that with more runs from a particular GCM, there is greater confidence and understanding of the GCM’s tendencies. This is desirable and might merit greater weight than a GCM with only one realization. The latter introduces sizable uncertainty to the ensemble as it is unknown if additional realizations from the GCM with a single realization would yield similar results or vary widely. In practice, the most prudent approach is a case by case consideration of these and other methods to determine the most appropriate path forward. In the Study, the results were found to be insensitive to the method by which summary statistics were computed (ensemble mean streamflow projections were within 1 percent of each other under both approaches). Results presented throughout the following sections weight all GCM realizations equally simply describing summary statistics based on the 112 available projections. Acknowledging that a summary statistic alone cannot capture the complexity of these results, ranges, percentiles and other distributional measures are also provided.

8.3.1 Climate

Climate projections from the 112-projection ensemble indicate a strong continued warming throughout the Basin. Figure B-37 shows the Basin average temperature and precipitation projections for 1950 to 2099 (the length of the GCM projection period) in relation to the 1950 to 2005 (the length of the observed climate period) historical observed climate. The projection ensemble indicates substantial warming, with a median increase in annual temperature of about

1.3 ºC by 2025, 2.4 ºC by 2055, and 3.3 ºC by 2080. All projections are consistent in the direction of the temperature change, but vary in terms of climate sensitivity. Annual precipitation trends are not apparent in this Basin-wide analysis. Roughly half of the projections indicate a wetter future, while the other half indicate drier conditions. The uncertainty in future annual precipitation appears to be increasing with time, while the median of the projections is relatively unchanged.

Figure B-38 presents the change in mean annual temperature (absolute change) and precipitation (percent change) for three future periods: 2011 to 2040 (2025), 2041 to 2070 (2055), and 2066 to 2095 (2080), relative to the 30-year historical period 1971 to 2000 (1985). For most of the Basin, temperature increases are within 1.0 °C to 1.5 °C, 2.0 °C to 2.5 °C, and 3.0 °C to 4.0 °C for 2025, 2055, and 2080, respectively. The Upper Basin is projected to warm more than the Lower Basin. Projected precipitation changes are relatively modest in 2025. However, by the 2055 and 2080 periods, precipitation decreases by up to 10 percent in much of Lower Basin. In contrast, precipitation increases by up to 10 percent in the Upper Basin at higher elevation and toward the north (Green River Basin).

Maps of seasonal changes in temperature and precipitation for the three future 30-year periods are included in appendix B6 and are summarized here.

The seasonal analysis shows that 2055 projected seasonal temperature changes exhibit minimal geographic variation in the fall. Winter and summer temperatures in the Upper Basin increase slightly more than those in the Lower Basin. Projected temperature increases are lowest in winter, ranging from 1.5 °C to 2.5 °C. The largest projected temperature increases occur in summer, and range from 2.5 °C to 3.0 °C.

The 2055 change in projected mean winter precipitation is highly varied throughout the Basin, with values in the Lower Basin decreasing from 0 to 15 percent and the values in the Upper Basin increasing from 0 to 15 percent. However, it should be noted that on an absolute basis, the Upper Basin receives considerably more rainfall than the Lower Basin, such that a 15 percent change is substantially more total precipitation in that region. During spring, precipitation is projected to decrease throughout the Basin. The most severe reductions (on a percentage basis) occur in the southwestern region, where the decline is up to 30 percent. Summer is the only season in which projected precipitation shows a decrease in the Upper Basin and an increase or no change in the Lower Basin. Trends in fall precipitation closely resemble those of the winter season, but the projected percent changes for fall are lower in magnitude.

Figure B-39 summarizes projected changes in climate conditions on a watershed basis, as indicated by the 112-projection ensemble for the three future 30-year periods. Each point represents a single watershed (one for each contributing area). The location of a point in the figure is determined by the mean projected change in temperature between the future periods and the simulated historical period 1971 to 2000, and the mean projected change in precipitation between the future periods relative to the simulated historical period. Change in temperature is measured in ºC, while change in precipitation is measured as a percentage.

FIGURE B-37
Historical (line series with markers) and Projected Annual Average Temperature (top) and Projected Annual Total Precipitation (bottom) Smoothed as a 10-year Mean
Shading represents a range of projections and the solid line represents a median of projections.

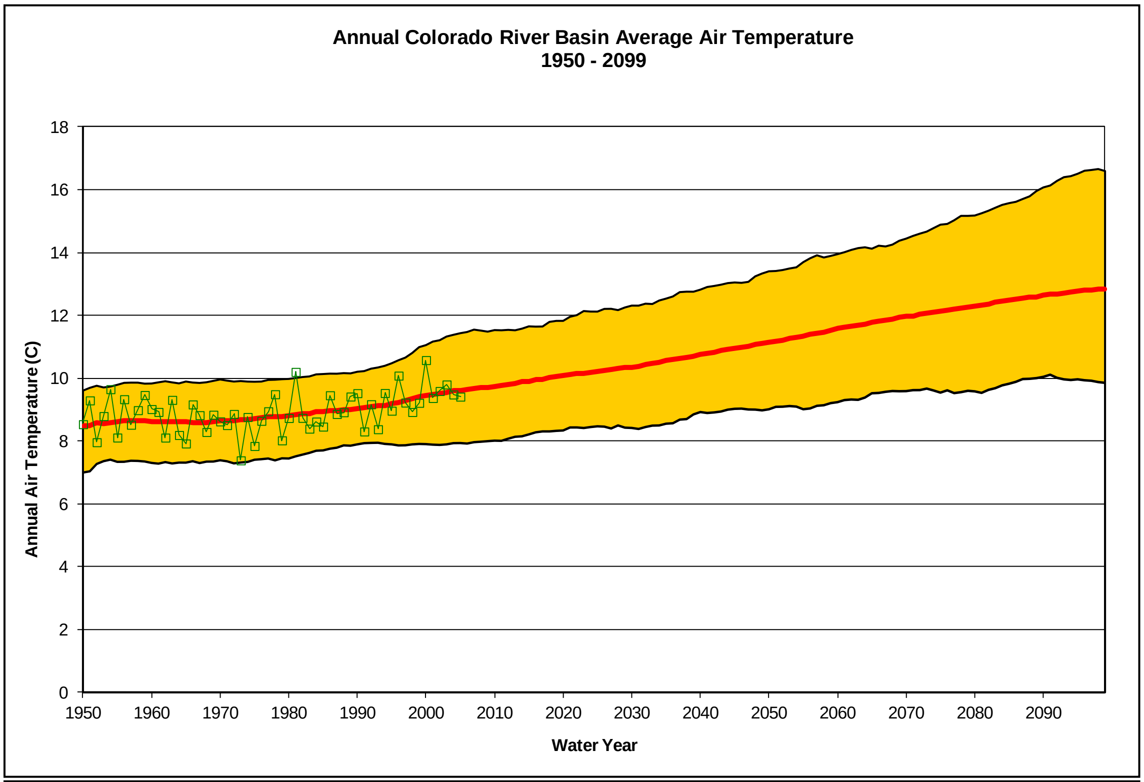

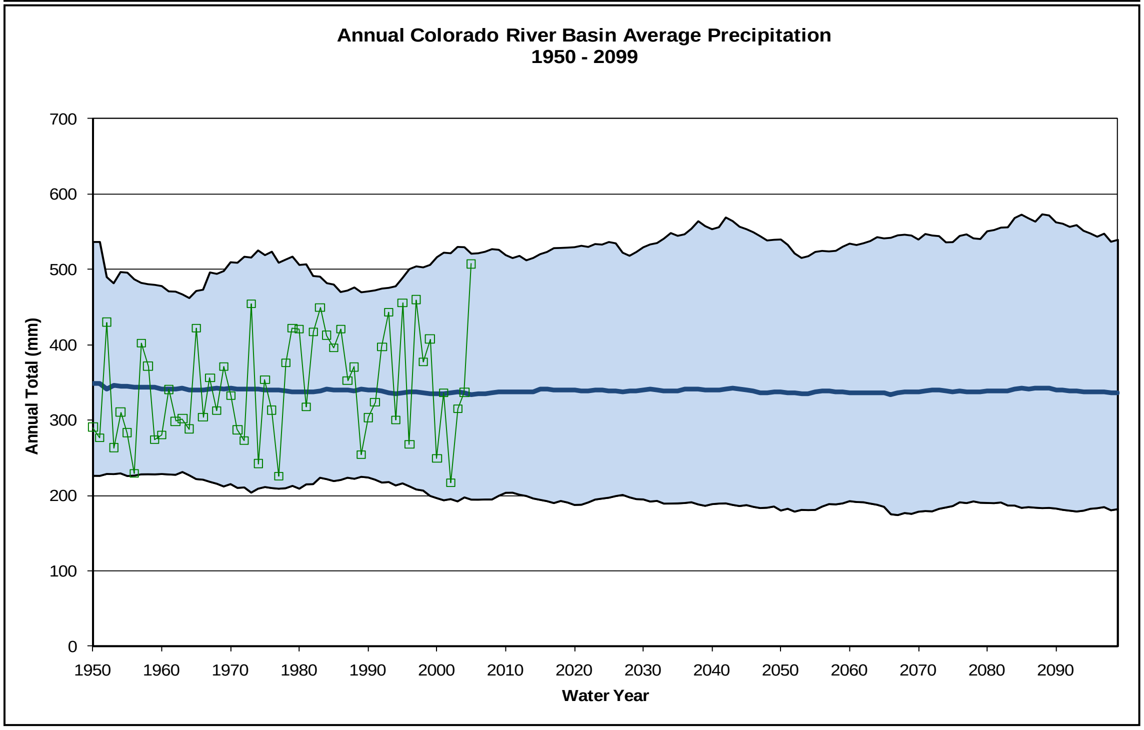

FIGURE B-38
Mean Projected Change in Annual Temperature and Precipitation
2025 (2011–2040) versus 1985 (1971–2000), 2055 (2041–2070) versus 1985 (1971–2000), and 2080 (2066–2095) versus 1985 (1971–2000).

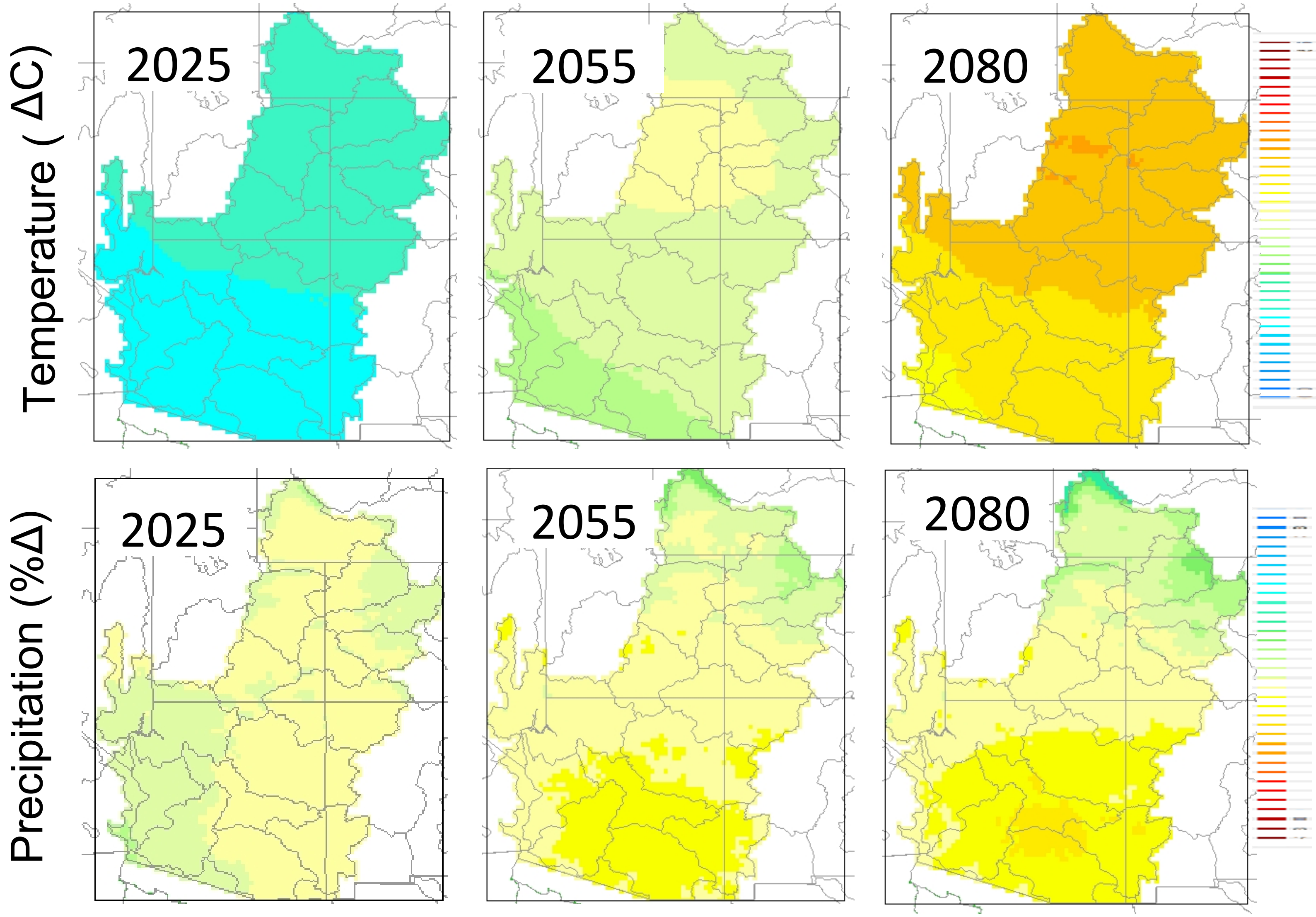

FIGURE B-39
Projected Changes in Mean Seasonal and Annual Temperature and Precipitation for the Colorado River Basin
Periods are 2025 (2011–2040); 2055 (2041–2070); and 2080 (2066–2095), compared to the 1985 (1971–2000) historical period (hollow symbols represent Lower Basin locations, while solid symbols indicate Upper Basin locations).

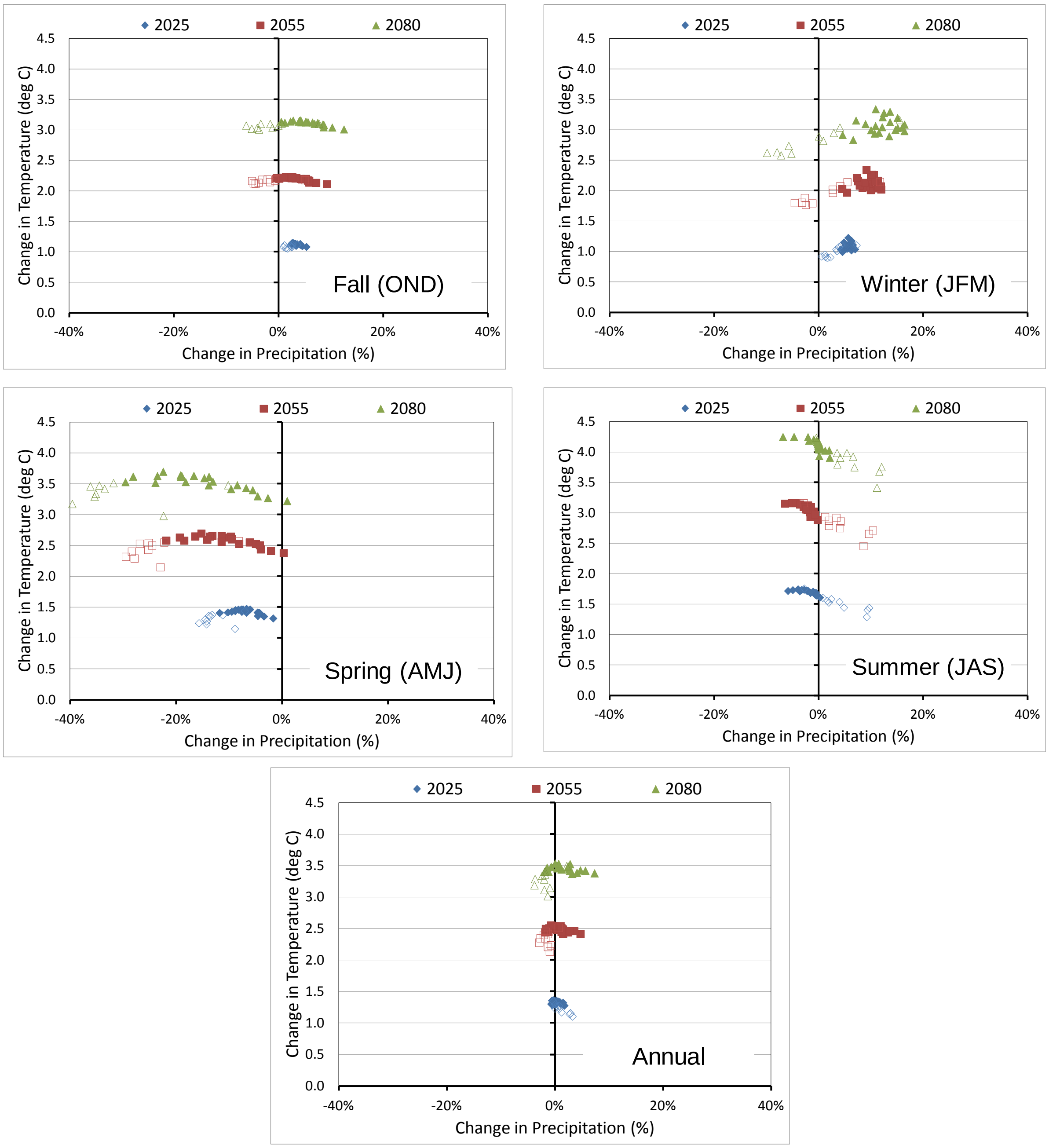

For a given season and future time period, projected changes in temperature are relatively consistent across all watersheds, with little variation throughout the Basin. By 2025, temperatures are projected to increase at least 1.0 °C in nearly all watersheds for all four seasons. Spring and summer show the greatest warming, with seasonal temperatures in most watersheds increasing 3 °C to 4 °C by 2080. Annual temperature increases are projected at 1.0 °C to 1.5 °C, 2.0 °C to 2.5 °C, and 3.0 °C to 3.5 °C for 2025, 2055, and 2080, respectively.

Projected changes in seasonal precipitation vary widely across watersheds and seasons. In general, relative precipitation variability increases with time. On an annual basis, projected precipitation through 2080 is generally within 5 percent of historical precipitation, with half of the Basin's watersheds exhibiting positive change and half exhibiting negative change. The most significant and monotonic change in precipitation occurs in spring, during which all watersheds show a decrease in precipitation for each of the future time periods. By 2080, the decrease in spring precipitation ranges from 0 to 40 percent, with the values well distributed within the range. During fall and winter, small increases (less than 10 percent) are projected for 2025, but bimodal patterns of increases in the Upper Basin (about 20 percent for winter in 2080) and decreases or neutral changes in the Lower Basin (about 10 percent for winter in 2080) begin to appear in the 2055 and 2080 time periods. Summer is the only season in which the bimodal pattern is reversed with decreases in precipitation projected in the Upper Basin and increases in the Lower Basin (see appendix B6 for projected seasonal precipitation maps). The summer pattern is likely due to a more active monsoon and increased moisture flow from the Gulf of California during this season simulated in the GCMs, although the summer precipitation associated with the monsoon is poorly simulated in most climate models (Lin et al. 2008; Gutzler et al. 2005).

8.3.2 Summary of Changes in Climate

- Warming is projected to increase across the Basin, with the largest changes in spring and summer and larger changes in the Upper Basin than in the Lower Basin. Annual Basin-wide median temperature increases are projected to be approximately 1.3 °C, 2.4 °C, and 3.3 °C for 2025, 2055, and 2080, respectively, with less warming in winter and higher warming in summer.

- Precipitation patterns continue to be spatially and temporally complex, but projected seasonal trends toward drying are significant in certain regions. Precipitation patterns are complex due to influence of oceans, storm tracks, changes in atmospheric circulation patterns (e.g., Hadley cell expansion), and the interplay with mountainous regions (orographic considerations). A general trend toward drying is present in the Basin, although increases are projected in the higher elevation and most hydrologically productive regions. Consistent and expansive drying conditions are projected for the spring throughout the Basin. For much of the Basin, drying conditions are projected in the summer, although some areas of the Lower Basin are expected to experience slight increases in precipitation which may be due to the monsoonal influence in this region. Upper Basin precipitation is projected to increase in the fall and winter, while the Lower Basin is expected to experience a decrease. Despite drying spring conditions in the Upper Basin, annual precipitation is projected to increase in the higher elevations due to higher winter precipitation increases in these regions. Projections demonstrate a bi-modal pattern of precipitation changes in fall and winter, with the Upper Basin projected to experience increases and the Lower Basin projected to experience decreases. The division of wetter versus drier conditions in the winter moves northward with continued warming through time, consistent with an expansion of the Hadley cell and more northerly storm tracks (Seager and Vechhi, 2010).

8.3.3 Hydrologic Processes

Figures B-40 and B-41 present grid cell-based VIC model output via Basin-wide spatial plots for ET, runoff, soil moisture, and SWE. For each future time period and for each parameter, the mean projected annual changes are presented. Projected seasonal changes for these parameters can be found in appendix B6.

Figure B-40 shows the percent change in mean annual ET and mean annual runoff. ET is projected to increase in most high elevation and northerly areas of the Upper Basin and is strongly related to the availability of soil moisture. In the Lower Basin, where decreased precipitation is projected (and subsequently reduced soil moisture), ET is projected to decrease substantially, particularly in the 2055 and 2080 periods. Runoff is projected to decrease substantially (up to 30 percent) across large areas of the Basin, with greatest reductions in the south and at high elevation. Elsewhere, projected decreases are generally within 15 percent of the historical period through 2080. Runoff is projected to increase for small areas in the northeastern portion of the Basin (Green River Basin primarily). The increases in the northern portion of the Basin are an important finding and contribute significantly to mitigate reduced runoff trends for much of the rest of the Basin.

Figure B-41 shows the mean percent change in April 1 SWE and July 1 soil moisture. With few exceptions, April SWE is projected to decline by up to 30 percent throughout the Basin by 2025 as more precipitation falls as rain and as warmer conditions lead to earlier snowmelt. This process becomes more pronounced in the 2055 and 2080 periods. July 1 soil moisture is projected to decrease by 5 to 10 percent throughout the Basin for the three future time periods. The loss of soil moisture is primarily the result of the greater moisture availability for ET earlier in the year (more rain less snow and earlier melt of snowpack) in the higher elevation Upper Basin and reduced overall precipitation in the Lower Basin. The most substantial decline occurs in the northeast portion of the Basin.

Maps of seasonal changes in ET, runoff, soil moisture, and SWE for the three future 30-year periods are included in appendix B6 and are summarized here.

Projected 2055 changes in ET vary substantially throughout the Basin. In general, ET is projected to increase during fall and winter, but decrease during summer for the majority of the Basin. Projected ET changes exhibit considerable geographic variability and range in magnitude during spring, when portions of the Upper Basin have ET increases of up to 30 percent and portions of the Lower Basin have ET decreases of up to 30 percent. Both phenomena are related to soil moisture availability. Increases in Upper Basin ET are due to greater soil moisture availability, while Lower Basin decreases are due to reduced available soil moisture. During summer, projected 2055 changes in ET range from -5 to -10 percent in most locations.

Projected 2055 changes in runoff also vary substantially throughout the Basin. In most seasons, runoff declines throughout the Basin. However, increases are projected for portions of the Upper Basin in fall and winter, and for the extreme southwestern portion of the Basin for all seasons. The projected decline in runoff is most substantial during spring, when several areas in both the Upper and Lower Basins feature a runoff reduction of up to 30 percent. Portions of the Upper Basin exhibit a reduction of similar magnitude during both summer and fall.

FIGURE B-40
Mean Projected Percent Change in Annual ET and Median Projected Percent Change in Runoff[1]
2025 (2011–2040) versus 1985 (1971–2000), 2055 (2041–2070) versus 1985 (1971–2000), and 2080 (2066–2095) versus 1985 (1971–2000).

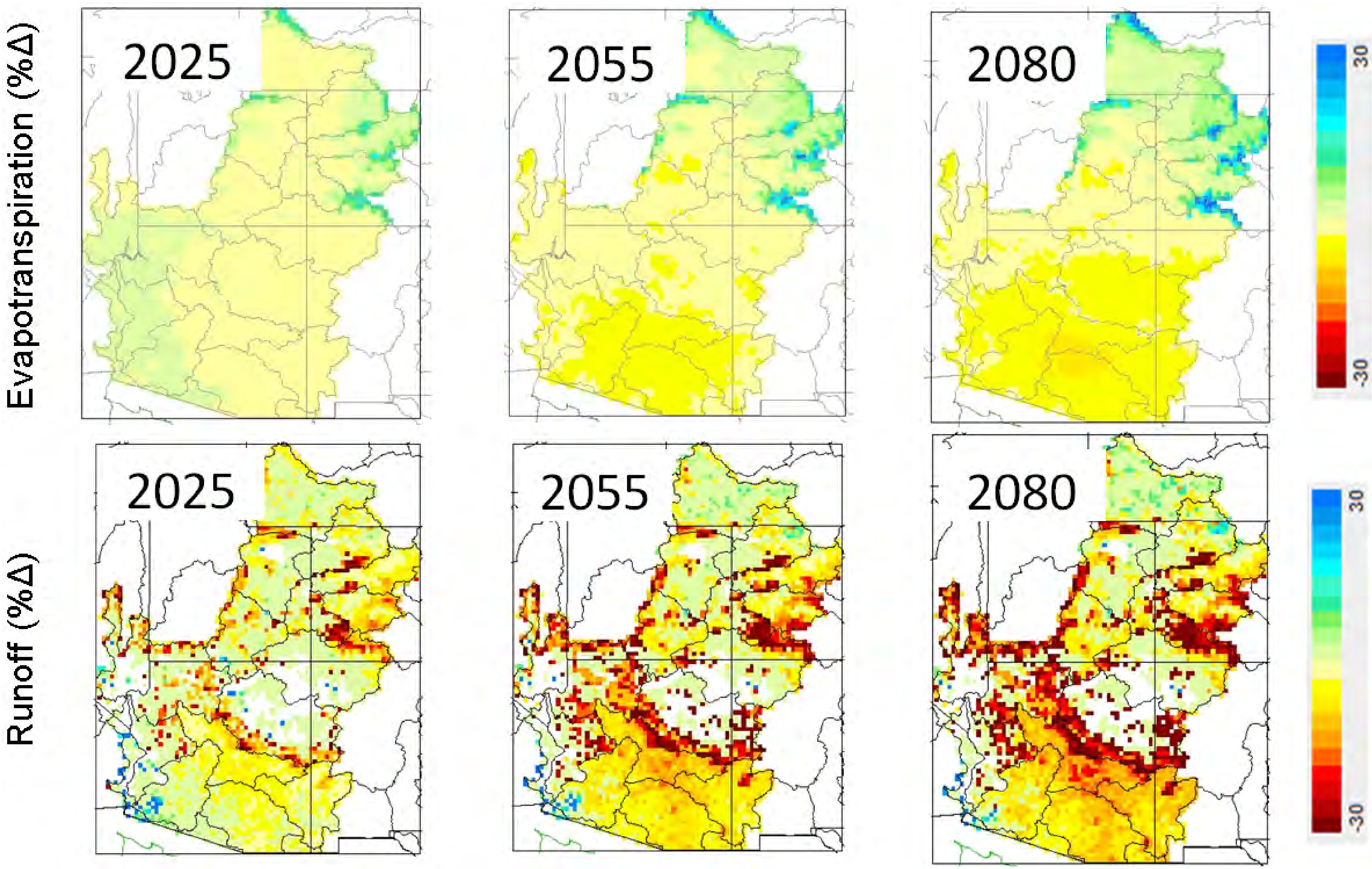

[1] Median is used for runoff percent change, rather than mean because regions of extreme low historical precipitation may show disproportionately high percentage changes.

FIGURE B-41
Mean Projected Percent Change in April 1 SWE and July 1 Soil Moisture
2025 (2011–2040) versus 1985 (1971–2000); 2055 (2041–2070) versus 1985 (1971–2000); and 2080 (2066–2095) versus 1985 (1971–2000).

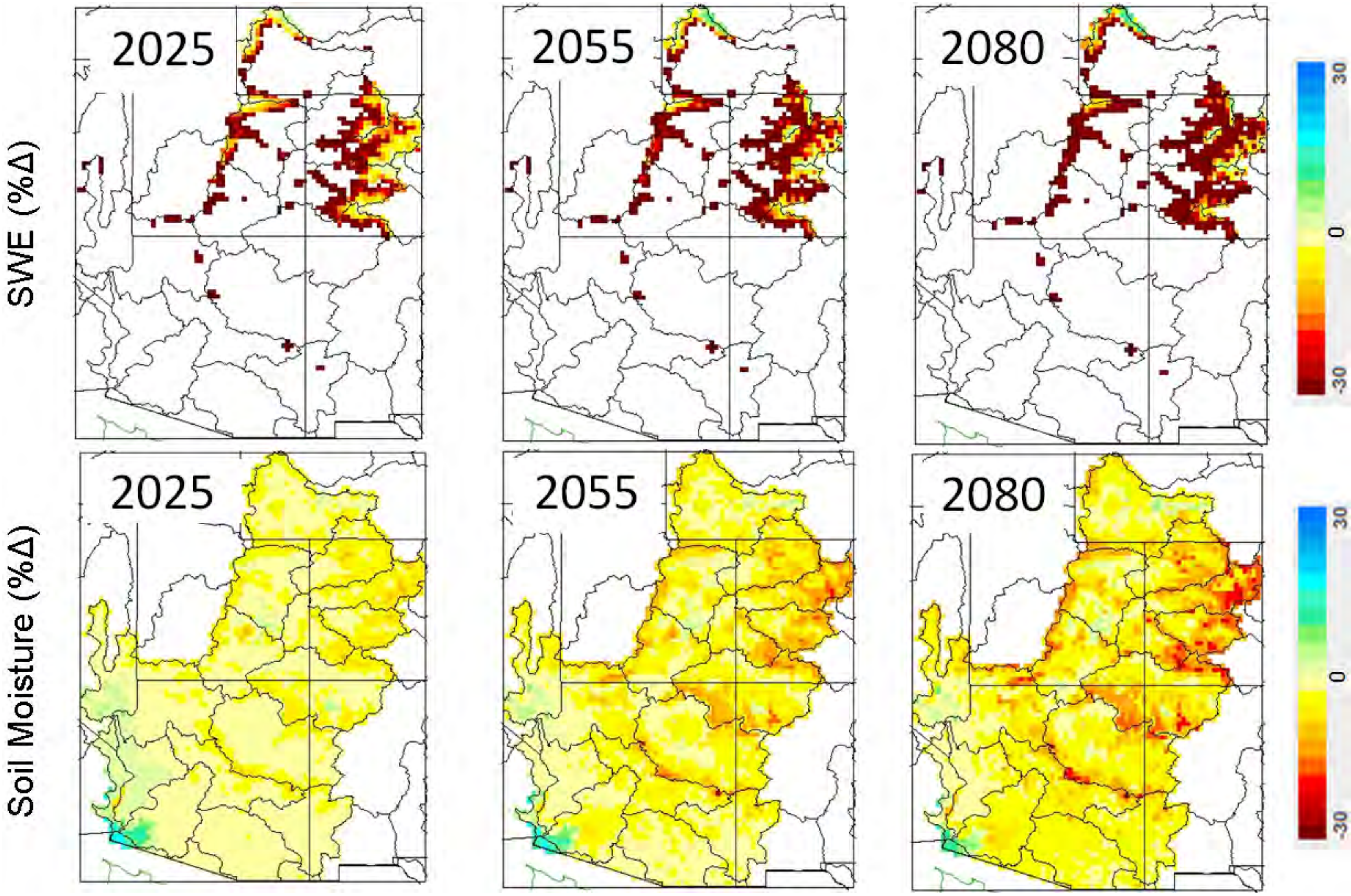

The results of the watershed-based statistical analysis of VIC model output (climatological and hydrologic parameters) are presented for two representative Basin watersheds. The selected watersheds are those immediately upstream of the Colorado River at Glenwood Springs, Colorado, and the Colorado River at Hoover Dam. These select watersheds represent a high elevation headwaters region in the Upper Basin and a lower elevation, warmer region in the Lower Basin. Additional locations representing a more-robust cross-section of the Basin are included in appendix B6.

Figures B-42 and B-43 each present the changes in six hydrologic parameters (precipitation, temperature, ET, runoff, SWE, and soil moisture) from the 30-year historical period (1971 to 2000) to three future 30-year periods: 2011 to 2040 (2025); 2041 to 2070 (2055); and 2066 to 2095 (2080). Figure B-42 presents these hydrologic parameter changes for the Colorado River at Glenwood Springs, Colorado. The results for this watershed are representative of those for other watersheds in the high elevation Upper Basin:

- Precipitation: In the three future time periods, the Upper Basin watersheds experience a shift in the timing of precipitation; more precipitation occurs in fall and winter (November through March) and less occurs in spring (April through June) relative to historical conditions. For this watershed, the increases in precipitation in fall/winter are greater than the reductions in spring/summer, resulting in a net increase.
- Temperature: Monthly temperatures increase from 1.0 °C to 1.5 °C by 2025, and by 2.5 °C to 4.0 °C by 2080 relative to the 30-year historical period of 1971 to 2000.
- ET: Although ET is relatively unchanged from September through March, spring months (April through June) feature a marked increase.
- SWE: Snowpack, as indicated by SWE, is consistently less in the future than in the historical period, particularly from March through June. Shifts in both runoff and soil moisture indicate that some portion of the reduction in spring SWE may be related to earlier snowmelt.
- Runoff: Runoff is projected to increase in March, April, and May, while both precipitation and SWE are reduced during April and May. This suggests an earlier snowmelt that supplies the increased runoff from March through May and contributes to a reduction in snowpack. This is further supported as runoff is substantially reduced in June and July, suggesting that the melting snowpack, which historically supplied runoff during these months, has been substantially reduced by this time.
- Soil moisture: Soil moisture is increased from February through April in conjunction with increased snowmelt infiltration. However, relative to historical conditions, the projected soil moisture is lower for the remainder of the year, exhibiting the most substantial reduction in June.

Figure B-43 presents these plots for the Colorado River at Hoover Dam. The results for this watershed are representative of those for other watersheds in the Lower Basin. Due to the limited snowpack in the Lower Basin and its resulting limited role in the hydrologic processes of this region, the SWE results for the Lower Basin are not considered in these plots. Relative to the

FIGURE B-42
Projected Change in Mean Monthly Climatological and Hydrologic Parameters: 01-Colorado River at Glenwood Springs, Colorado (Upper Basin)

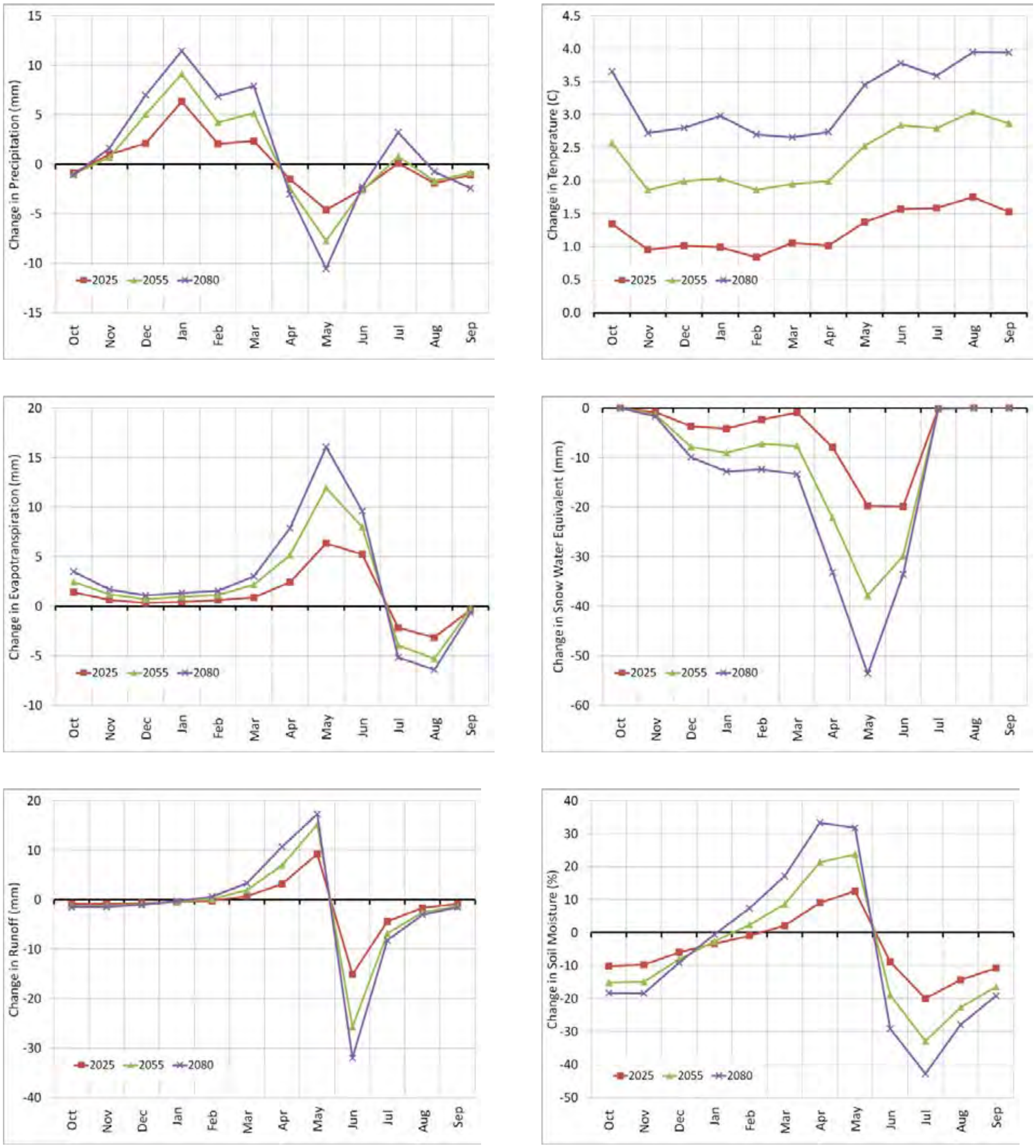

FIGURE B-43
Projected Change in Mean Monthly Climatological and Hydrologic Parameters: 25-Colorado River at Hoover Dam

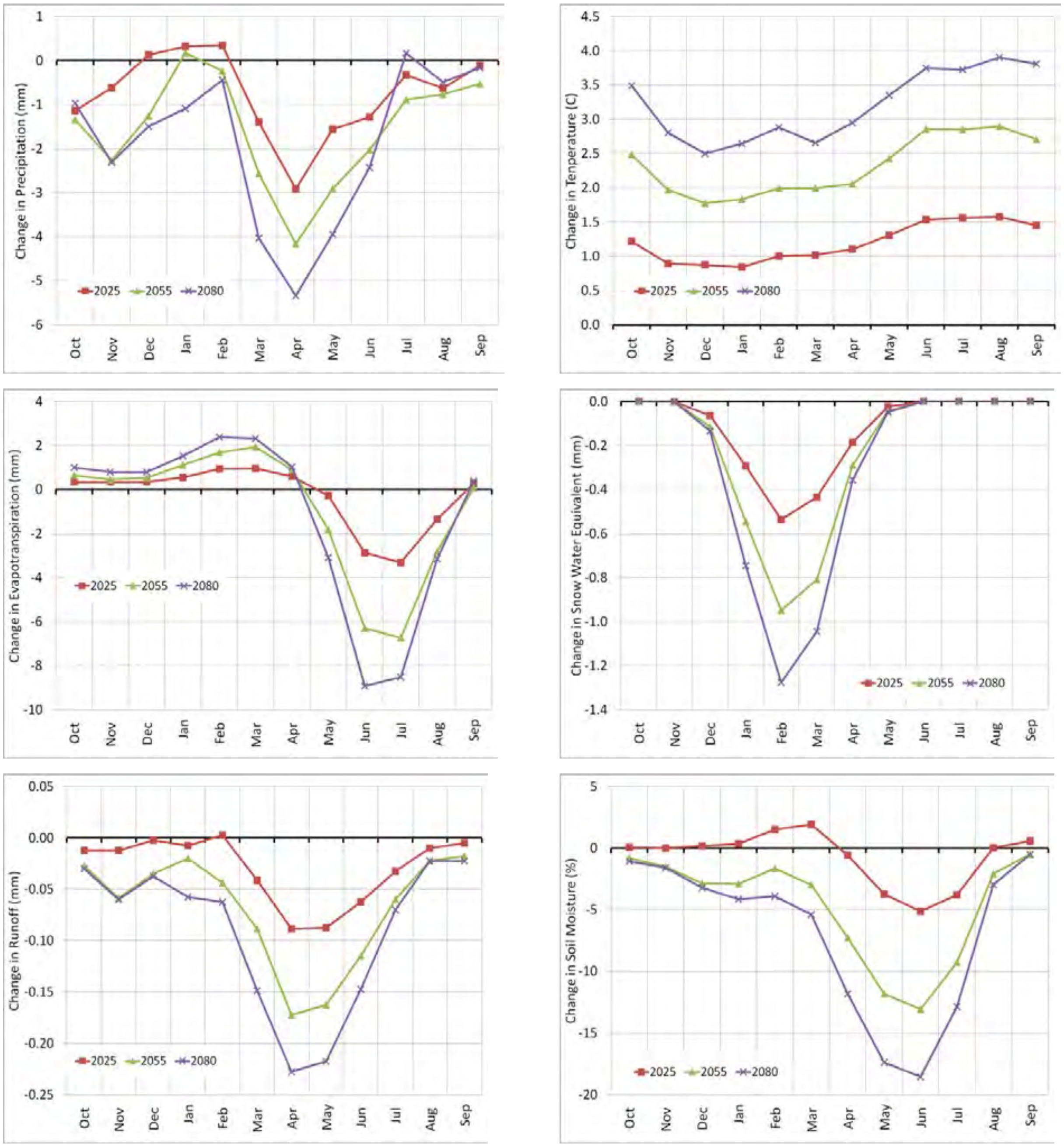

Upper Basin, the changes projected for the Lower Basin are smaller in magnitude on an absolute scale (e.g., change in mm rather than change in percentage):

- Precipitation: In the Lower Basin, precipitation is projected to decrease during half of the year, with spring exhibiting the most notable decline.
- Temperature: Monthly temperature increases are projected throughout the year ranging from 1.5 °C by 2025 to 4.0 °C by 2080.

- Evapotranspiration: ET is noticeably reduced in late spring and early summer, though modest increases are projected for winter. The marked reductions in late spring and early summer are likely due to the reductions in precipitation, runoff, and soil moisture that occur during these times.
- Runoff: Runoff is reduced during all seasons at this location and is more pronounced in the 2055 and 2080 time periods. Reductions result from the compounding effects of decreased precipitation and increased winter and early spring ET. It should be noted that runoff in this watershed (and similar watersheds in the Lower Basin) is very small and contributes little to the overall flow in the Colorado River. Runoff is usually less than 5 to 10 percent of the precipitation in this region.
- Soil Moisture: Soil moisture is projected to be lower year round, with the largest reductions occurring in the spring.

In the future, the Lower Basin is generally projected to have less water in the form of precipitation and soil moisture year round, and especially during winter and spring. However, the magnitude of these reductions is modest.

8.3.4 Summary of Changes in Hydrologic Processes

- PET generally increases with warmer conditions and suggests a theoretical increase in ET demand. Actual ET, which is limited by soil moisture availability, is projected to increase across the Basin during seasons of highest available soil moisture. ET increases are projected in the Upper Basin (at lower elevations) and the Lower Basin in fall and winter as snowpack is not significant and warmer temperatures exist. Substantial ET decreases in the Upper and Lower Basin are projected in summer as soil moisture is depleted earlier than under historical conditions. During spring, peak increases in ET are projected in the Upper Basin (at higher elevations) as higher winter precipitation and earlier snowmelt allow a higher percentage of PET to be satisfied. Conversely, in the Lower Basin, the largest decreases are projected during the spring as precipitation, runoff, and soil moisture are reduced during this time. ET changes described here are from natural watershed and non-irrigated areas. ET effects on irrigated areas and water demand are discussed in *Technical Report C – Water Demand Assessment*.
- Snowpack is projected to decrease as more precipitation falls as rain rather than snow and warmer temperatures cause an earlier melt. Decreases in snowpack in the fall and early winter are expected in areas where precipitation is not changed or is increased, and is caused by a greater liquid form of precipitation due to warming. Substantial decreases in spring snowpack are expected and projected to be widespread, due to earlier melt or sublimation of snowpack.
- Soil moisture represents a significant portion of the seasonal watershed storage and buffers monthly changes in water availability and consumptive use. The interplay among precipitation, snowpack, ET, and runoff causes changes in soil moisture conditions. In general, soil moisture is depleted earlier in the year, and deficits persist longer into the late fall and early winter compared to historical conditions. In regions with overlying snowpack, earlier melt implies earlier contribution to soil moisture storage and an earlier opportunity for ET to consumptively use this stored water. In all regions, there is projected to be increased

PET due to warming. However, actual ET is governed by water availability; and when such soil moisture storage is depleted actual ET is curtailed. Reductions in soil moisture at the beginning of summer (approximated as July 1) are modest but consistent throughout the Basin. Larger reductions are projected in the higher elevation portions of the Basin where moisture persists longer. Overall, the watershed enters the winter season with larger soil moisture deficits and greater opportunity to store and consume winter precipitation.

- Runoff (both direct and baseflow), the balance of hydrologic processes affecting the supply and demand at the local grid-scale, is spatially diverse, but is generally projected to decrease, except in the northern Rockies. As with precipitation, runoff is projected to increase significantly in the higher elevation Upper Basin during winter, but exhibits decreases during spring and summer. Increases in runoff in the summer across the southwestern portion of the Basin are consistent with higher precipitation rates, possibly associated with a more active monsoon. However, the increases from an absolute change perspective are small (generally less than 5 mm [0.15 inch] per year) and do not contribute to substantial net supply to the Colorado River. Due to the minimal amount of annual rainfall in this region, however, caution should be taken in interpreting a percentage increase (a small increase from near zero is a large percentage increase).

8.3.5 Climate Teleconnections

Climate change projections of ENSO characteristics for the balance of this century are model-dependent and inconclusive. Not all the GCMs used in the Study simulate the dynamics of ENSO and other longer-term indices with fidelity. AchutaRao and Sperber (2002) evaluated ENSO simulations using 80-year control runs from 17 GCMs that participated in the CMIP3. They found that only a subset of the GCMs produce realistic amplitudes of NINO3 (index of the sea surface temperatures in the Pacific Ocean) and SOI, but ENSO often tends to occur at higher than observed frequency. In their recent study (AchutaRao and Sperber, 2006), though, they find the next generation GCMs that participated in the IPCC AR4 tend to be more realistic in representing the frequency with which ENSO occurs. The GCMs are better at locating enhanced temperature variability over the eastern Pacific Ocean. They suggest multi-century integrations of GCMs may be required to statistically assess model improvement of ENSO.

ENSO has an important role in western U.S. climate. Whether the frequency and characteristics of ENSO will be changed in a changing climate has strong practical importance. A few of the recent studies analyzed GCM simulations to address these questions (Yeh et al. 2009; Collins et al., 2010). However, there is no common consensus yet in the scientific community. Collins et al. (2010) argue that despite considerable progress in the understanding of the impact of climate change on many of the processes that contribute to El Niño variability, it is not yet possible to say whether ENSO activity will be enhanced or damped, or if the frequency of events will change. Yeh and Kirtman (2007) investigate two coupled GCMs—the Meteorological Research Institute’s model, and the Geophysical Fluid Dynamics Laboratory’s model—to analyze projected ENSO amplitude changes using a four times carbon dioxide emission scenario. They determine that despite the large changes in the tropical Pacific mean state, the changes in ENSO amplitude are highly model-dependent. Results suggest that the understanding of changes in ENSO statistics among various climate change projections is highly dependent on whether the model ENSO is in the linear or nonlinear regime. ENSO and PDO provide only limited skill in determining basin precipitation; thus, even improved simulation results for these indices may be of limited value in making assessments of future supply conditions. Further research is needed to investigate the teleconnections and the direction of these teleconnections in the future.

8.3.6 Streamflow

Natural streamflows were simulated at the 29 flow locations for each of the 112 climate projections. Figure B-44 displays all of the individual 112 sequences in the Downscaled GCM Projected scenario. The sequence bolded in figure B-44 also appears in figure B-45, which is a representative trace of the 112 sequences. In figure B-45, the mean annual flow of the 112 sequences at this location declines substantially over time due to changes in hydrologic processes. Mean annual flows for Colorado River at Lees Ferry, Arizona, for the 50-year period of the Study (2011 to 2060) are approximately 13.7 maf. This represents a reduction in streamflow of approximately 6 percent compared to the period 1950 to 1999 (14.6 maf), or approximately 9 percent compared to the long-term period 1906 to 2007 (15.0 maf). It should be noted that the median of the projections is nearly 1.0 maf lower (annual flow of around 12.7 maf) than the mean, indicating that the projection ensemble exhibits a strong drying trend but that some wetter projections are compensating in the mean statistic. A few projections (less than 10 percent) show considerably more annual variability than the observed record. Although simulated future minimum flows are similar to those in the observed record, the maximum annual flows are significantly higher.

Finally, figure B-46 shows the range of Colorado River flow projections under the Downscaled GCM Projected scenario as compared to the historical observed flows. Observed natural flows span from 1906 to 2007 while the projections begin in 1950 and extend through 2099. During the overlapping period of 1950 to 2007, the projection reflects the range of natural flows from the observed record. Interestingly, the projection ensemble indicates a declining trend starting in the 1990s and a significant expansion in variability starting in the late 2000s. A number of sequences in the Downscaled GCM Projected scenario exhibit occasional annual runoff conditions that far exceed the maximum in the observed or paleo records. Although it is possible that future climate will expand the magnitude and frequency of extreme events, it is also possible that some projections are simply extreme outliers from the ensemble. As shown in figure B-46, 5 to 10 percent of the projections show annual flows in excess of the maximum observed natural flow of 25 maf for any given year.

To better understand the issue of simulated extreme high flows and to determine whether specific GCMs or emission scenarios were driving this result, further analysis was conducted. For each downscaled climate projection, the cumulative difference from the simulated maximum flow to the maximum observed annual value of 25 maf over the study period 2011 to 2060 was computed. In addition, the total number of years in which the simulated flow exceeded 25 maf was counted for the 112 VIC model simulations. The results of this analysis are shown in figure B-47. Each of the 112 projections are listed and colored by the emission scenario (blue for A1B, red for A2, and green for B1). The corresponding dot represents the number of years in which that projection had simulated flows greater than 25 maf. The bar represents the cumulative flow above 25 maf. More than half of all GCM projections produced at least one event greater than 25 maf and these occurred regardless of emission scenario. None of the projections had more than 4 years in which they exceeded 25 maf. In addition, the GCMs with the largest deviations under one emission scenario produced fewer or no deviations under another emission scenario.

FIGURE B-44
Colorado River at Lees Ferry, Arizona Natural Flow for 112 Sequences for the Downscaled GCM Projected Scenario
The bolded line indicates a representative trace.

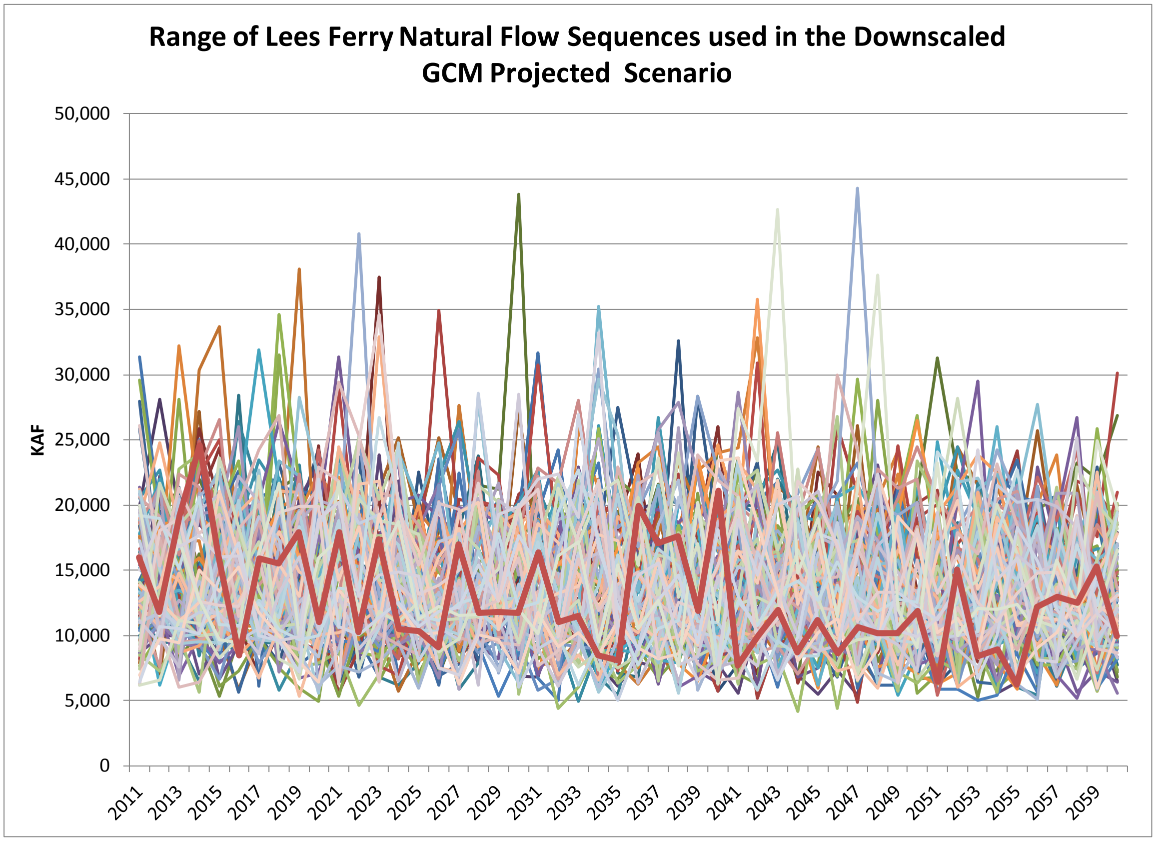

FIGURE B-45
Colorado River at Lees Ferry, Arizona Natural Flow Statistics for the Downscaled GCM Projected Scenario
Median (line), 25th–75th percentile band (dark shading), 10th–90th percentile band (light shading), max/min (whiskers), and 1906–2007 observed min and max (dashed lines). The red bolded line indicates a representative trace.

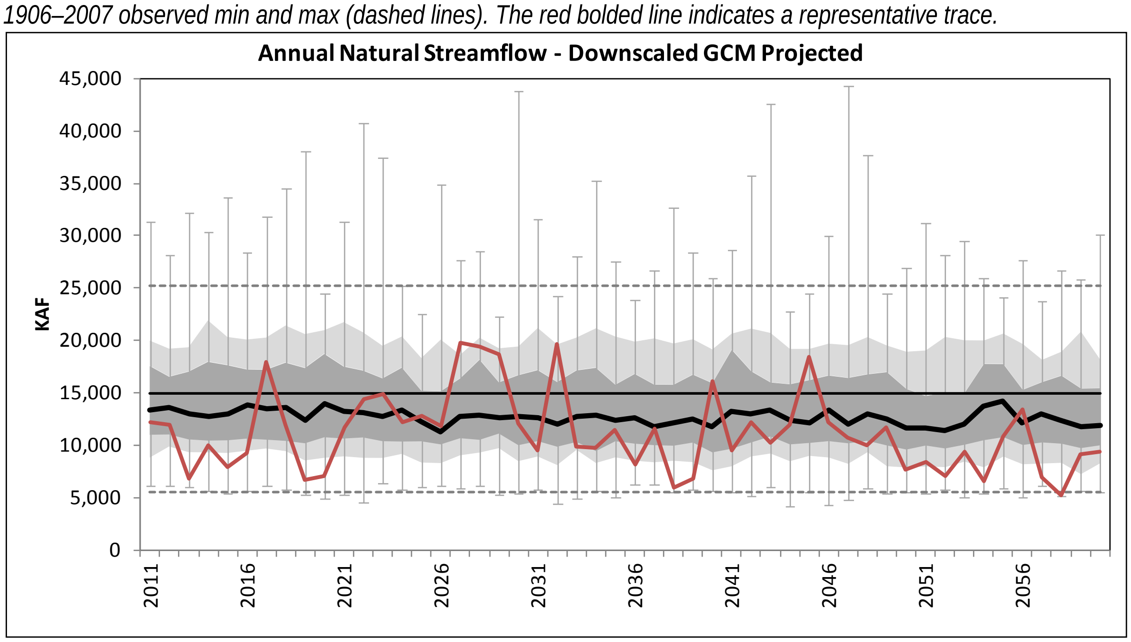

FIGURE B-46
Colorado River at Lees Ferry, Arizona Natural Flow Statistics for the Downscaled GCM Projected Scenario as Compared to Observed Flow

Median (line), 25th–75th percentile band (dark shading), 10th–90th percentile band (light shading), max/min (whiskers), and 1906–2007 observed (blue line).

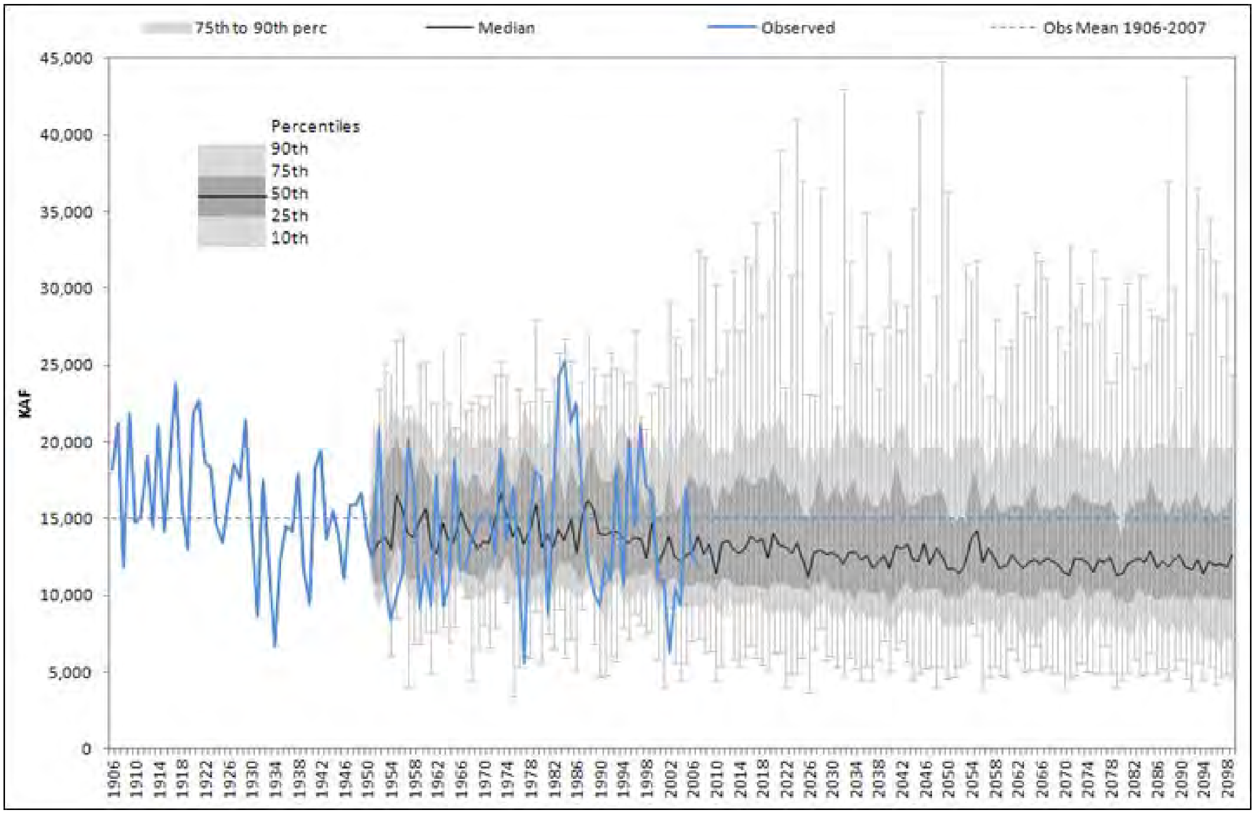

FIGURE B-47
Cumulative Difference from Simulated Annual Maximum Flow and 25 maf (bar) and Total No. of Years that Exceed 25 maf (dot) for Colorado River at Lees Ferry, Arizona for 112 Downscaled Projections for the Period 2011–2060

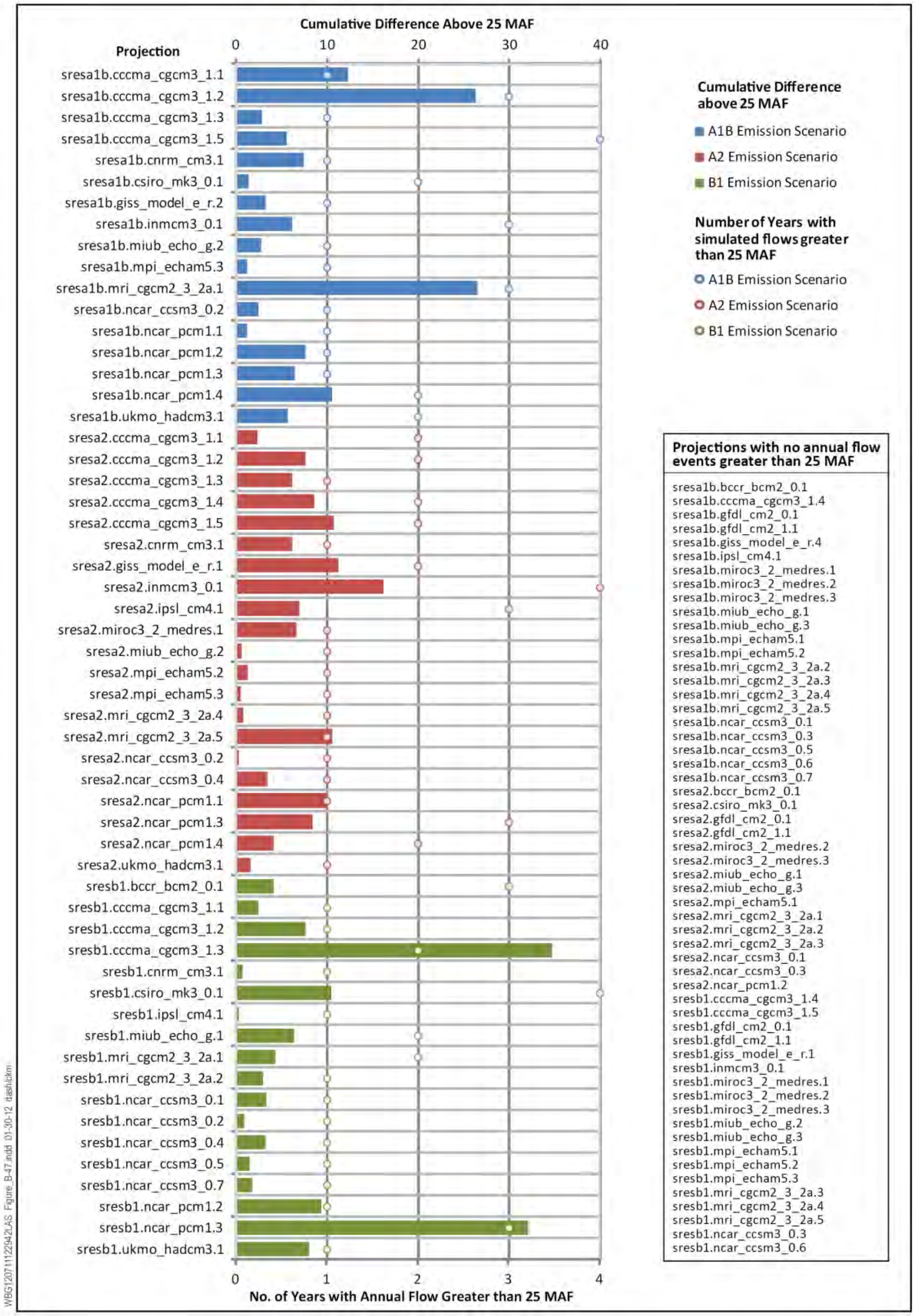

The analysis concluded that it is a rare occurrence for a projection to exceed 25 maf, but the potential is prevalent among the ensemble members regardless of emission scenario. The GCMs ECHAM5, CCSM, MIROC, and Geophysical Fluid Dynamics Laboratory, however, stood out in producing the fewest of these events (see appendix B2).

Figure B-48 shows the mean annual percent change in natural flow for all 29 locations for four future periods as compared to the 50-year historical period of 1950 to 1999. The comparison here is not made to the observed 1906 to 2007 period, but rather to the historical VIC-simulated period such that any inherent model biases are incorporated in both VIC-simulated periods. The future periods reflect the Study period (2011 to 2060) and three 30-year periods extending throughout the 21st Century (2011 to 2040, 2041 to 2070, and 2066 to 2095) to provide the time evolution of the projected flow changes.

FIGURE B-48
Simulated Relative Change in Mean Annual Flows (Ensemble Mean) for the Study Period (2011–2060), and Three Future Periods (2011–2040, 2041–2079, and 2066–2095), Compared to 1950–1999 for each of the 29 Natural Flow Locations

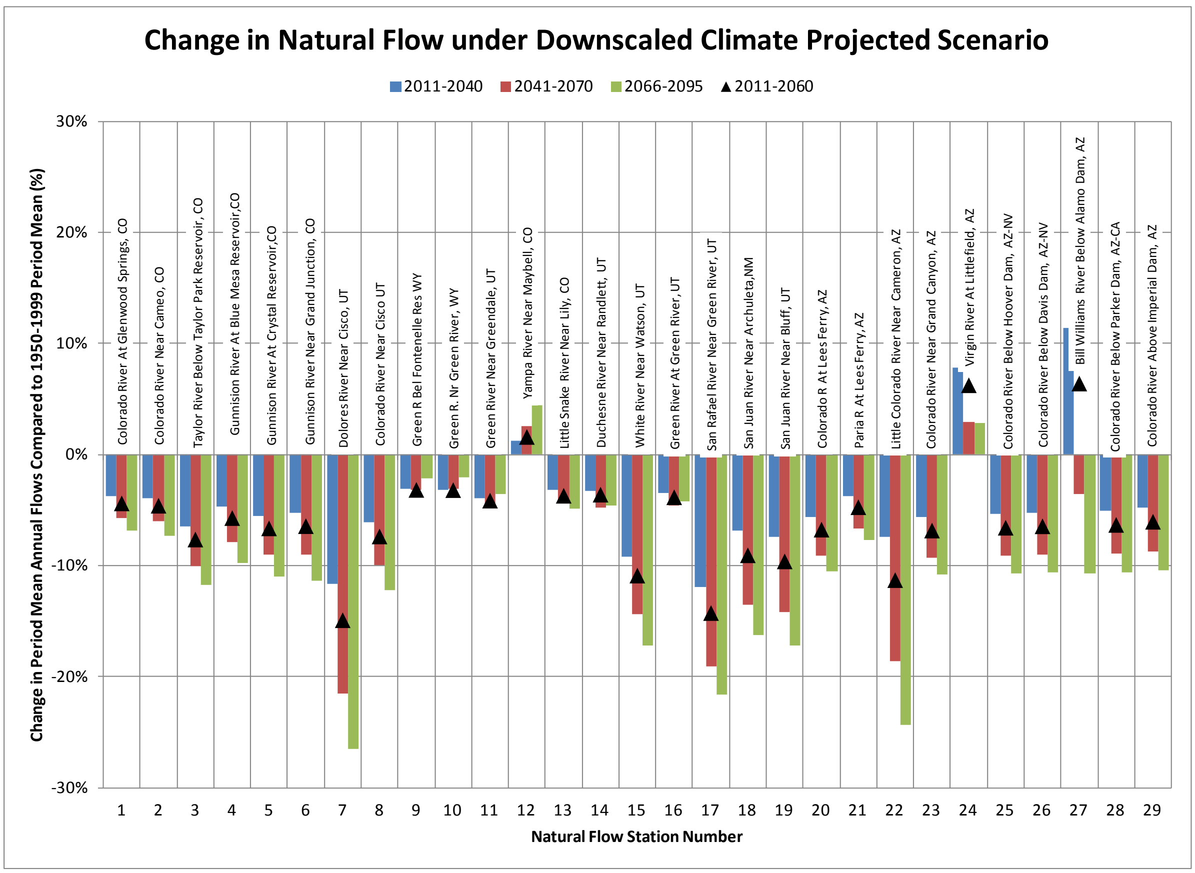

All locations except the Yampa River, Virgin River, and Bill Williams River are projected to experience decreasing annual flows. The Dolores River, White River, San Rafael River, Little Colorado River, and San Juan River are projected to experience the largest percentage decrease in annual flows (greater than 10 percent). The Green River and upper watershed of the Colorado River are projected to experience smaller reductions in streamflow (less than 5 percent). These spatial differences in streamflow changes appear to be largely related to the location of the watershed in relation to the precipitation pattern changes (more northerly) and the relative elevation differences among watersheds (higher elevation). In general, smaller sub-basins that are farther north and at higher elevations (such as the Yampa River) may be expected to have increasing flows given projected increases in precipitation. Although precipitation is projected to increase in some larger sub-basins at lower elevations (such as the Green River), a decrease in flow is projected, possibly a result of the dominant role of increased temperature in these regions.

The implicit assumption made with respect to the SRES emission scenarios used to drive the GCMs in the Study is that they are equally likely (or unlikely) and that they can be used in a multi-model ensemble. Climate projections through mid-century are dominated by the choice of GCM rather than individual emission scenarios. Table B-1 presents the range of projected change in Colorado River at Lees Ferry, Arizona streamflow associated with specific SRES emission scenarios, as compared to the ensemble of all emission scenarios. VIC simulations indicate streamflow reductions for all three SRES emission scenarios, and difference of less than 2 percent between emission scenario groupings for time periods covered in the Study. These results are expected since the climate system responds relatively slowly to changes in emissions. By late century, the differences between simulated streamflows across emission scenarios become substantially larger, reflecting both the response time of the climate system and the higher emissions. During the first period indicated in table B-1, it is noteworthy that the greatest streamflow reduction occurs under the A1B scenario. While the GHG emissions in this scenario fall between the A2 and B1 scenarios in the distant future, they actually represent the highest emission scenario (of the three) through about 2020 (see appendix B2). By the second and third periods (mid-century and beyond) the streamflow changes between emission scenarios are more intuitive with the general emission pathways.

TABLE B-1
Percentage Change in Mean Flow with Respect to Historical Mean (1950–1999) at the Colorado River at Lees Ferry, Arizona

	2011–2040	2041–2070	2066–2095	2011–2060
All Projections	-5.6	-9.1	-10.5	-6.8
SRESB1	-5.2	-7.9	-8.0	-6.0
SRESA1B	-6.7	-9.1	-10.5	-7.7
SRESA2	-4.9	-10.3	-13.2	-6.5

While annual flows show decreases and likely some expansion in variability, monthly flows exhibit a significant shift in timing. Figure B-49 shows the simulated mean monthly flows from the climate projections for the Colorado River at Lees Ferry, Arizona compared to the observed monthly flows. Commensurate with the seasonal changes in temperature, precipitation, and hydrologic processes, after 2025, the peak streamflow occurs about one month earlier (from June through May) and is approximately 500 thousand acre-feet (kaf) lower. In addition, increases occur in winter streamflow, while substantial reductions occur in spring and summer. The wintertime increases are likely associated with increased precipitation in the Upper Basin, while spring and summer decreases are likely associated with earlier melt of the snowpack and reduced precipitation patterns. Prior to the mid-century it appears that the transition to

FIGURE B-49
Comparison of Observed and Future Simulated Mean Monthly Flows at Colorado River at Lees Ferry, Arizona

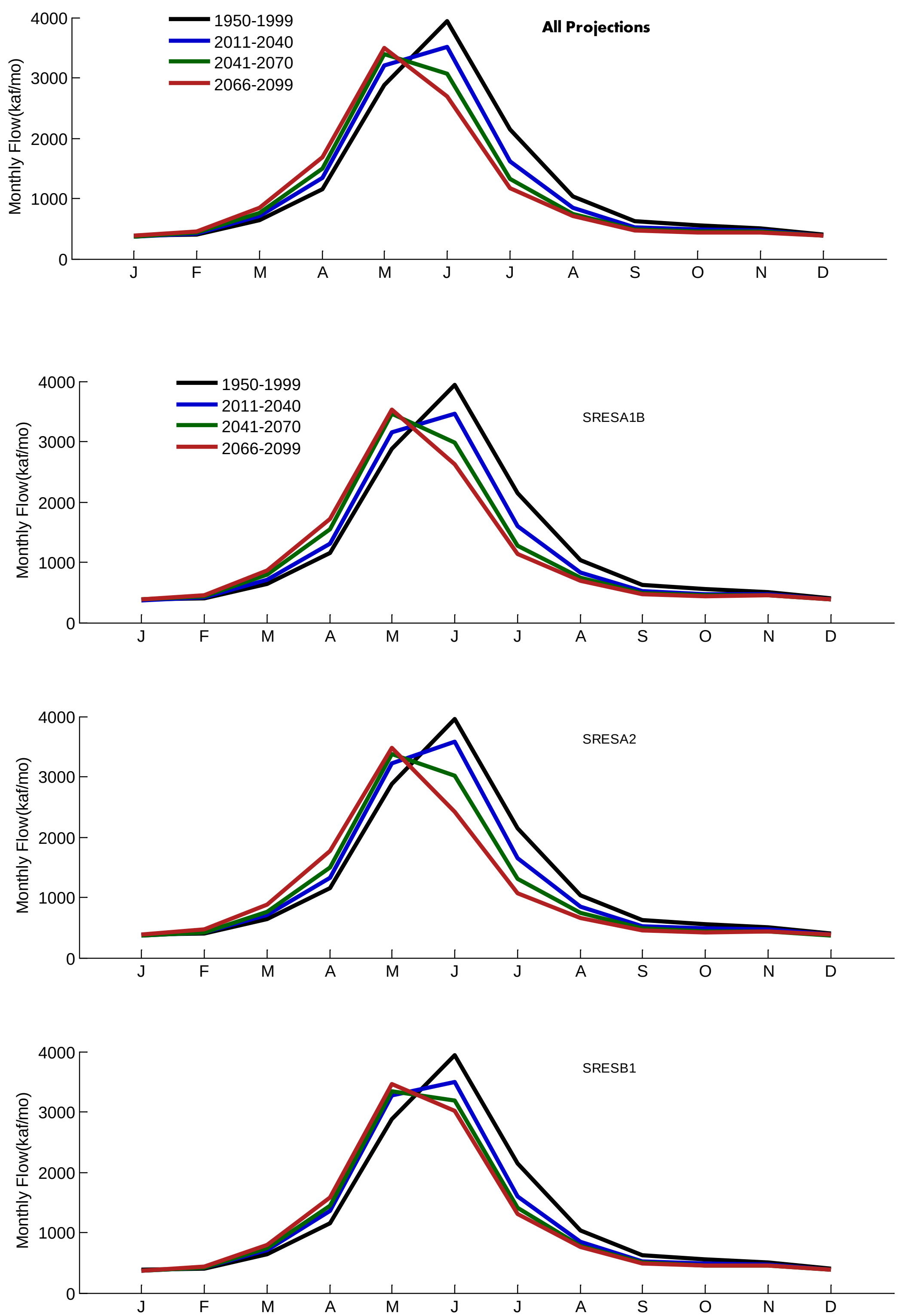

earlier runoff is underway with increasing May flows and decreases in June flows, but the full monthly shift has not yet occurred. The lower panels of figure B-49 also indicate that there is no substantial difference in the monthly timing trends between emission scenarios.

The inter-annual variability in streamflow is another important component of water supply. Deficit statistics using the identical methods as those described for the historical supply were computed for each of the 112 climate projections. The 1906 to 2007 observed mean of 15.0 maf was used to set the threshold for determining whether the system was in a deficit or surplus. For the purpose of this report, “deficit” is defined as a consecutive 2-year period when the mean is less than the observed long-term mean of 15.0 maf. Similarly, “surplus” is defined as a consecutive 2-year period when the mean is above 15.0 maf.

Figure B-50 illustrates the frequency and magnitude of both deficit and surplus spells. The inset figure shows the frequency occurrence of a specific spell length across all projections. The median exceedance probability of a surplus spell longer than 0 years is 30 percent, indicating that, when as measured against the 1906 to 2007 mean annual flow of 15 maf, about a third of the years in the future would be considered to not be a deficit. In addition, deficit length may extend greater than 20 years (indicated by the 90th percentile deficit length), as compared to the recent 9-year deficit. Under the Downscaled GCM Projected scenario (at the ensemble median) a 9-year deficit may occur up to 20 percent of the time and result in a cumulative deficit of 30 to 40 maf. The recent 9-year deficit is estimated to have a cumulative deficit of more than 28 maf. The results also suggest that under some climate projections, sustained periods of dryness will occur (deficit lengths greater than 50 years). Most projections result in long-term mean annual flows that are less than the 15 maf observed mean. The future climate essentially arrives at a new mean state. Thus deficits may need to be evaluated against the projection-specific, long-term mean to reflect this new inter-annual variability about the new mean.

Figure B-51 is identical to figure B-50 except that the threshold for deficit and surplus is determined from the projection-specific, long-term mean, rather than the observed mean. The drought depiction is considerably different under these conditions. As expected, deficit and surplus frequencies are roughly equal. In addition, deficit spell lengths do not exceed 17 years and are a maximum of 8 years at the median of the projections. Deficit magnitudes at the 9-year deficit remain in the 18 to 40 maf range. Under this perspective, the inter-annual variability is not substantially different than the recent observed period, but rather the Downscaled GCM Projected means are significantly reduced, leading to the perspective of relatively sustained deficit when measured against recent observed flows. There is no absolute correct perspective; thus, both methods are presented here.

FIGURE B-50
Simulated Deficit and Surplus Spell Length and Magnitude for All 112 Climate Projections
(Threshold Defined as 1906–2007 Mean Annual Flow ~15 maf)

Box plots show the median (dash), 25th–75th percentile band (shading), and max/min (whiskers).

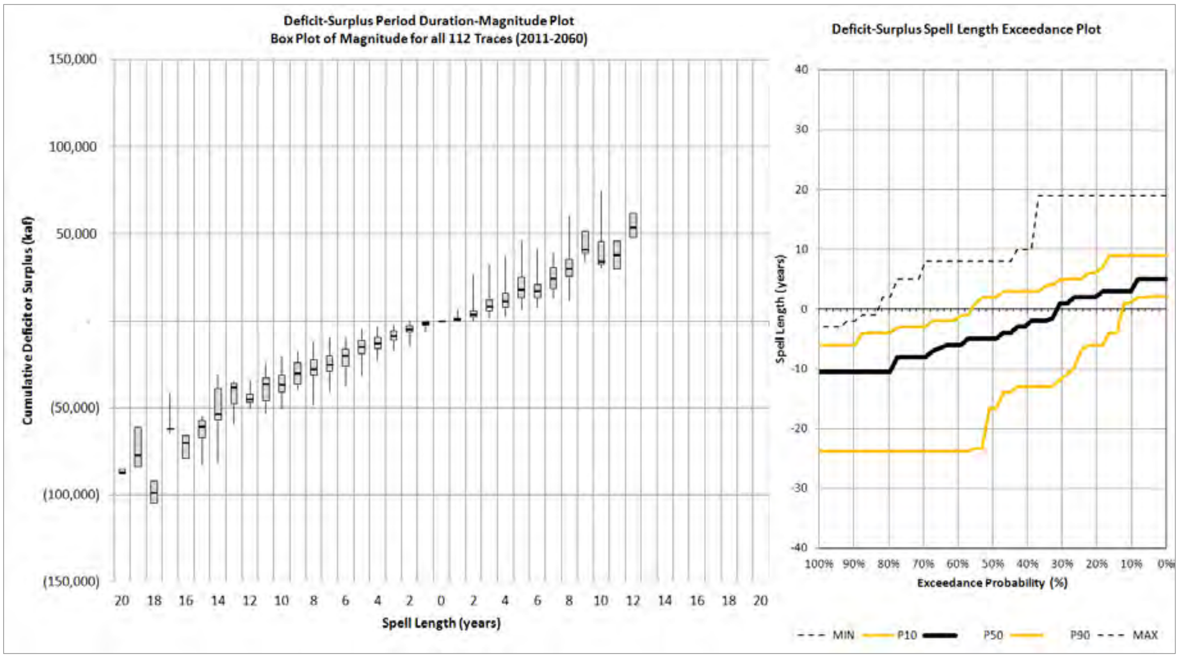

FIGURE B-51
Simulated Deficit and Surplus Spell Length and Magnitude for all 112 Climate Projections (Threshold Defined as Individual Projection Mean for 2011–2060)

Box plots show the median (dash), 25th–75th percentile band (shading), and max/min (whiskers).

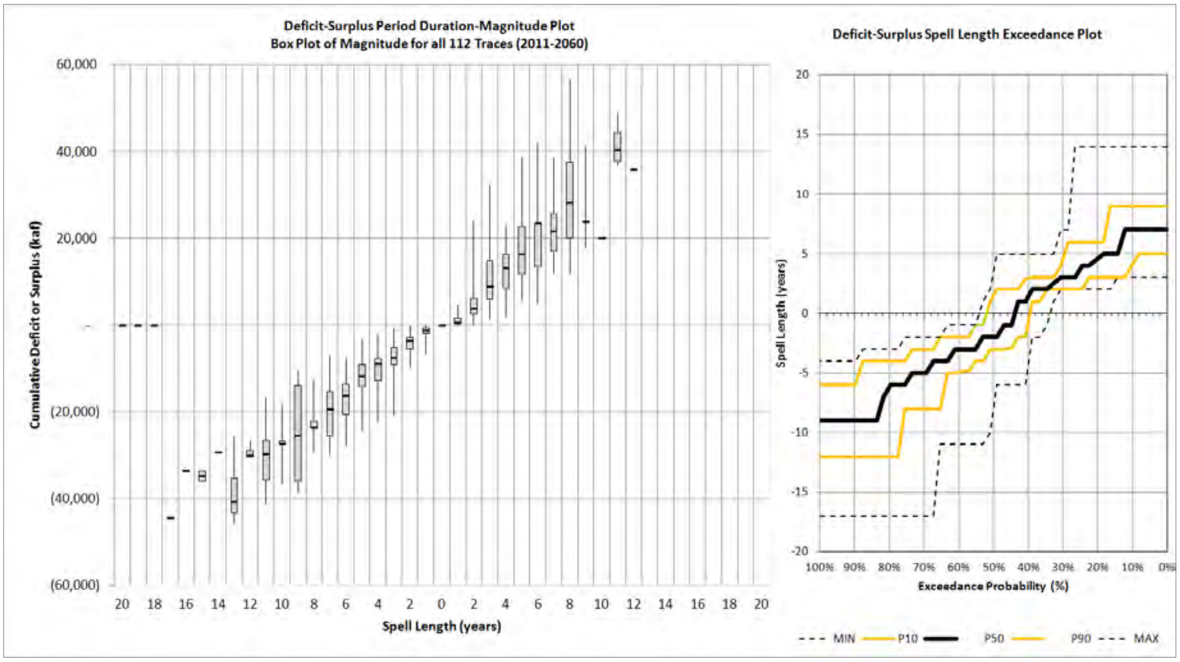

9.0 Comparison of Future Supply Scenarios

The water supply assessment described in this report includes four distinct supply scenarios that attempt to bracket the range of conditions that might be experienced over the next 50 years. The scenarios include direct use of the observed record (Observed Resampled scenario), direct use of the paleo reconstructions (Paleo Resampled scenario), blends of observed and paleo sequences (Paleo Conditioned scenario), and use of future climate projections and hydrologic modeling (Downscaled GCM Projected scenario). Figure B-52 shows the range of annual flows for the Colorado River at Lees Ferry, Arizona for each of the scenarios in a four-panel series.

The Observed Resampled, Paleo Resampled, and Paleo Conditioned scenarios have similar mean annual flows and a similar range of annual variability. The Paleo Resampled scenario contains individual years of flows lower than Observed Resampled, but a narrower band of variability within the inter-quartile range. The Paleo Conditioned scenario, by design, includes a similar range of annual flows as the Observed Resampled. The Downscaled GCM Projected scenario reflects possible changes in climate beyond what occurred historically and has lower mean annual flows while expanding the annual variability range through increased maximum annual flows. Mean annual natural flows for the Colorado River at Lees Ferry, Arizona range from 14.7 to 15.0 maf for the Observed Resampled, Paleo Resampled, and Paleo Conditioned scenarios. The Downscaled GCM Projected scenario results in mean annual flows of approximately 13.7 maf.

Each supply scenario includes multiple realizations, resulting in a range of flow statistics. Figure B-53 graphically depicts these annual flow statistics. The range of mean flows is greatest under the Downscaled GCM Projected scenario, with the inter-quartile range spanning roughly 12.5 to 15 maf and the absolute range covering 10 to 17 maf. Especially with respect to the use of climate projections, the ensemble mean or median should be considered more useful than any individual projections. This ensemble mean or median has been shown to perform better than any individual projection against a range of historical climate metrics and variability and trend significance, largely due to the cancelling out of natural internal GCM model variability and cancelling out of individual model errors (see Gleckler et al. [2008], and Pierce et al. [2009], for a more-complete discussion of this topic). The Paleo Resampled scenario, despite the large absolute range, has a smaller standard deviation than the other scenarios due to the tightness of the bulk of the realizations. Skew is a measure of the shape of the annual flow distribution. A skew of zero implies a normal distribution, in which wetter years and magnitudes are evenly balanced with drier years. Most scenarios have a positive skew, suggesting a bias to the drier side of the distribution. This is particularly noticeable in the Downscaled GCM Projected scenario. The Paleo Resampled scenario has the highest year-to-year correlation as measured by the backward lag-1 correlation. This high degree of correlation is attributable in part to the method used to develop the reconstructions. The minimum annual flows are fairly consistent across the scenarios, with the Paleo Resampled scenario exhibiting the most extreme low-flow condition. The Downscaled GCM Projected scenario exhibits a range of maximum annual flows well beyond those seen in any of the other scenarios.

FIGURE B-52
Annual Colorado River at Lees Ferry, Arizona Natural Flow Time Series for Supply Scenarios
Median in bold black line, inter-quartile range in dark shading, 10th–90th percentile range in light shading, selected individual sequence in bold colored line, max/min as whiskers, and 1906–2007 observed max/min (dashed lines).

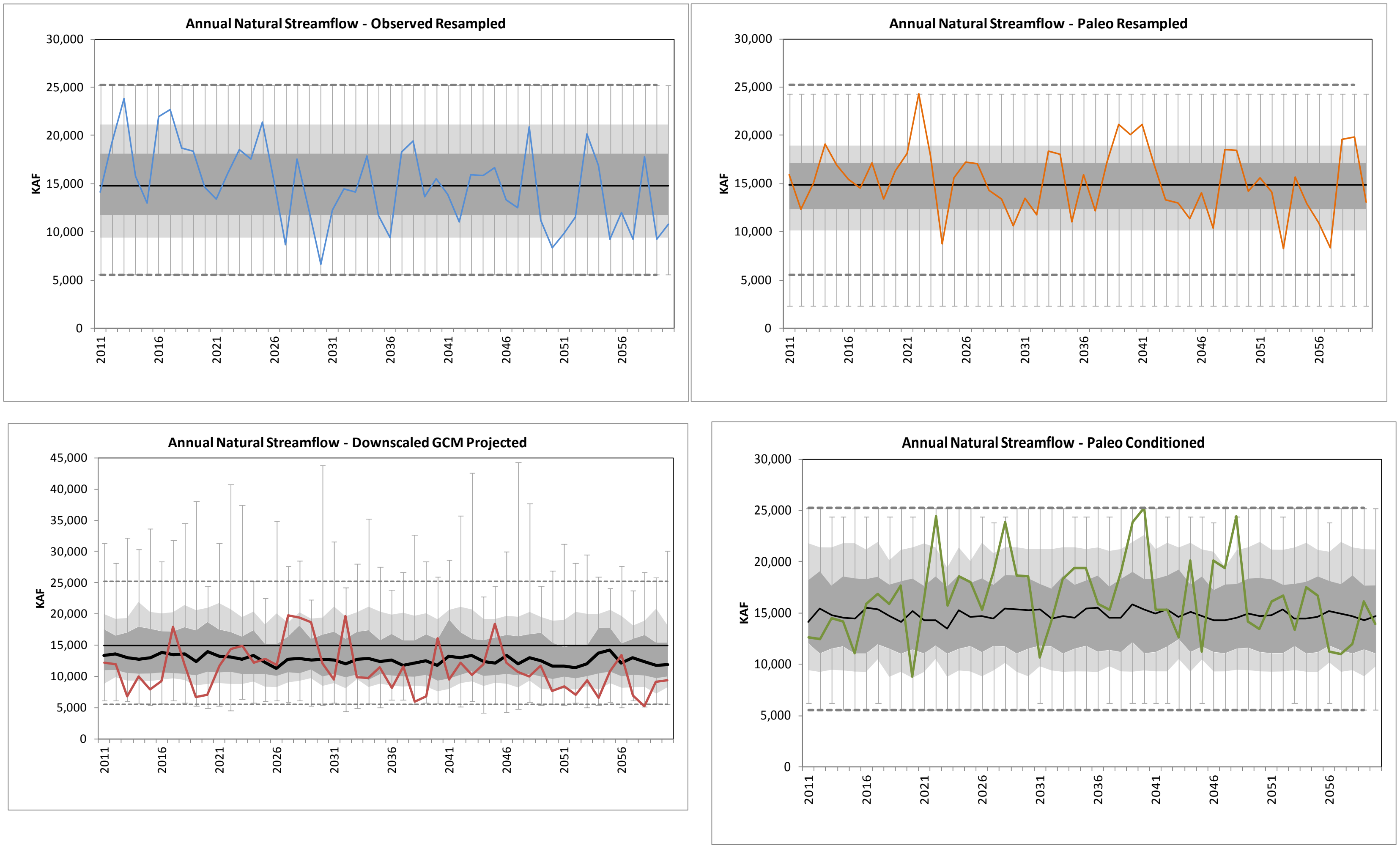

FIGURE B-53
Summary Statistics for Annual Colorado River at Lees Ferry, Arizona Natural Flows for Supply Scenarios (for 2011–2060)
Figure shows the median (dash), 25th–75th percentile band (box), and max/min (whiskers).

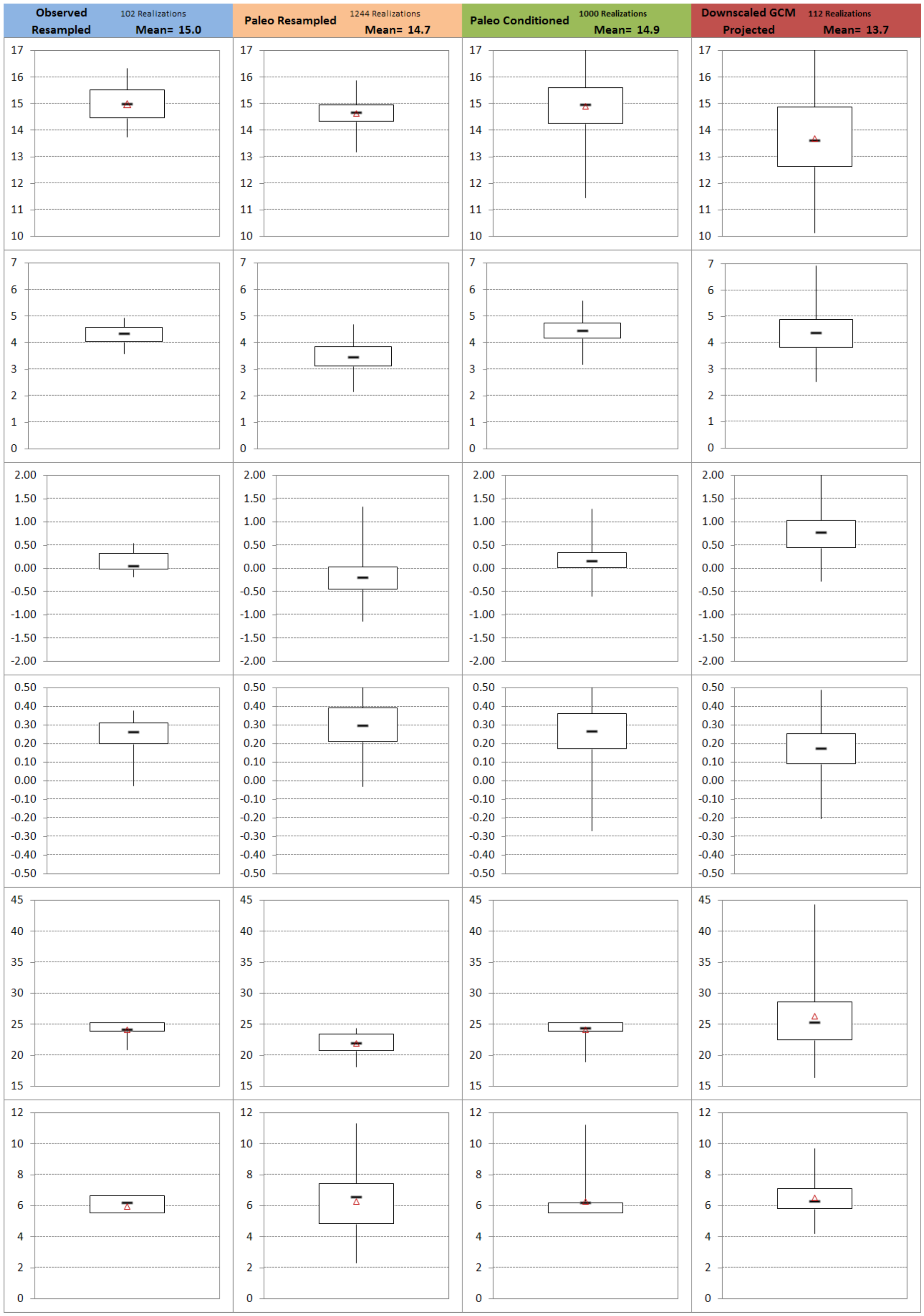

Figure B-54 provides a side-by-side comparison of each of the scenarios over the study horizon and the monthly flow range. Again, the Downscaled GCM Projected scenario demonstrates both higher high flows and lower low flows, measured as a 5-year average. This range, combined with the reduced mean annual natural flows in this scenario, makes the Downscaled GCM Projected scenario likely the most challenging supply condition within which to manage the Basin. The figure also shows that the monthly variability of the Downscaled GCM Projected scenario is significantly larger than any other scenario. This is particularly true in the winter and spring, when the Upper Basin hydrologic processes are most active and subject to change under climate warming. The shift in peak flow timing from June through May is apparent in figure B-55, and becomes more pronounced when analyzing results for the later 30-year time periods (table B-3).

FIGURE B-54
Annual Colorado River at Lees Ferry, Arizona 5-Year Natural Flow Time Series (top) and Monthly Variability across Supply Scenarios (bottom) (for 2011–2060)

Figure shows the median (dash), 25th–75th percentile band (box), and max/min (whiskers).

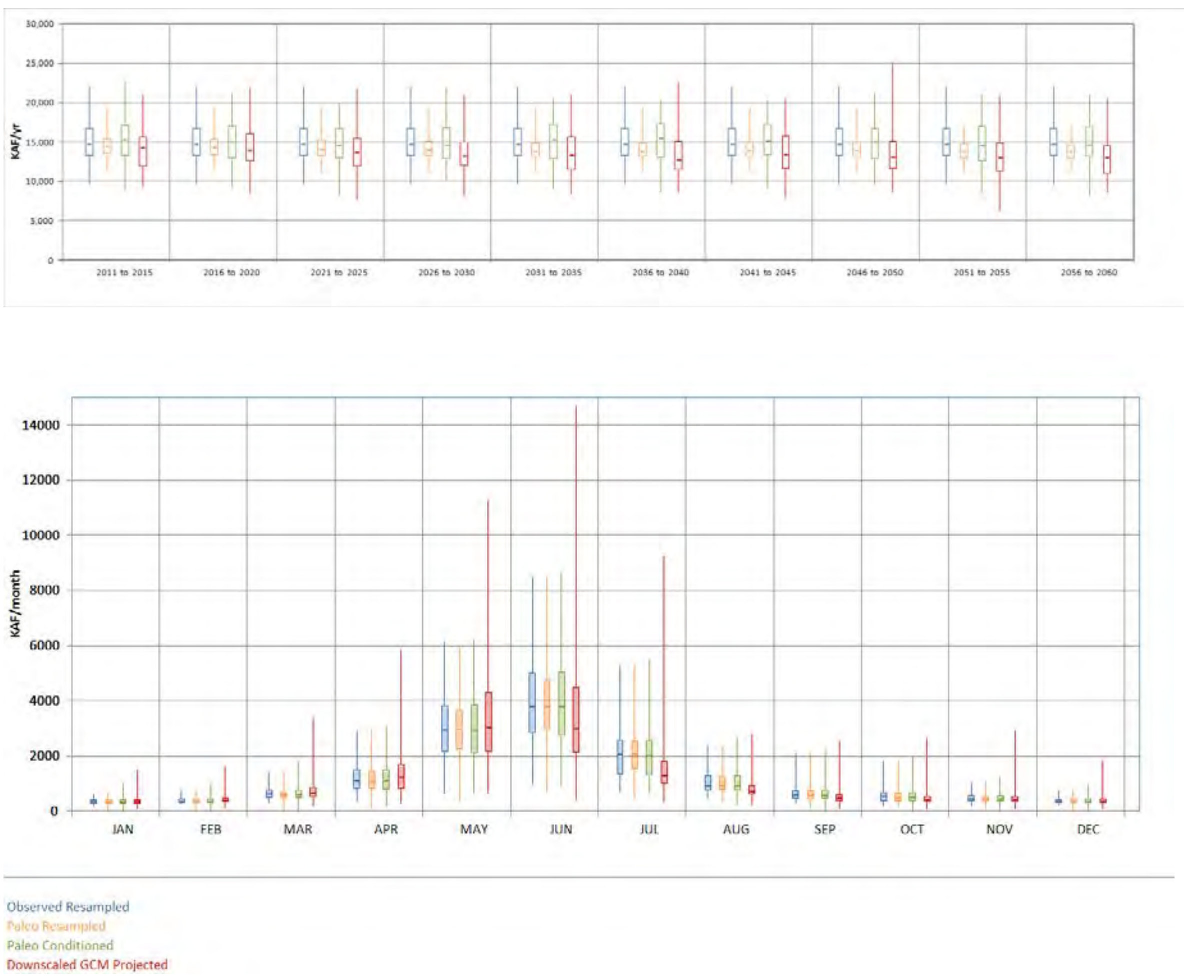

FIGURE B-55
Monthly Colorado River at Lees Ferry, Arizona Natural Flow Variability for Supply Scenarios (for 2011–2060)
Figure shows the median (dash), 25th–75th percentile band (shading), and max/min (whiskers).

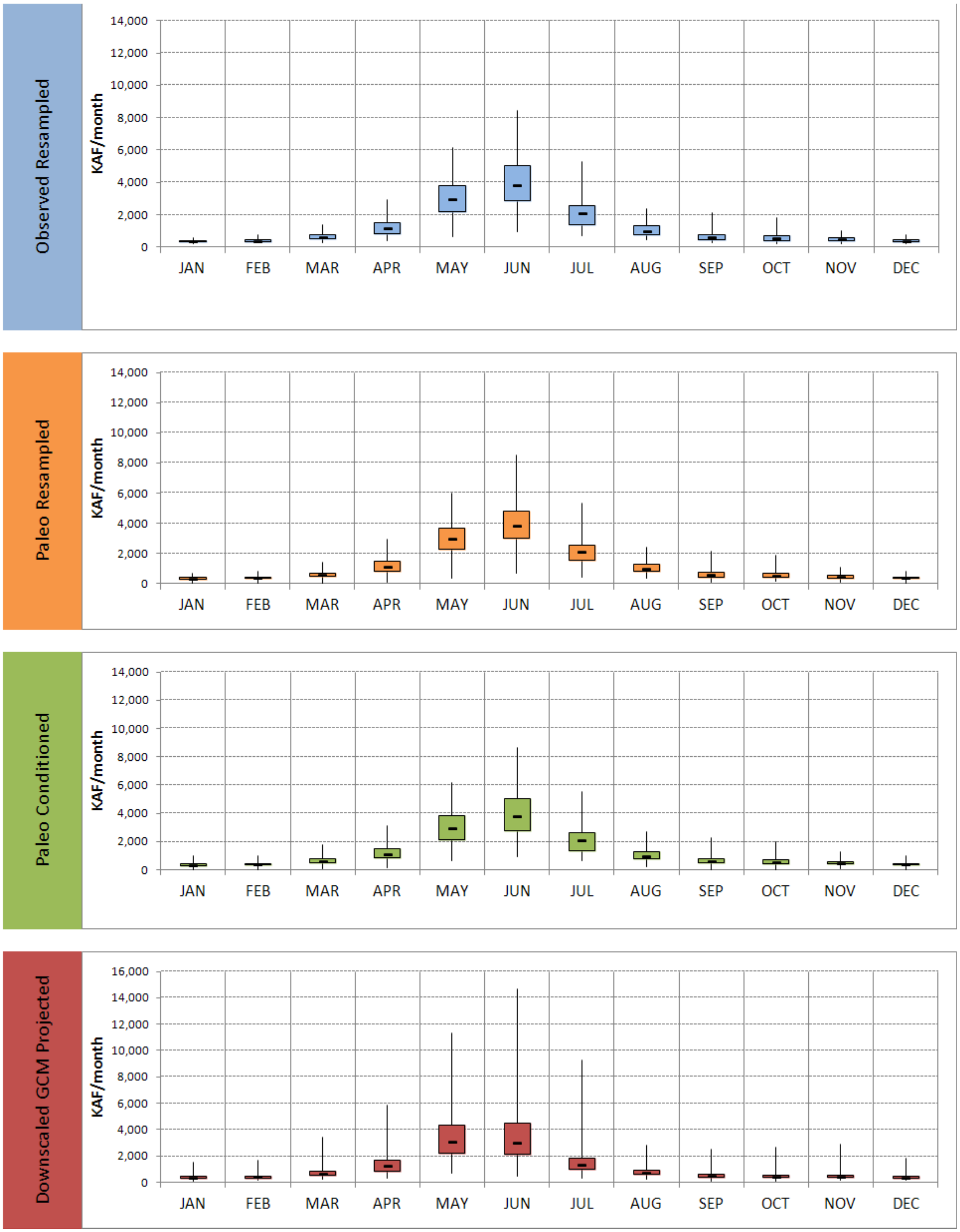

The inter-annual variability of streamflow across the scenarios is characterized by determining the frequency, duration, and magnitude of deficit and surplus periods. Figure B-56 is a four-panel figure showing the length and magnitude of such spells. For example, the maximum length of sustained deficit through 2007 in the Observed Resampled scenario was 8 years (note that this length would be 9 years if the observed record extended through 2010), while the maximum sustained surplus is 7 years. In comparison, the Paleo Resampled, Paleo Conditioned, and Downscaled GCM Projected scenarios all produce deficit periods of 15 years or longer. The maximum deficit accumulated is approximately 60 maf over the 15 years of deficit (both Paleo Conditioned and Downscaled GCM Projected scenarios). However, the reduced mean annual flow in the Downscaled GCM Projected scenario causes many of the realizations to be in a sustained deficit using the recent observed flows as the measure.

FIGURE B-56

Frequency, Duration, and Magnitude of Deficit and Surplus Periods for Supply Scenarios (for 2011–2060)

Top figures (left to right) are the Observed Resampled and Paleo Resampled scenarios. Bottom figures (left to right) are the Paleo Conditioned and Downscaled GCM Projected scenarios. Box plots show the median (dash), 25th–75th percentile band (shading), and max/min (whiskers).

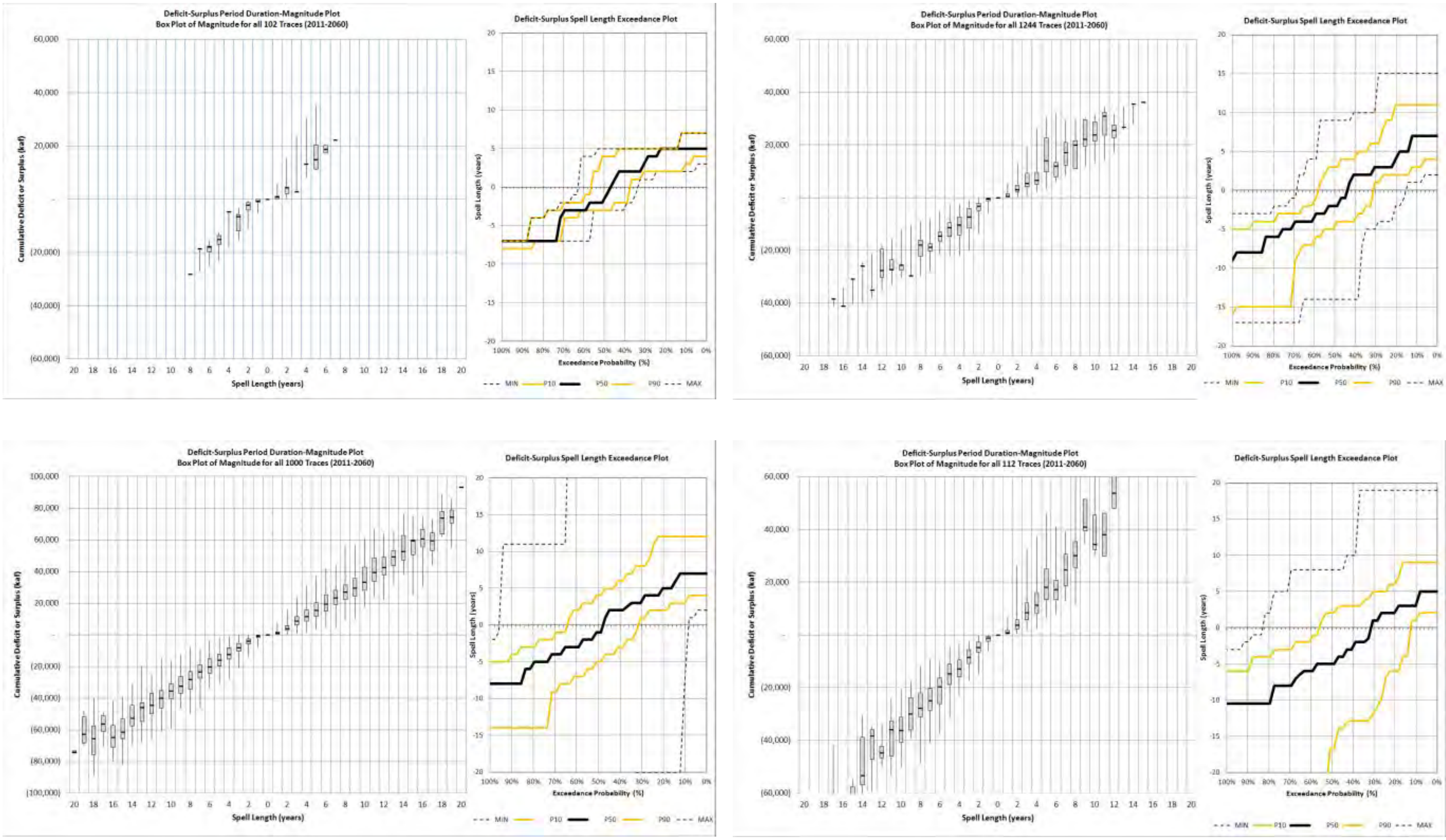

Table B-2 summarizes the key statistics for each water supply scenario and generally provides a tabular presentation of the information presented in the figures in this section. Similarly, table B-3 summarizes the annual and monthly statistics for the Downscaled GCM Projected scenario for three distinct future periods (2011 to 2040, 2041 to 2070, and 2066 to 2095) to assist in the evaluation of temporal trends. It should be noted that the last of these three periods is beyond the Study period, but is shown to assist in understanding trajectory of projected changes. Under this scenario, mean annual flows are projected to continue to decrease over time (from -7.5 percent around 2025 to -10.9 percent around 2055, to -12.4 percent around 2080) as compared to the 1906 to 2007 mean. At the same time, the shift in peak streamflow timing evolves from a current peak in June to an eventual peak in May due to earlier snowmelt and increased rain-to-snow ratios in response to warming.

TABLE B-2
Summary of Key Streamflow Statistics for Each Water Supply Scenario for the Period 2011–2060

		Scenario			
	Statistic	**Observed Resampled**	**Paleo Resampled**	**Paleo Conditioned**	**Downscaled GCM Projected**
Annual (Water Year)	Average Annual Flow (maf)	15.0	14.7	14.9	13.7
	Percent Change from Long-Term Mean (1906–2007)	0%	-2%	-1%	-8.7%
	Median (maf)	15.0	14.7	15.0	13.6
	25th Percentile (maf)	14.5	14.3	14.2	12.6
	75th Percentile (maf)	15.5	15.0	15.6	14.9
	Minimum Year Flow (maf)	5.6	2.3	5.6	4.2
	Maximum Year Flow (maf)	25.2	24.3	25.2	44.3
Monthly	Peak Month	June	June	June	June
	Peak Month Mean Flow (kaf)	4,007	3,914	4,000	3,393
	Peak Month Maximum Flow (kaf)	8,467	8,531	8,678	14,693
	Month at Which Half of Annual Flow (Water Year) is Exceeded	June	June	June	June
Deficit Periods[1]	Maximum Deficit (maf)	28.2	38.4	98.5	246.1
	Maximum Spell Length (years)	8	17	24	50
	Intensity (Deficit/Length) (maf/year) [median]	3.5	2.3	4.1	7.4
	Frequency of 5+ Year Spell Length (Percent) [median]	22%	30%	25%	48%
	Maximum 8-year Deficit (longest in 1906–2007 observed record, maf)	28.2	29.8	50	48.6
Surplus Periods[2]	Maximum Surplus (maf)	22.2	36.2	88	74.7
	Maximum Spell Length (years)	7	15	25	19
	Intensity (Surplus/Length) (maf/year)	3.2	2.4	3.5	13.2
	Frequency of 5+ Year Spell Length (Percent)	28%	15%	18%	<1%
	Maximum 7-year Surplus (longest in 1906–2007 observed record, maf)	22.2	29.2	44	39.2

[1] A deficit period occurs whenever the 2-year running average flow is below the observed average from 1906–2007 of 15.0 maf.

[2] A surplus period occurs whenever the 2-year running average flow is above the observed average from 1906–2007 of 15.0 maf.

TABLE B-3
Summary of Annual and Monthly Streamflow Statistics for the Downscaled GCM Projected Scenario for the 3 Future 30 Year Time Periods: 2011–2040 (2025), 2041–2070 (2055), and 2066–2095 (2080)

	Statistic	**Downscaled GCM Projected 2011–2040 (2025)**	**Downscaled GCM Projected 2041–2070 (2055)**	**Downscaled GCM Projected 2066–2095 (2080)**
Annual (Water Year)	Average Annual Flow (maf)	13.9	13.4	13.1
	Percent Change from Long-Term Mean (1906–2007)	-7.5%	-10.9%	-12.4%
	Median (maf)	13.8	13.3	13.4
	25th Percentile (maf)	12.8	12.0	11.2
	75th Percentile (maf)	15.1	14.6	14.5
	Minimum Year Flow (maf)	4.4	3.9	3.7
	Maximum Year Flow (maf)	43.8	44.3	44.3
Monthly	Peak Month	June	May	May
	Peak Month Mean Flow (kaf)	3,535	3,388	3,495
	Peak Month Maximum Flow (kaf)	14,693	10,830	12,991
	Month at Which Half of Annual Flow (Water Year) is Exceeded	June	May	May

The last time period is beyond the Study period, but is shown for informational purposes.

10.0 Summary and Limitations

This report documents the current and future water supply assessment for the Study. The research and development program initiated by Reclamation in 2004 resulted in the development of the Paleo Resampled and Paleo Conditioned scenarios. These scenarios are described in appendix N of the 2007 Interim Guidelines Final EIS (Reclamation, 2007), as is the Observed Resampled scenario. The Downscaled GCM Projected scenario is the newest addition to the set of scenarios and has not been previously used in any Reclamation long-term planning activities. The VIC modeling associated with the projected climate forcings suggests changes in streamflows resulting from this scenario are consistent with past efforts, particularly that of Christensen and Lettenmaier (2007).

The streamflow bias correction that has been included in this report compensates for biases in climate and hydrologic data as well as for biases in the hydrology model (VIC) structure. This step is important for the use of results other than “change” metrics in subsequent analyses. However, in evaluating biases and VIC model performance, the need for model calibration at finer resolutions is found to be a necessary next step and will reduce the level of bias correction needed in the future. Care should be taken in attempting to apply the “raw” VIC results for smaller watersheds in the Basin. The improvements in hydrologic model calibration and application should parallel progress in climate modeling and methods to develop higher-resolution climate information.

The role of snowpack development and melt, ET, and soil moisture are found to be very important in determining the available supply in the Basin. However, limited Basin-wide data are available to better understand these dynamics. The elevational sensitivity of snowpack, effect of warming and increased carbon dioxide on ET, and the role of summer and fall soil moisture on water supply are areas in need of further study.

In addition, newer GCMs and downscaling techniques will soon be available under the IPCC Fifth Assessment Report. The improved resolution and model physics of some of the new GCMs may refine patterns of precipitation changes (such as the increases in the Green River Basin and Upper Colorado, and monsoonal effects in the Lower Basin).

11.0 References

AchutaRao, K. M., and K. R. Sperber. 2002. "Simulation of the El Niño Southern Oscillation: Results from the Coupled Model Intercomparison Project." *Climate Dynamics*, Vol. 19: 191-209, DOI 10.1007/s00382-001-0221-9.

AchutaRao, K. M., and K. R. Sperber. 2006. "ENSO Simulation in Coupled Ocean-Atmosphere Models: Are the Current Models Better?" *Climate Dynamics*, Vol. 27: 1-15, DOI: 10.1007/s00382-006-0119-7.

Andreadis, K. M., and D. P. Lettenmaier. 2006. "Trends in 20th-Century Drought over the Continental United States." *Geophysical Research Letters*, 33, L10403, DOI:10.1029/2006GL025711.

Becker, E.J., E.H. Berbery, and R.W. Higgins. 2011. "Modulation of Cold-Season U.S. Daily Precipitation by the Madden–Julian Oscillation." *J. Climate*, 24, 5157–5166.

Bond, N. A., and G.A. Vecchi. 2003. "The influence of the Madden–Julian oscillation on precipitation in Oregon and Washington." *Wea. Forecasting*, 18, 600–613.

Bureau of Reclamation (Reclamation). 2007. *Colorado River Interim Guidelines for Lower Basin Shortages and Coordinated Operations for Lake Powell and Lake Mead Final Environmental Impact Statement*.

Bureau of Reclamation (Reclamation). 2011a. Colorado River Natural Flow Data. Retrieved from http://www.usbr.gov/lc/region/g4000/NaturalFlow/index.html.

Bureau of Reclamation (Reclamation). 2011b. *Literature Synthesis on Climate Change Implications for Water and Environmental Resources*.

Bureau of Reclamation (Reclamation). 2011c. *SECURE Water Act Section 9503(c) – Reclamation Climate Change and Water 2011*.

Cayan, D.R., T. Das, D.W. Pierce, T.P. Barnett, M. Tyree, and A. Gershunov. 2010. "Future dryness in the southwest US and the hydrology of the early 21st century drought." *Proceedings of the National Academy of Sciences*, 107(50), 21271-21276, DOI: 10.1073/pnas.0912391107.

Cayan, D.R., S.A. Kammerdiener, M.D. Dettinger, J.M. Caprio, and, D.H. Peterson. 2001. "Changes in the Onset of Spring in the Western United States." *Bulletin of the American Meteorological Society*, 82, 399–415.

Cayan, D.R., K.T. Redmond, , and L.G. Riddle. 1999. "ENSO and Hydrologic Extremes in the Western United States." *Journal of Climate*, 12, 2881-2893.

Christensen, N.S. and D.P. Lettenmaier. 2007. "A Multimodel Ensemble Approach to Assessment of Climate Change Impacts on the Hydrology and Water Resources of the Colorado River Basin." *Hydrology and Earth System Sciences*, 11, 1417–1434.

Christensen, N.S., A.W. Wood, N. Voisin, D.P. Lettenmaier, and R.N. Palmer. 2004. "The Effects of Climate Change on the Hydrology and Water Resources of the Colorado River." *Climatic Change*, 62, 337–363.

Clark, M.P., M.C. Serreze, and G.J. McCabe. 2001. "The Historical Effect of El Niño and La Niña Events on the Seasonal Evolution of the Mountain Snowpack in the Columbia and Colorado River Basins." *Water Resources Research*, 37, 741-757.

Colorado Water Conservation Board. 2010. *Colorado River Water Availability Study*. Draft Report.

Collins, M., S. An, W. Cai, A. Ganachaud, E. Guilyardi, F. Jin, M. Jochum, M. Lengaigne, S. Power, A. Timmermann, G. Vecchi, and A. Wittenberg. 2010. "The Impact of Global Warming on the Tropical Pacific Ocean and El Niño." *Nature*, 3, 391-397. doi: 10.1038/ngeo868

Das, T., D.W. Pierce, D.R. Cayan, J.A. Vano, and D.P. Lettenmaier. 2011. "The Importance of Warm Season Warming to Western U.S. Streamflow Changes." *Geophys. Res. Lett.*, DOI: 10.1029/2011GL049660.

Diaz, H.F., and G.N. Kiladis. 1992. "Atmospheric Teleconnections Associated with the Extreme Phases of the Southern Oscillation." Diaz, H.F., and V.A. Markgraf (eds.). *El Niño: Historical and Paleoclimatic Aspects of the Southern Oscillation*.

Edwards, L. M., and K.T. Redmond. 2005. "Climate Factors on Colorado River Basin Water Supply." In *Colorado River Basin Climate: Paleo, Present, Future*. Special publication for Association of California Water Agencies and Colorado River Water Users Association Conferences, California Department of Water Resources, pp. 14-22.

Fassnacht, S. R. 2006. "Upper Versus Lower Colorado River Sub-basin Streamflow: Characteristics, Runoff Estimation, and Model Simulation." *Hydrological Processes*, 20, 2187–2205.

Gleckler, P.J., K.E. Taylor, and C. Doutriaux. 2008. "Performance Metrics for Climate Models." *Journal of Geophysical Research* 46, DOI: 10.1019/2007JD008972.

Gleick, P.H. 1987. "Climatic changes, water resources, and institutional responses: A look at the United States, Mexico, and the Colorado River." In the Proceedings of the Symposium on Climatic Change in the Southern United States: Future Impacts and Present Policy Issues (May 28-29, 1987). U.S. Environmental Protection Agency/University of Oklahoma. pp. 450–465.

Groisman, P. Ya., R.W. Knight, and T.R. Karl. 2001. "Heavy Precipitation and High Streamflow in the Contiguous United States: Trends in the Twentieth Century." *Bulletin of the American Meteorological Society*, 82, 219–246.

Gutzler, D.S., H.K Kim, R.W. Higgins, H. Juang, M. Kanamitsu, K. Mitchell, K. Mo, P. Pegion, E. Ritchie, J.K. Schemm, S. Schubert, Y. Song, and R. Yang. 2005. "The North American Monsoon Model Assessment Project: Integrating numerical modeling into a field-based process study." *Bulletin of the American Meteorological Society* 86: 1423–1429.

Hamlet, A.F., and D.P. Lettenmaier. 1999. "Effects of climate change on hydrology and water resources objectives in the Columbia River Basin." *Journal of the American Water Resources Association*, 35(6),pp.1597-1625.

Hamlet, A. F., P.W. Mote, M.P. Clark, and D.P. Lettenmaier. 2005. "Effects of Temperature and Precipitation Variability on Snowpack Trends in the Western United States." *Journal of Climate*, 18, 4545–4561.

Hamlet, A.F, E.P. Salathé, and P. Carrasco. 2010. *Statistical Downscaling Techniques for Global Climate Model Simulations of Temperature and Precipitation with Application to Water Resources Planning Studies*.

Hidalgo, H., T. Piechota, and J. Dracup. 2009. "Alternative Principal Components Regression Procedures for Dendrohydrologic Reconstructions." *Water Resources Research*, Vol. 45, W06417, DOI:10.1029/2008WR007201.

Hirschboeck, K.K., Meko, D.M. 2005. *A Tree-Ring Based Assessment of Synchronous Extreme Streamflow Episodes in the Upper Colorado & Salt-Verde-River Basins – Final Report*.

Hoerling, H., D.P. Lettenmaier, D. Cayan, and B. Udall. 2009. "Reconciling Projections of Colorado River Streamflow." *Southwest Hydrology*. May/June.

Hu, Q., and S. Feng. 2010. "Influence of the Arctic oscillation on central United States summer rainfall." *J. Geophys. Res.*, 115, D01102. DOI: 10.1029/2009JD011805.

Intergovernmental Panel on Climate Change (IPCC). 2000. *Emissions Scenarios*. Special Report of the Intergovernmental Panel on Climate Change [Nakicenovic, N., and R. Swart (eds.)].

Intergovernmental Panel on Climate Change (IPCC). 2007. *Climate Change 2007: The Physical Science Basis*. Contribution of Working Group I to the Fourth Assessment Report of the Intergovernmental Panel on Climate Change [Solomon, S., D. Quin, M. Manning, Z., Chen, M. Marquis, K.B. Averyt, , M. Tignor, and H.L. Miller. (eds.)].

Lee, T., J.D. Salas, and J. Keedy. 2006. *Simulation Study for the Colorado River System Utilizing a Disaggregation Model*.

Liang, X., D.P. Lettenmaier, and E.F. Wood. 1996. *Surface Soil Moisture Parameterization of the VIC-2L Model: Evaluation and Modification*.

Liang, X., D.P. Lettenmaier, E.F. Wood, and S.J. Burges. 1994. "A Simple Hydrologically Based Model of Land Surface Water and Energy Fluxes for General Circulation Models." *Journal of Geophysical Research*, Vol. 99, 14415–14428.

Lin, J., B.E. Mapes, K.M. Weickmann, G.N. Kiladis, S.D. Schubert, M.J. Suarez, J.T. Bacmeister, and M. Lees. 2008. "North American monsoon and convectively coupled equatorial waves simulated by IPCC AR4 Coupled GCMs." *J. Climate*, 21:2919–2937.

Lohmann, D., R. Nolte-Holube, and E. Raschke. 1996: "A large-scale horizontal routing model to be coupled to land surface parameterization schemes." *Tellus*, 48, 708–721.

Lohmann, D., E. Raschke, B. Nijssen, and D.P. Lettenmaier. 1998. "Regional Scale Hydrology: I. Formulation of the VIC-2L Model Coupled to a Routing Model." *Hydrological Sciences Journal*, 43, 131–141.

Maurer, E. P., L. Brekke, T. Pruitt, and P.B. Duffy. 2007. "Fine-Resolution Climate Projections Enhance Regional Climate Change Impact Studies." *Eos, Transactions, American Geophysical Union*, 88 (47), 504.

Maurer, E.P. 2007. "Uncertainty in hydrologic impacts of climate change in the Sierra Nevada, California under two emissions scenarios." *Climatic Change*, Vol. 82, No. 3-4, 309-325, DOI: 10.1007/s10584-006-9180-9.

Maurer, E.P., A.W. Wood, J.C. Adam, D.P. Lettenmaier, and B. Nijssen. 2002. "A Long-Term Hydrologically-Based Data Set of Land Surface Fluxes and States for the Conterminous United States." *Journal of Climate*, 15(22), 3237-3251.

McCabe, G.J., D.M. Wolock. 1999a. "General circulation model simulations of future snowpack in the western United States." *Journal of the American Water Resources Association*, Vol. 35, 1473–1484.

McCabe, G.J., D.M. Wolock. 1999b. "Estimates of runoff using water-balance and atmospheric general circulation models" [abst.]. *Journal of the American Water Resources Association*, Vol. 35(6), 1341–1350.

McCabe, G.J., D.M. Wolock. 2002. "A Step Increase in Streamflow in the Conterminous United States." *Geophysical Research Letters*, 29, 2185, DOI:10.1029/2002GL015999.

McCabe, G.J., M.A. Palecki, and J.L. Betancourt. 2004. "Pacific and Atlantic Ocean Influences on Multi-Decadal Drought Frequency in the United States." *Proceedings of the National Academy of Sciences*, 101, 4136–4141.

Meko, D.M., C.A. Woodhouse, C.A. Baisan, T. Knight, J.J. Lukas, M.K. Hughs, and M.W. Salzer. 2007. "Medieval Drought in the Upper Colorado River Basin." *Geophysical Research Letters*, 34(5), L10705, DOI: 10.1029/2007GL029988.

Miller, W.P., and T.C. Piechota. 2008. "Regional Analysis of Trend and Step Changes Observed in Hydroclimatic Variables around the Colorado River Basin." *Journal of Hydrometeorology*, 9(5), 1020, DOI:10.1175/2008JHM988.1.

Mo, K.C., J.E. Schemm, and S. Yoo. 2009. "Influence of ENSO and the Atlantic Multi-Decadal Oscillation on Drought over the United States." *Journal of Climate*, 22(22), 5962–5982, DOI:10.1175/2009JCLI2966.1.

Mote, P.W. 2003. "Trends in snow water equivalent in the Pacific Northwest and their climatic causes." *Geophys. Res. Lett*., 30(12), 1601, DOI:10.1029/2003GL017258.

Mote, P. W. 2006. “Climate-Driven Variability and Trends in Mountain Snowpack in Western North America.” *Journal of Climate*, 19, 6209–6220.

Mote, P.M. Clark, and A. Hamlet. 2008. “Variability and Trends in Mountain Snowpack in Western North America.” 20th Conference on Climate Variability and Change. American Meteorological Society. New Orleans, Louisiana.

Mote, P.W., A.F. Hamlet, M.P. Clark, and D.P. Lettenmaier. 2005. “Declining Mountain Snowpack in Western North America.” *Bulletin of the American Meteorological Society*, 86, 39–49.

Nash, L.L., and P.H. Gleick. 1991. “The sensitivity of streamflow in the Colorado Basin to climatic changes.” *Journal of Hydrology*, Vol. 125, 221–241.

Nash, L., and P. Gleick. 1993. *The Colorado River Basin and Climatic Change: The Sensitivity of Streamflow and Water Supply to Variations in Temperature and Precipitation*. U.S. Environmental Protection Agency. EPA230-R-93-009.

National Oceanic and Atmospheric Administration (NOAA). 2011. Retrieved June 30, 2011, from http://www.ncdc.noaa.gov/oa/ climate/normals/usnormals.html.

National Research Council (NRC). 2007. *Colorado River Basin Water Management: Evaluating and Adjusting to Hydroclimatic Variability*.

Nijssen, B., D.P. Lettenmaier, X. Liang, S.W. Wetzel, and E.F. Wood. 1997. “Streamflow simulation for continental-scale river basins.” *Water Resource Research*, 33, 711–724.

Nowak, K., J. Prairie, B. Rajagopalan, and U. Lall. 2010. “A nonparametric stochastic approach for multisite disaggregation of annual to daily streamflow.” *Water Resources Research*, 46.

Ouarda, T., J.W. Labadie, and D.G. Fontane.1997. “Index sequential hydrologic modeling for hydropower capacity estimation.” *J. of the American Water Resources Association*, 33(6), 1337–1349.

Pagano, T., and D. Garen. 2005. “A Recent Increase in Western U.S. Streamflow Variability and Persistence.” *Journal of Hydrometeorology*, 6, 173–179.

Painter, T.H., J.S. Deems, J. Belnap, A.F. Hamlet, C.C. Landry, and B. Udall. 2010. “Response of Colorado River runoff to dust radiative forcing in snow.” Proceedings of the National Academy of Sciences on Climate Change and Water in Southwestern North America.

Pederson, G.T. , S.T. Gray, C.A.Woodhouse, J.L. Betancourt, D.B. Fagre, J.S. Littell, E. Watson, B.H. Luckman, L.J. Graumlich. 2011. “The Unusual Nature of Recent Snowpack Declines in the North American Cordillera.” *Science*, 333, 332 (2011).

Piechota, T. C., J. Timilsena, G.A. Tootle, and H. Hidalgo. 2004. “The Western U.S. Drought: How Bad is it?” *Eos, Transactions, American Geophysical Union*, 85, 301–308.

Pierce, D.W., T.P. Barnett, B.D. Santer, and P.J. Gleckler. 2009. “Selecting Global Climate Models for 12 Regional Climate Change Studies.” *Proceedings of the National Academy of Sciences*.

Prairie, J., K. Nowak, B. Rajagopalan, U. Lall, and T. Fulp. 2008. “A Stochastic Nonparametric Approach for Streamflow Generation Combining Observational and Paleoreconstructed Data.” *Water Resources Research*, Vol. 44, W06423, DOI: 10.1029/2007WR006684.

Redmond, K.T., and R.W. Koch. 1991. “Surface Climate and Streamflow Variability in the Western United States and Their Relationship to Large-Scale Circulation Indices.” *Water Resources Research*, 27, 2381–2399.

Regonda, S.K., B. Rajagopalan, M.P. Clark, and J. Pitlick. 2005. “Seasonal Shifts in Hydroclimatology over the Western United States.” *Journal of Climate*, 18, 372–384.

Sabo, J.L., S. Tushar, L.C. Bowling, G.H.W. Schoups, W.W. Wallender, M.E. Campana, K.A. Cherkauer, P.E. Fuller, W.L. Graf, J.W. Hopmans, J.S. Kominoski, C. Taylor, S.W. Trimble, R.H. Webb, and E.E. Wohl. 2010. “Climate Change and Water in Southwestern North America Special Feature: Reclaiming freshwater sustainability in the Cadillac Desert.” *Proc Natl Acad Sci*, 107:21263–21270.

Salathé, E.P. 2005. “Downscaling simulations of future global climate with application to hydrologic modeling.” *Int J Climatol*, 25, 419–436.

Seager, R. and G.A. Vecchi. 2010. “Greenhouse warming and the 21st century hydroclimate of southwestern North America.” *Proc Natl Acad Sci*, 107, 21277–21282.

Stockton, C.W., and G.C. Jacoby. 1976. “Long-term Surface Water Supply and Streamflow Trends in the Upper Colorado River Basin.” *Lake Powell Research Project Bulletin*, No. 18.

Webb, R.H., and J.L. Betancourt. 1992. *Climatic Variability and Flood Frequency of the Santa Cruz River, Pima County, Arizona*. U.S. Geological Survey. Water-Supply Paper 2379.

Wilby, R.L., L.E. Hay, and G.H. Leavesley. 1999. “A comparison of downscaled and raw GCM output: implications for climate change scenarios in the San Juan River Basin, Colorado.” *Journal of Hydrology*, 225, 67–91.

Wood, A.W., E.P. Maurer, A. Kumar, and D.P. Lettenmaier. 2002. “Long-Range Experimental Hydrologic Forecasting for the Eastern United States.” *Journal of Geophysical Research-Atmospheres*, 107(D20), 4429.

Wood, A.W., L.R. Leun, V. Sridhar, and D.P. Lettenmaier. 2004. “Hydrologic Implications of Dynamical and Statistical Approaches to Downscaling Climate Model Outputs.” *Climatic Change*, 15(62):189–216.

Woodhouse, C.A., and P.M. Brown. 2001. “Tree-ring evidence for Great Plains drought.” *Tree-Ring Research*, 57:89–103.

Woodhouse, C.A., and J.J. Lukas. 2006. “Multi-Century Tree-Ring Reconstructions of Colorado Streamflow for Water Resource Planning.” *Climatic Change*, 78, 293–315.

Woodhouse, C.A., S. Gray, and D. Meko 2006. “Updated Streamflow Reconstructions for the Upper Colorado River Basin.” *Water Resources Research*, 42(5), W05415, DOI: 10.1029/2005WR004455.

Woodhouse, C.A., D.M. Meko, G.M. MacDonald., D.W. Stahle, and E.R. Cook. 2010. “A 1,200-year perspective of 21st century drought in southwestern North America.” *Proc Natl Acad Sci*, 107, 21283–21288.

World Meteorological Organization. 2011. Retrieved from http://www.wmo.int/pages/index_en.html.

Yeh, S., and B.P. Kirtman. 2007. "ENSO Amplitude Changes Due To Climate Change Projections In Different Coupled Models." *Journal of Climate*, 20(2), 203. DOI:10.1175/Jcli4001.1.

Yeh, S-W, J.S. Kug, B. Dewitte, M.H. Kwon, B.P. Kirtman, and F.F. Jin. 2009. "El Niño in a Changing Climate." *Nature*, 461:511-U570.

Disclaimer

The Colorado River Basin Water Supply and Demand Study (Study) is funded jointly by the Bureau of Reclamation (Reclamation) and the seven Colorado River Basin States (Basin States). The purpose of the Study is to analyze water supply and demand imbalances throughout the Colorado River Basin and those adjacent areas of the Basin States that receive Colorado River water through 2060; and develop, assess, and evaluate options and strategies to address the current and projected imbalances.

Reclamation and the Basin States intend that the Study will promote and facilitate cooperation and communication throughout the Basin regarding the reliability of the system to continue to meet Basin needs and the strategies that may be considered to ensure that reliability. Reclamation and the Basin States recognize the Study was constrained by funding, timing, and technological and other limitations, and in some cases presented specific policy questions and issues, particularly related to modeling and interpretation of the provisions of the Law of the River during the course of the Study. In such cases, Reclamation and the Basin States developed and incorporated assumptions to further complete the Study. Where possible, a range of assumptions was typically used to identify the sensitivity of the results to those assumptions.

Nothing in the Study, however, is intended for use against any Basin State, any federally recognized tribe, the federal government or the Upper Colorado River Commission in administrative, judicial or other proceedings to evidence legal interpretations of the Law of the River. As such, assumptions contained in the Study or any reports generated during the Study do not, and shall not, represent a legal position or interpretation by the Basin States, any federally recognized tribe, federal government or Upper Colorado River Commission as it relates to the Law of the River. Furthermore, nothing in the Study is intended to, nor shall the Study be construed so as to, interpret, diminish or modify the rights of any Basin State, any federally recognized tribe, the federal government, or the Upper Colorado River Commission under federal or state law or administrative rule, regulation or guideline, including without limitation the Colorado River Compact (45 Stat. 1057), the Upper Colorado River Basin Compact (63 Stat. 31), the Utilization of Waters of the Colorado and Tijuana Rivers and of the Rio Grande, Treaty Between the United States of America and Mexico (Treaty Series 994, 59 Stat. 1219), the United States/Mexico agreement in Minute No. 242 of August 30, 1973 (Treaty Series 7708; 24 UST 1968), or Minute No. 314 of November 26, 2008, or Minute No. 318 of December 17, 2010, or Minute No. 319 of November 20, 2012, the Consolidated Decree entered by the Supreme Court of the United States in Arizona v. California (547 U.S 150 (2006)), the Boulder Canyon Project Act (45 Stat. 1057), the Boulder Canyon Project Adjustment Act (54 Stat. 774; 43 U.S.C. 618a), the Colorado River Storage Project Act of 1956 (70 Stat. 105; 43 U.S.C. 620), the Colorado River Basin Project Act of 1968 (82 Stat. 885; 43 U.S.C. 1501), the Colorado River Basin Salinity Control Act (88 Stat. 266; 43 U.S.C. 1951) as amended, the Hoover Power Plant Act of 1984 (98 Stat. 1333), the Colorado River Floodway Protection Act (100 Stat. 1129; 43 U.S.C. 1600), the Grand Canyon Protection Act of 1992 (Title XVIII of Public Law 102-575, 106 Stat. 4669), or the Hoover Power Allocation Act of 2011 (Public Law 112-72). In addition, nothing in the Study is intended to, nor shall the Study be construed so as to, interpret, diminish or modify the rights of any federally recognized tribe, pursuant to federal court decrees, state court decrees, treaties, agreements, executive orders and federal trust responsibility. Reclamation and the Basin States continue to recognize the entitlement and right of each State and any federally recognized tribe under existing law, to use and develop the water of the Colorado River system.